Chair of High-Power Converter Systems
Technical University of Munich Prof. Marcelo Lobo Heldwein

Arcisstr. 21 Email: hlu@ed.tum.de Tel.: +49 (0)89 289 28358
80333 Munich Web: www.epe.ed.tum.de/hlu Fax: +49 (0)89 289 28336

PRACTICAL COURSE

Simulation of Controlled Electrical Drives for MSPE

Edition: Summer Semester 2025

Lecturer:
Wei Tian
Room Z905 (Building 9)
Arcisstr. 21
D-80333 Munich

Tel.: +49 (0)89 289 28426
E-Mail: wei.tian@tum.de

Important Notes

Location and Time

The practical course is scheduled in room **0901** (Building 9) from **09:00** to **13.00** (Group A) and from **14:00** to **18:00** (Group B) as stated in the **schedule** in TUMonline.

The preliminary meeting is scheduled in room **3999** (Building 9) on **29.08.2025** at **13:00**

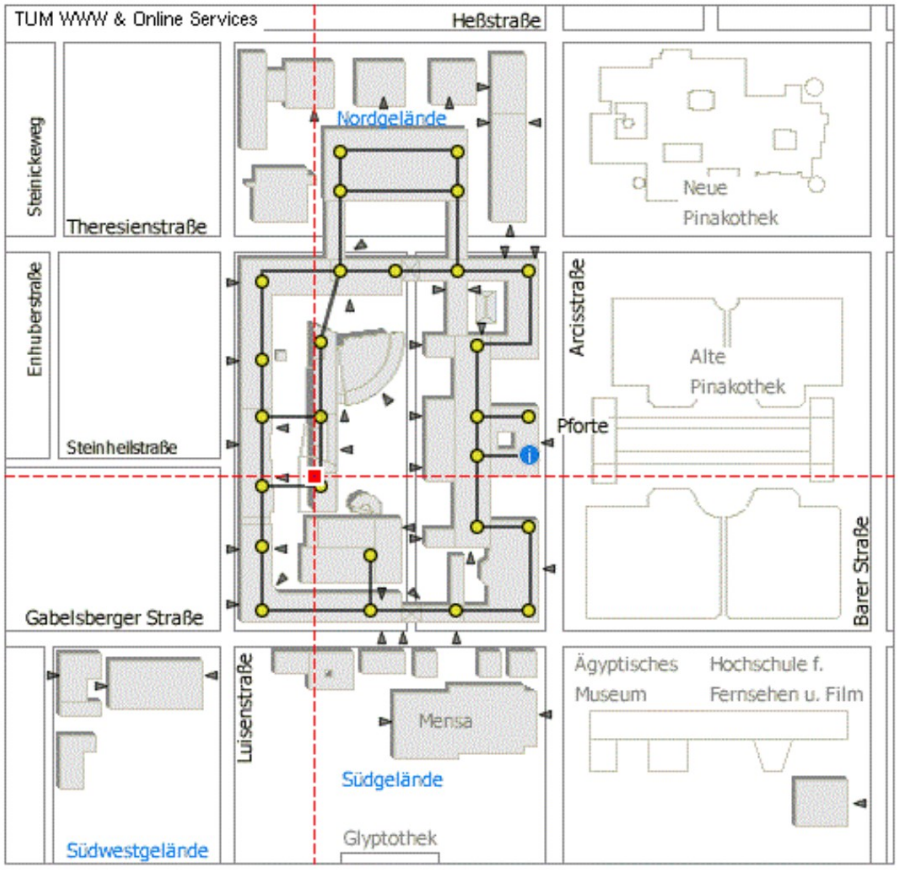

Preparation of the Experiments

The lab course consists of five simulation studies. Between each lab sessions at least one day off is provided, which shall be utilized to prepare for the following simulation studies by getting familiar with the given instructions. Problems labelled with an asterisk (*) shall be solved before the experiment. For solutions and deeper understanding the denoted literature can be consulted.

Grading

The final grade is calculated from the preparation of the experiments (30%), the implementation of the models by participation and comprehension in respective discussions (40%) and the result in the final written exam (30%).

Contents

Introduction

Modern industrial production lines are getting increasingly complex due to progress in technology. Therefore it is more difficult to handle and control them. Machinery downtimes, as well as sophisticated test rigs cause unwanted costs. For this reason development engineers have hardly any room to test novel open- or closed-loop control strategies at respective systems. Hence in past years computer simulation has become an important tool for conception, analysis, design and optimization of controlled drives. This development was made possible by the simultaneous progress in computer performance. The general objective of simulation studies is to predict the behavior of the investigated physical system by means of a mathematical model. There are a large number of different simulation programs, which are customized to specific applications.
This practical course provides an opportunity to obtain an insight to modern computer simulation. Within five experiments *mechatronic* systems will be simulated. These models include controlled electro-mechanical energy conversion units as illustrated in figure 1. The models will be implemented and optimized. Therefore the most important machine types, the separately excited direct current machine and alternating current machines, such as induction machine and permanent magnet synchronous machine will be investigated.
For the implementation of the experiments, the simulation tool `MATLAB/Simulink` is used. It is suitable for investigating linear, nonlinear, time-continuous and discrete systems. The graphical interface is intuitive to learn and operate.

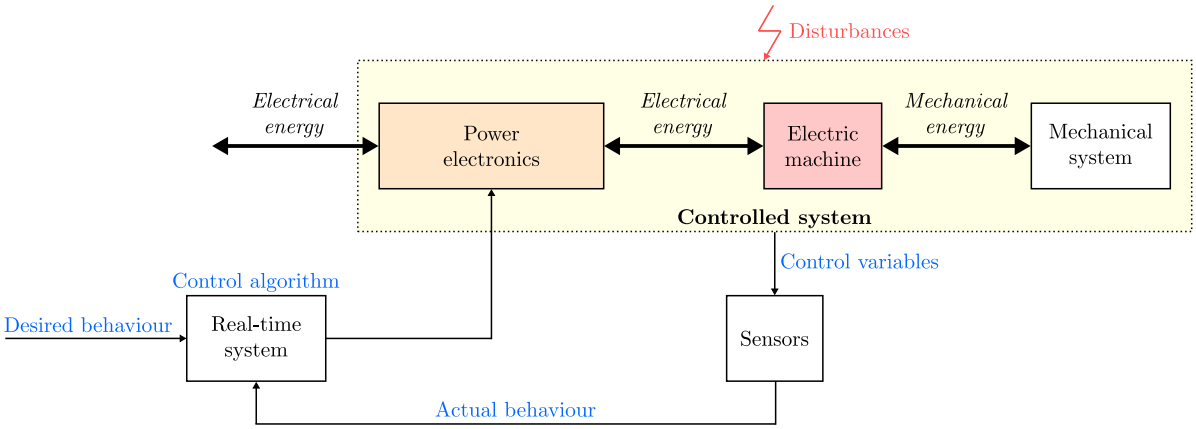

Figure 1: Components of a Mechatronic System

Experiment 1
Model of the DC Machine

1.1 Overview

The first two experiments cover the *controlled direct current drive*, also called DC drive. This type of drive system consists of the *direct current machine* and the DC converter as an electronic actuator. The actuator controls the electrical energy flow to the machine and thereby enables its closed-loop control. The control takes place through the output of a controller, that compares the measured control variable to a given reference value.
Within the practical course the *H-bridge* is considered. It is commonly used for separately excited DC machines in industrial systems. First experiment covers the modelling of a DC/DC converter, the separately excited DC machine and the associated sensors. Using these models, the open-loop operation of the DC machine and in particular the steady-state torque-speed-characteristic are investigated. The design of the controller and the analysis of the closed-loop control system will be the content of the second experiment.

1.2 H-Bridge Converter

1.2.1 Operating Principle

The *H-bridge converter* belongs to the class of DC/DC converters. Based on a constant input voltage U_{dc}, it outputs an adjustable pulsating output voltage u_A. In consideration of possible voltage and current polarities, single-quadrant converters and multi-quadrant converters are distinguished. In the following, four-quadrant converters are considered, which are able to supply positive as well as negative voltages and conduct currents bidirectionally (Fig. 1.1).

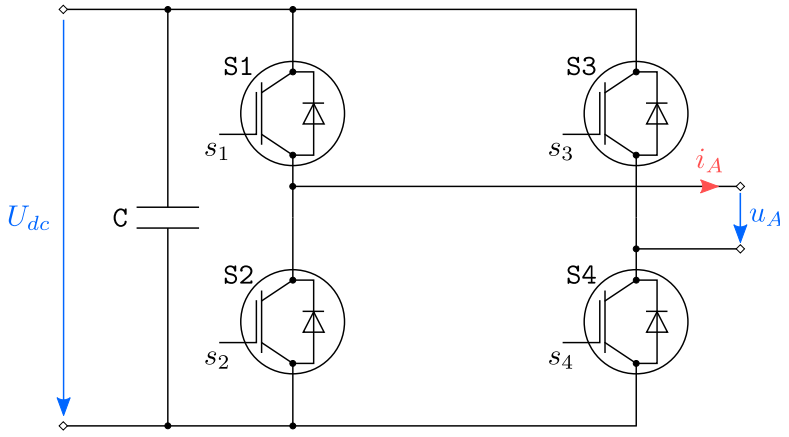

Figure 1.1: Circuit Diagram of H-Bridge Converter

Figure 1.1 displays the switching elements `S1` to `S4` (IGBT modules with integrated freewheeling diodes). They are assumed to behave as ideal switches and can be closed by the binary control

signals s_1 to s_4 (short notation s_x, $x \in \{1..4\}$) or opened (short notation $\neg s_x$, $x \in \{1..4\}$) arbitrarily. Whenever one of the switches in a half-bridge is closed, the other one has to be opened to avoid a short circuit of the *DC-bus voltage* U_{dc}. Thus, the following logical relations between the control signals and the output voltage are derived:

$$\begin{aligned} (s_1 \wedge \neg s_2) \wedge (\neg s_3 \wedge s_4) &\Rightarrow u_A = U_{dc} \\ (\neg s_1 \wedge s_2) \wedge (s_3 \wedge \neg s_4) &\Rightarrow u_A = -U_{dc} \\ [(s_1 \wedge \neg s_2) \wedge (s_3 \wedge \neg s_4)] \vee [(\neg s_1 \wedge s_2) \wedge (\neg s_3 \wedge s_4)] &\Rightarrow u_A = 0 \end{aligned} \tag{1.1}$$

Considering the relations given above, the switching signals s_2 and s_4 can be generated by logical negation of the signals s_1 and s_3.

1.2.2 Replication of Continuous Voltage Values

As shown in the equations (1.1), the converter can supply three discrete output voltages. By switching between these three states a mean voltage in the interval $[-U_{dc}; U_{dc}]$ can be generated. This behavior is achieved when the control signals s_1 and s_3 are generated by pulse-width-modulation (PWM).

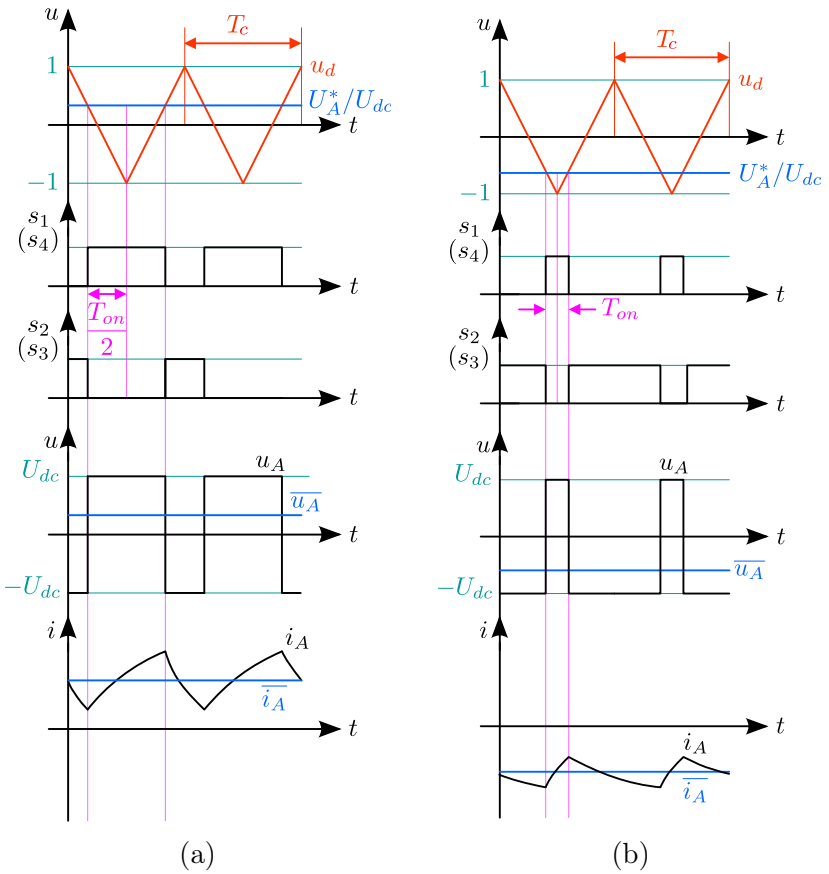

Figure 1.2: Functionality of Pulse-Width-Modulation
(a) $d > 0.5$ or $\overline{u_A} > 0$; (b) $d < 0.5$ or $\overline{u_A} < 0$

The principle of the PWM is illustrated in figure 1.2, where the following symbols are used:

U_A^*	desired voltage
u_d	carrier signal
T_c	period of the carrier signal
T_{on}	on-time of switch `S1` during one carrier period
u_A	instantaneous value of the output voltage
U_{dc}	direct current bus voltage

$\overline{u_A}$ corresponds to the moving average of the output voltage of one carrier period:

$$\overline{u_A}(t) = \frac{1}{T_c} \int_t^{t+T_c} u_A(t')\,\mathrm{d}t' \tag{1.2}$$

The binary signal s_1 is generated by comparison of the ratio from the desired voltage U_A^* and the DC-bus voltage U_{dc} and the reference signal u_d (*carrier signal*), as shown below:

$$s_1 = \begin{cases} 1 & \text{if} \quad U_A^*/U_{dc} \geq u_d \\ 0 & \text{else} \end{cases} \tag{1.3}$$

The duty cycle d of the signal s_1 therefore is:

$$d = \frac{T_{on}}{T_c} = \frac{T_{on}/2}{T_c/2} = \frac{1 + U_A^*/U_{dc}}{2} \tag{1.4}$$

To prevent the simultaneous closing of the switches `S1` and `S2`, the activation of `S2` takes place by the signal $s_2 = \neg s_1$. When $s_3 = s_2 = \neg s_1$ and $s_4 = \neg s_3 = s_1$ are chosen, u_A can take the values U_{dc} and $-U_{dc}$ according to (1.1). In advantage, only one signal is enough for the control of the converter . By varying the duty cycle in the interval $[0; 1]$, a mean voltage $\overline{u_A}$ in the range of $[-U_{dc}; U_{dc}]$ can be set. In that case, the third logical relation in (1.1) is not used, which is negligible since a mean voltage of zero can also be achieved appropriately setting the duty cycle to $d = 0.5$.

In figure 1.2 a triangular signal is used as carrier signal. Other signal types, for example a saw-tooth, are also possible. Figure 1.2(a) displays the command signal as well the resulting output voltage and current in case of an **ohmic-inductive** load with $U_A^* > 0$ respectively $d > 0.5$. Figure 1.2(b) shows the corresponding behaviour for $U_A^* < 0$ i.e. $d < 0.5$.

1.2.3 Dynamical Behaviour after Command Value Changes

When the desired voltage value U_A^* is changed, it takes a delay time T_w until the moving average of the output voltage is set accordingly. This is shown in figure 1.3. The four-quadrant converter can be regarded as an amplifier with a time lag.

In summary, a constant voltage source U_{dc} in combination with a H-bridge converter leads to an adjustable voltage source with output voltages in the interval $[-U_{dc}; U_{dc}]$. Furthermore, the energy flow can be lead bidirectionally. Thus the H-Bridge is suitable for the armature circuit as well as the excitation circuit of a DC machine.

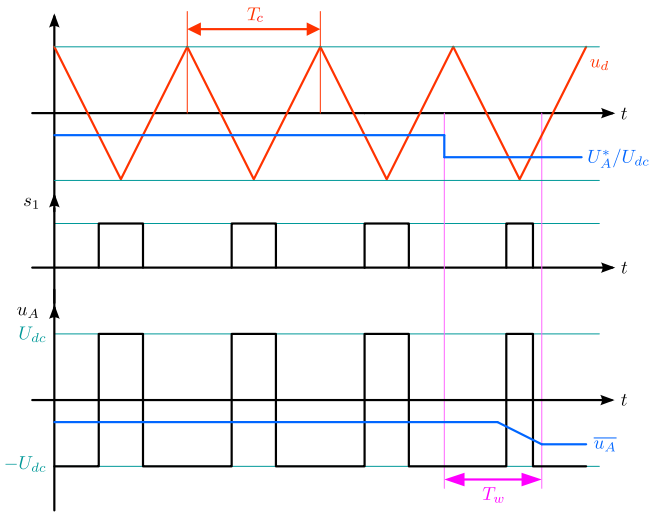

Figure 1.3: Delay Time for Changes of the Desired Value

1.3 Separately Excited DC Machine

1.3.1 Modeling

The fundamental structure of a direct current machine is depicted schematically in figure 1.4. Inside the machine electromechanical and thermal processes with partly nonlinear effects take place. Hence it represents a complex system. To conclude the relations between the electrical and mechanical domain in a manageable model, the following assumptions are made:

- The influence of the armature current to the air gap field (*armature reaction*) is neglected. The armature reaction deterioriates the machine behavior and it is tried to eliminate this effect by appropriate designs (e.g. compensation winding in larger machines).[1], [2]).
- Temperature effects due to the armature and excitation resistances are not taken into account.
- Regarding magnetic material properties, only the influence of magnetic saturation to the excitation circuit is considered. Taking certain construction measures, the minimization of hysteresis- and eddy-current-effects is achieved. The relation between excitation current and field flux linkage is described by a nonlinear function.

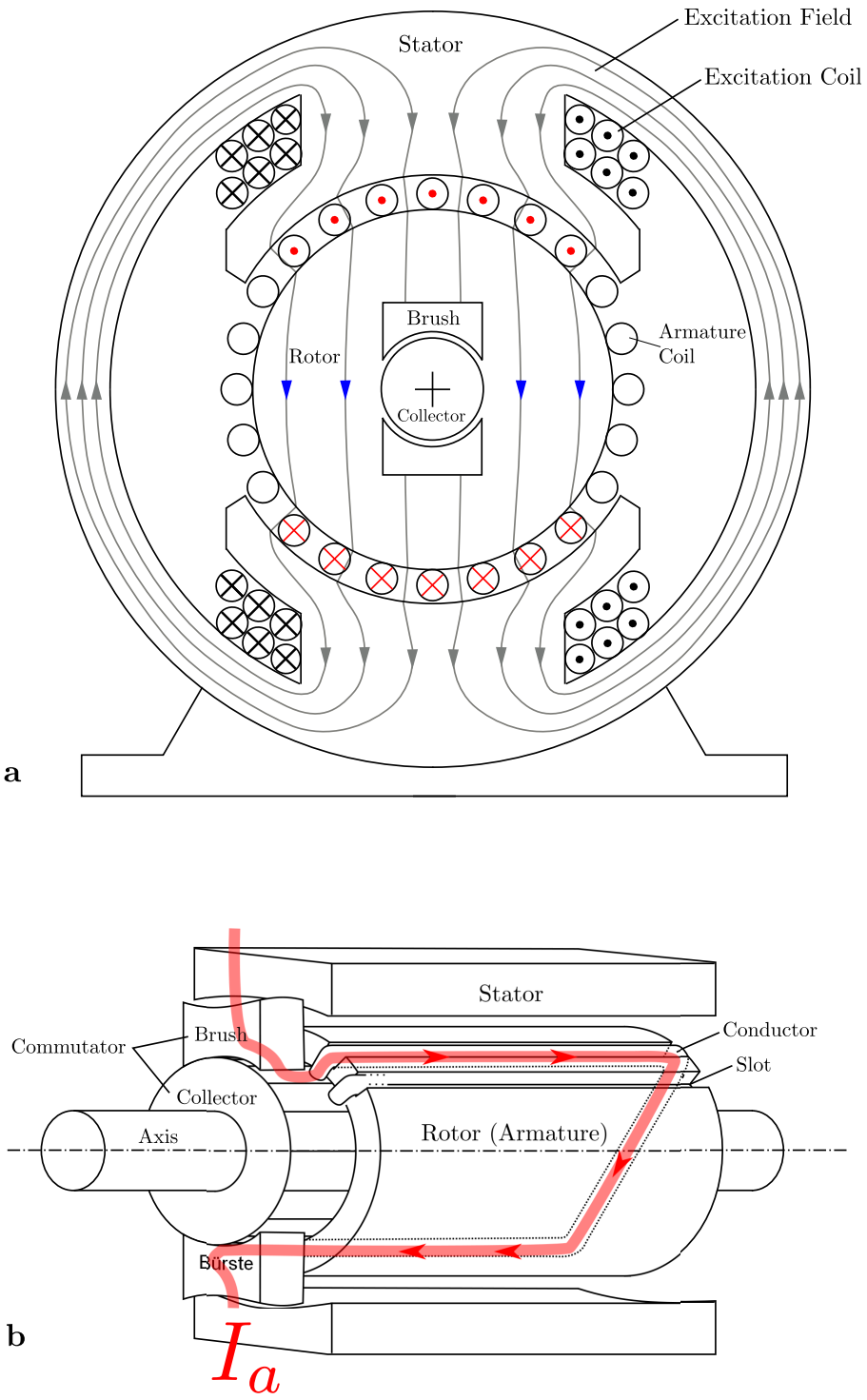

Figure 1.4: Structure of DC Machine
(a) Cross section; (b) Side view

Taking these assumptions into consideration, the following relationships between the electrical and mechanical variables (described in table 1.1) can be established:

$$\text{Armature Circuit:} \qquad U_A = E_A + R_A\, I_A + L_A \frac{\mathrm{d}I_A}{\mathrm{d}t} \tag{1.5a}$$

$$E_A = C_M\, \Psi_E\, \Omega_M \tag{1.5b}$$

$$M_M = C_M\, \Psi_E\, I_A \tag{1.5c}$$

$$\text{Excitation Circuit:} \qquad U_E = R_E\, I_E + \frac{\mathrm{d}\Psi_E}{\mathrm{d}t} \tag{1.5d}$$

$$\Psi_E = f(I_E) \text{ with } \Psi_E(0) = 0 \tag{1.5e}$$

$$\text{Mechanic:} \qquad M_M - M_L = \Theta_M \frac{\mathrm{d}\Omega_M}{\mathrm{d}t} \tag{1.5f}$$

Symbols	Physical Values	Symbols	Physical Values
U_A	Armature Voltage	I_E	Excitation Current
I_A	Armature Current	R_E	Excitation Resistance
R_A	Armature Resistance	C_M	Machine Constant
L_A	Armature Inductance	M_M	Air Gap Torque
E_A	Electromotive Force (EMF)	M_L	Load Torque
Ψ_E	Excitation Field Flux Linkage	Θ_M	Rotor Moment of Inertia
U_E	Excitation Voltage	Ω_M	Rotor Angular Speed

Table 1.1: Explanation of Symbols Used in (1.5)

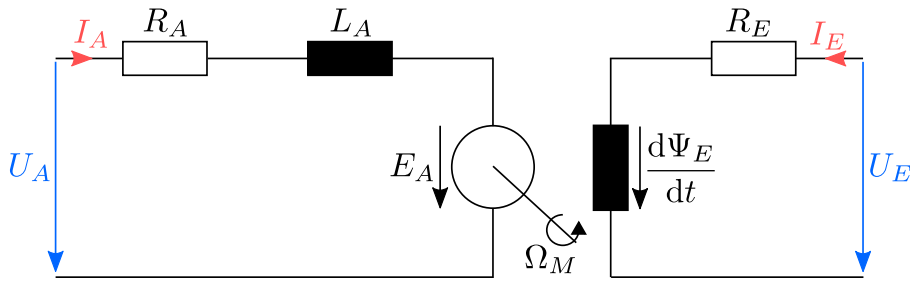

Figure 1.5: Equivalent Circuit Diagram of the Armature and Excitation Circuit

1.3.2 Steady-State Behavior

Motor Characteristics

In *steady-state* operation, at the time when the energy stored in the machine is constant and the state variables I_A, Ω_M and I_E do not change ($\mathrm{d}I_A/\mathrm{d}t = \mathrm{d}\Omega_M/\mathrm{d}t = \mathrm{d}I_E/\mathrm{d}t = 0$), the absorbed power is equal to the supplied power. Consequently, for a certain armature voltage U_A there exists a strict relation between torque and rotational speed. If a certain load is applied, then

a related rotation speed will be set. On the contrary, if a specific rotational speed Ω_M is set, the machine provides a corresponding torque. This is in accordance to the known operation of a DC machine supplied by a constant voltage source.
The stationary relation between torque and rotational speed can be derived from the system of equations (1.5). The armature voltage U_A and armature current I_A are replaced in terms of torque and rotational speed in equation (1.5a).

From $$U_A = E_A + I_A\ R_A + L_A \cancelto{0}{\frac{\mathrm{d}I_A}{\mathrm{d}t}}$$

under consideration of $$I_A = \frac{M_M}{C_M\ \Psi_E} \quad \text{and} \quad E_A = C_M\ \Psi_E\ \Omega_M$$

follows $$U_A = R_A \frac{M_M}{C_M\ \Psi_E} + C_M\ \Psi_E\ \Omega_M. \tag{1.6}$$

On the basis of $$M_M - M_L = \Theta_M \cancelto{0}{\frac{\mathrm{d}\Omega_M}{\mathrm{d}t}}$$

finally results $$\Omega_M = \frac{U_A}{C_M\ \Psi_E} - \frac{R_A}{C_M^2\ \Psi_E^2} M_L. \tag{1.7}$$

Equation (1.7) expresses the linear relation between the torque and angular velocity (see figure 1.6). The constant term corresponds to the *no-load speed* Ω_{M0}. This speed is reached, if no mechanical energy is taken from the machine, $M_L = 0$. If the motor gets loaded by the torque $M_L = M_{L1}$, the speed reduces and consequently so does the induced voltage. The voltage drop across the resistor of the armature winding leads to a rising current. Thus the generated torque of the machine increases until a new state of equilibrium is reached. The resulting operating point is (M_{L1}, Ω_1).
If the rotor is blocked, no voltage is induced in the armature winding. Then the voltage U_A across the armature resistor increases. Consequently the current I_S is named *short circuit current*. In this situation, the machine delivers *the stall torque*:

$$M_S = C_M\ \Psi_E\ I_S = C_M\ \Psi_E \frac{U_A}{R_A} \tag{1.8}$$

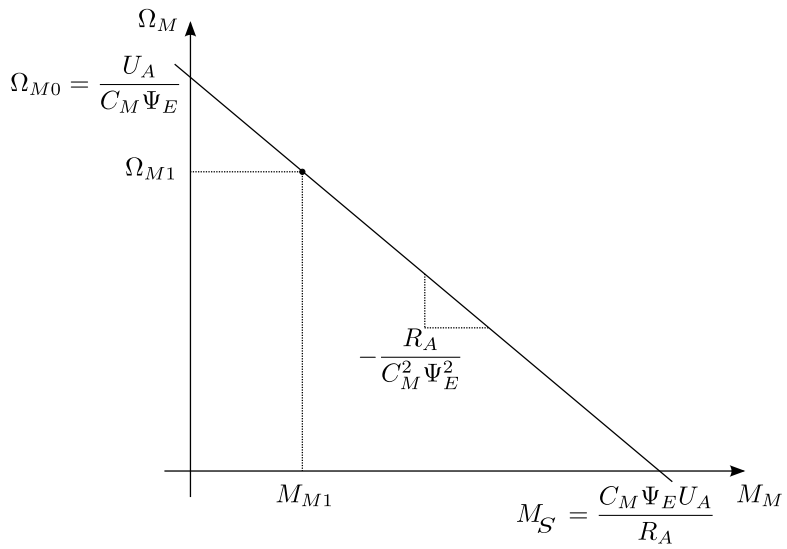

Figure 1.6: Steady-State Torque-Speed-Characteristic for the DC Machine

Influence on the Stationary Characteristic Curve

Besides the machine parameters C_M, R_A also the variables U_A and Ψ_E have influence on the characteristic curve. If the armature voltage U_A is set by connecting the voltage source to the armature terminals, the excitation flux can be adjusted by the excitation voltage according to (1.5d). Hence the machine characteristics can be influenced in two different ways:
When the armature voltage is varied, but excitation flux linkage is kept constant at the nominal value Ψ_{EN}, the intersecting points of the characteristic curve move along the Ω_M-axis without changing the slope. This approach is named as *armature control* (see Fig. 1.7). Since the insulation of the rotor windings, as well the area between two adjacent commutator segments have a limited insulation strength, the armature voltage is not allowed to exceed above the nominal value U_{AN}. For that reason, only operating points below the nominal characteristics are allowed.
In practice a small value for the armature resistor is targeted in the machine design to maximize the efficiency. However, this would lead to a heating loss $P = U_{AN}^2/R_A$ due to the current flow under rated voltage at standstill, which could damage the insulation of the rotor winding. Due to that effect the armature current is limited to the value $I_{max} < I_S$. Operation in the left area, where the nominal curve interacts the x-axis is therefore excluded.

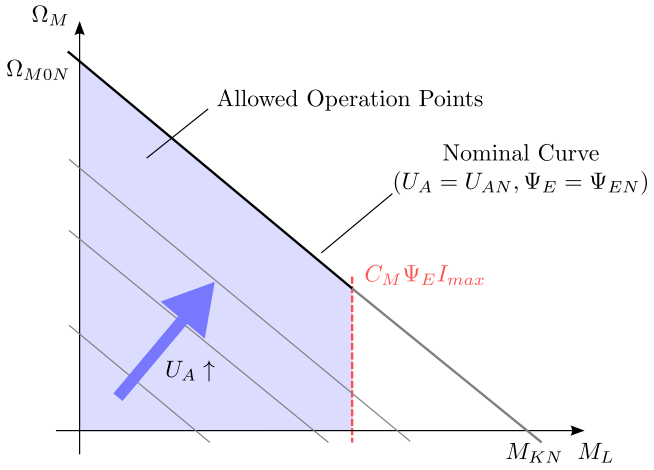

Figure 1.7: Operation in Armature Control

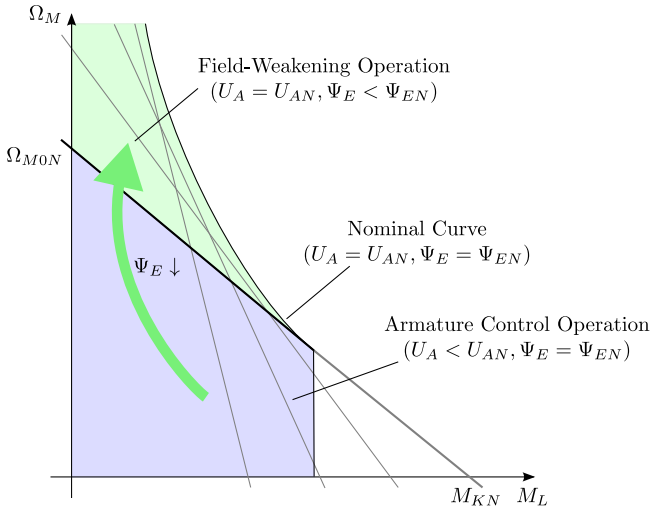

Figure 1.8: Extension of the Operation Range by Field Weakening

Stationary operating points above the nominal curve can be reached if the excitation flux is weakened at nominal armature voltage. This approach is named as *field weakening*. As shown in (1.5b) this leads to a lower counter-voltage, that is induced in the armature winding at the rotational speed Ω_M. Higher motor speeds can then be achieved. When reducing the excitation, the generated torque at a certain armature current I_A is lower (see (1.5c)). The reduction of the magnetic excitation corresponds to a clockwise rotation of the torque-speed-characteristic (Fig. 1.8).

1.4 Sensing

If a DC machine operates at a test bench the access to physical variables such as motor speed and armature current is only possible through installation of specific sensors. The recorded signals are time delayed, noisy, distorted or affected by offsets, nonlinearities and quantization errors. These errors represent a fundamental performance bottleneck of the drive system. Therefore, the most important causes of measurement errors are analyzed in the following section .

1.4.1 Current Measurement

The current is mostly measured with *shunt resistors* or *closed-loop transducers*. A *shunt* is a calibrated, low resistance component, across which the voltage drop is proportional to the current. Due to generated heat loss in the shunt resistor, the measured voltage has to be kept low. Therefore, the voltage has to be amplified to approximately $[-10V; 10V]$ by an analog circuit before digitization via an analog-digital-converter (ADC). This results in a relative strong noise component.

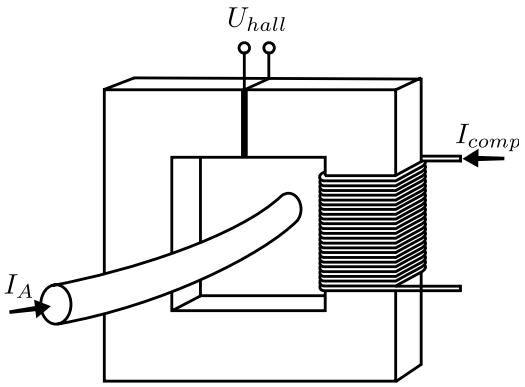

Figure 1.9: Structure of a Closed-Loop Transducer

Figure 1.9 shows the elementary components of a closed-loop transducer. An iron core encloses the conductor that carries the current of interest I_A. A hall-sensor captures the magnetic field in the iron core and outputs a corresponding voltage U_{hall}. This voltage drives a *compensation current* I_{comp} in the secondary winding that neutralizes the magnetic field. Hence the compensation current is proportional to the measured current. The proportionality factor is defined by the number of turns of the secondary winding. In general the compensation current gets transformed by a shunt resistor to a voltage that is evaluated by an ADC. With regard to low currents in secondary winding, a higher resistance can be chosen to improve the signal-to-noise ratio. Due to the operation principle of the hall sensor and the remanence of the iron core this measurement leads to larger *offsets* in the measured values.

In summary, measurement noise and offsets are the most significant sources of errors in current measurements. In this practical course the offset is neglected, but the current is superimposed with a noise term in the model. As depicted in figure 1.10 the measured signal is represented with a superscript ^{m} (filtered values with $\hat{}$).

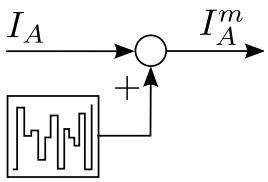

Figure 1.10: Model of Current Measurement

1.4.2 Speed Measurement

In practice mainly the derivation of the rotor angle is used for speed measurement, which is recorded by an encoder fixed to the rotor shaft.

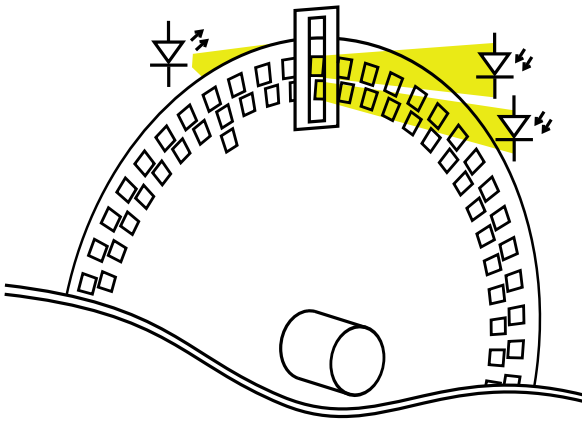

Figure 1.11: Drawing of an Optical Incremental Encoder

The most frequently used position-sensors are *incremental encoders* and *resolvers*. In the following only incremental encoders are considered.
The physical principle of position measurement is of magnetic or optical nature. In its simplest form the optical sensor consists of an incremental wheel, a light source and two photo sensors (see Fig. 1.11). There are two tracks of equidistantly placed slots, e.g. 1024, arranged along the perimeter of the disc. Both tracks are shifted by a quarter of the distance between to marks. Hence the photo diodes detect rectangular pulse signals which are shifted 90° to each other. This enables a higher resolution and also detection of the rotational direction. With a 1024-pulses-encoder up to 4096 discrete positions per revolution can be distinguished. For magnetic incremental encoders magnetically hard material is used, whose border regions are made of alternating magnetic polarities.
In simulation the speed detection is modelled according to the behaviour of the incremental encoder. The engine speed of the DC machine gets integrated to an angle which quantifies the corresponding amount of encoder pulses. The resulting signal then gets differentiated (see Fig. 1.12).

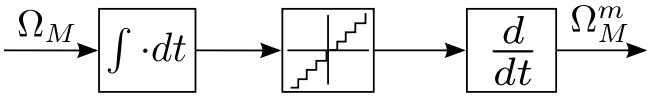

Figure 1.12: Model of the Speed Measurement

1.5 Model of the DC Machine

Note: The exercises marked by a * should be solved as preparation.

1.) * Transfer the basic equations (1.5) to the Laplace domain and draw the signal flow diagram of the separately excited direct current machine (input variables: U_A, U_E, M_L; output variables: I_A, Ω_M).

2.) * Complete the diagram in figure 1.13, by naming the operation modes of quadrants II, III and IV. Which requirement does the load torque have to fulfill, that a *steady state* operation in quadrant II and III is possible?

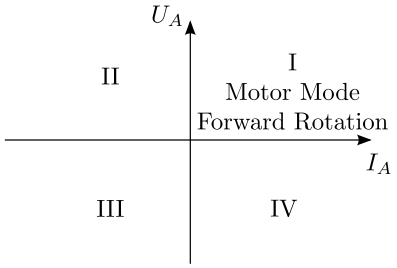

Figure 1.13: Quadrants in the I_A-U_A-Diagram

3.) * Indicate the operating point of maximum mechanical power $P_{M,max}$ in the M-Ω diagram for a given armature voltage U_A in the armature control range. Derive the expression of $P_{M,max}$ as a function of the no-load-speed Ω_{M0} and the stall torque M_S.

1.5.1 Behavior of the DC Machine

The behaviour of a DC machine, with the parameters summarized in table 1.2, shall be investigated. Initially it is assumed that the machine is fed by an ideal dc voltage source.

Physical Parameter	**Symbol and Value (SI)**			
Nominal Power	P_N	=	200	[W]
Nominal Engine Speed	N_N	=	2 000	[min^{-1}]
Nominal Torque	M_{MN}	=		[Nm]
Nominal Armature Voltage	U_{AN}	=	220	[V]
Nominal Armature Current	I_{AN}	=	1	[A]
Nominal Excitation Voltage	U_{EN}	=	220	[V]
Nominal Excitation Current	I_{EN}	=	0,1	[A]
Max. Armature Current	$I_{A,max}$	=	3	[A]
Max. Excitation Current	$I_{E,max}$	=	0.3	[A]
Armature Inductance	L_A	=		[H]
Armature Resistor	R_A	=		[Ω]
Excitation Resistor	R_E	=		[Ω]
Rotor Inertia Moment	Θ_M	=		[kg m^2]

Table 1.2: Parameters of the Investigated DC Machine

4.) * To identify the missing parameters of table 1.2, different experiments have been undertaken. The results are given in figure 1.14 and 1.15.

(a) Calculate the nominal torque and excitation resistance.

(b) Determine the armature resistance and armature inductance from the current waveform in figure 1.14. State the value of armature time constant T_A.

(c) Calculate the value of the machine constant C_M. Assume $\Psi_{EN} = 1\,[\text{Vs}]$.

(d) The diagram in figure 1.15 displays the rotor velocity for acceleration and deceleration with constant motor torque. As you can see the speed changes almost linear in time. Determine the derivative of the angular velocity during acceleration and deceleration from the graph. Which physical effect causes the difference between the two values? Calculate the rotor inertia.

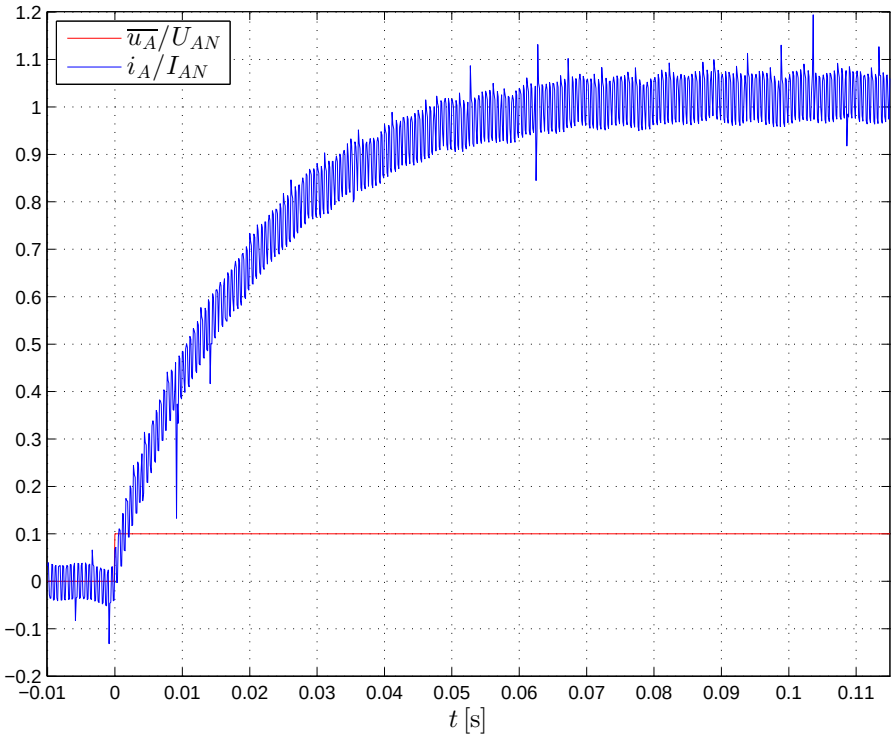

Figure 1.14: Armature Current Response on Voltage Step ($\Psi_E = 0\,[\mathrm{Vs}]$)

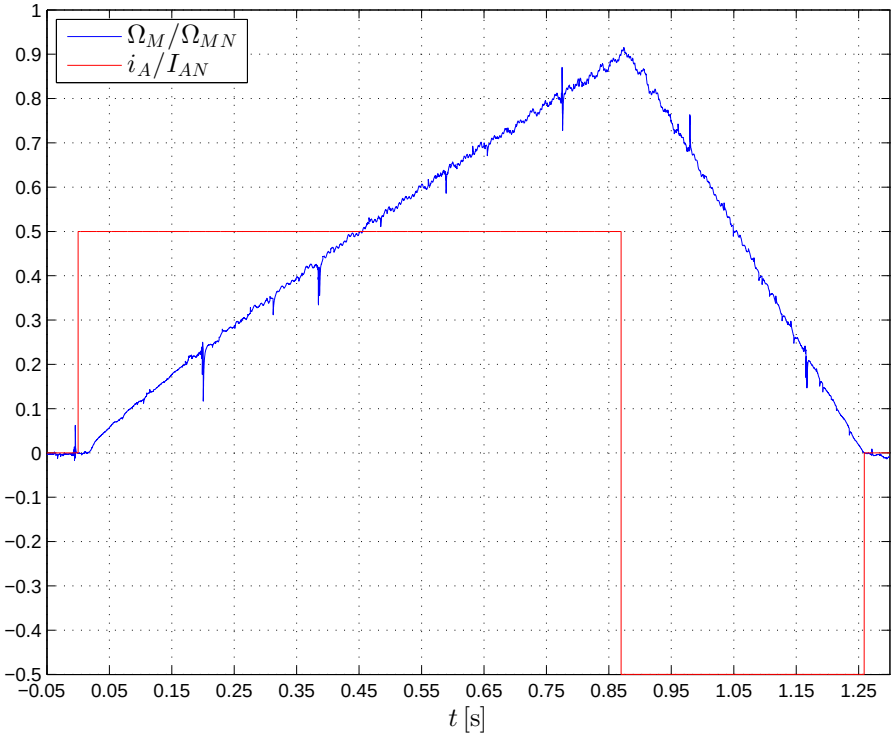

Figure 1.15: Rotor Velocity During Acceleration and Deceleration and Armature Current Waveform

The relation between excitation current and excitation flux undergoes remarkable hysteresis behaviour as depicted in figure 1.16. In our simulation studies the hysteresis loop gets approximated by the magnetizing curve, that is represented by:

$$\frac{\Psi_E}{\Psi_{EN}} = a_1 \operatorname{atan}\left(\frac{I_E}{I_{EN}}\right) + a_2 \operatorname{atan}\left(\frac{2I_E}{I_{EN}}\right) + a_3 \operatorname{atan}\left(\frac{3I_E}{I_{EN}}\right) \tag{1.9}$$

$$\text{where } a_1 = -1{,}122,\ a_2 = 2{,}553 \text{ and } a_3 = -0{,}759$$

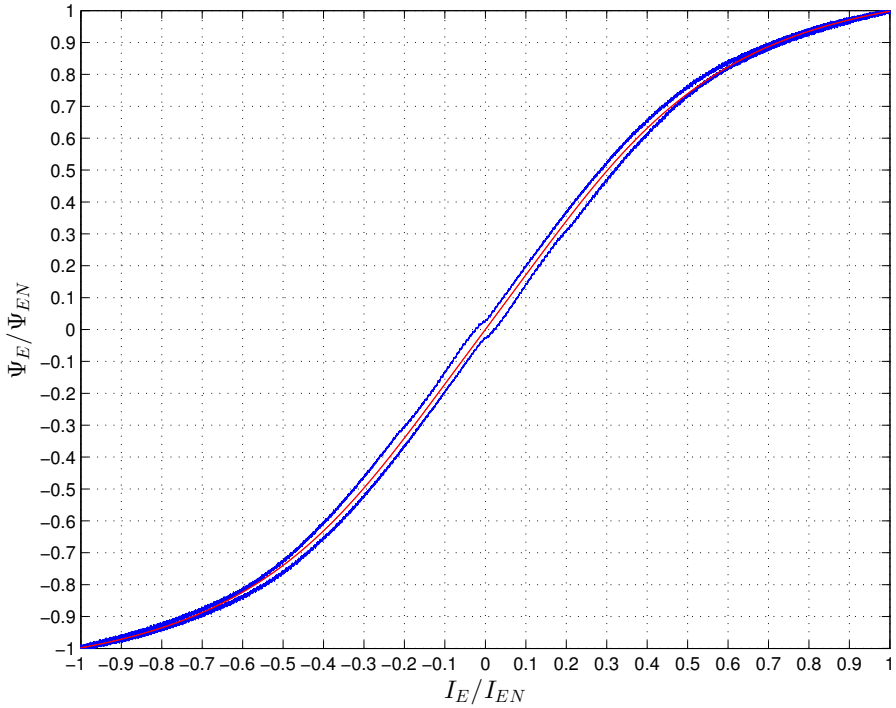

Figure 1.16: Excitation Flux Linkage as a Function of the Excitation Current (Recorded Hysteresis Loop and Approximated Magnetizing Curve)

In the following, the operation of an electrical machine with an adjustable DC voltage source is investigated.

5.) Open the file `Experiment_1_DCM_Parameter.m` in the directory `Experiment_1` in `MATLAB`. Complete it with the calculated parameters at the relevant positions and save the changes. Open the file `DCM_Ideal_Supply.slx` in `Simulink` and complete the armature circuit of the separately excited DC machine. Set U_{AN} and U_{EN} to their nominal values and load the machine at the time $t = 1\,[\mathrm{s}]$ with the torque $M_L = M_{MN}$.
Before starting the simulation adopt the model parameters by double clicking on the block `Initialize`. Evaluate the signals of the machine model (block `Direct Current Machine`). Observe and explain the trajectories in the M-Ω diagram.

6.) Think about a method to display the steady-state torque-speed-characteristic at a given armature voltage U_A using a ramp-shaped load torque. What do you have to consider when choosing the slop of the load torque?
Record one curve that runs through the quadrants I, II and IV to verify your proposal and evaluate the result.

7.) Record the steady state curve for the values $U_A = 0{,}5\,U_{AN}$ and $U_A = U_{AN}$ in **quadrant I** (the transients are allowed to enter the other quadrants) of the M-Ω diagram (see Fig. 1.7) and explain your result.

8.) **Dynamic armature control:** Investigate the dynamic transition between the stationary curves when applying the following voltage:

$$\frac{U_A}{U_{AN}} = \begin{cases} 0{,}4 & \text{for} \quad t \leq 3\,[\text{s}] \\ 0{,}8 & \text{for} \quad 3 < t \leq 5\,[\text{s}] \\ 1 & \text{for} \quad t > 5\,[\text{s}] \end{cases} \tag{1.10}$$

Display the resulting trajectory in the M-Ω diagram. Check that it doesn't leave quadrant I and explain the shape of the trajectory based on physical arguments.

9.) **Field weakening range:** Set the voltage source in the armature circuit to the value U_{AN}. Use the following course for the excitation voltage, to show the nominal steady state curve and a respective field weakening characteristic:

$$\frac{U_E}{U_{EN}} = \begin{cases} 1 & \text{for} \quad t \leq 3\,[\text{s}] \\ 0{,}5 & \text{for} \quad t > 3\,[\text{s}] \end{cases} \tag{1.11}$$

Both characteristics **shall be shown limited to quadrant I** (similar to Fig. 1.8). Interpret the obtained relation in the M-Ω diagram.

1.5.2 Converter Supplied Operation

In this section the operation of the DC machine with a H-bridge converter is investigated. The properties of the converter are summarized in table 1.3.

Physical Parameters	**Symbol and Value (SI)**
DC Bus Voltage	$U_{dc} = 220$ [V]
Maximum Number of Switching Operations of an IGBT per Time Interval	$r_{max} = 2\,000$ [s^{-1}]

Table 1.3: Parameters of the Converter

10.) * The pulse converter is driven by a PWM-signal. Which maximum carrier frequency $f_{c,\,max}$ results from the data in table 1.3?

11.) * Analogously to figure 1.2, draw the waveform of the command signals s_1 and s_2 of the converter and its output voltage u_A for a desired voltage of $U_A^* = 0$ V. Include also the resulting current i_A for a RL-load.
Which value does the duty cycle d take in that case?

12.) Open the file `DCM_Pulse_Converter.slx`. Double click on the block `Pulse Converter with Load` to have its content visible.
Build a H-bridge converter with the available elements, including resistive-inductive load

and EMF. If necessary look up the documentation of the blocks in the help menu.
Use the calculated values for parameters R_A and L_A. Set $E_A = 200$ V and save your changes.
Explain the functionality of the `Simulink`-block `Modulator`. Adjust the parameter T_c to the appropriate value in `Experiment_1_DCM_Parameter.m`, to obtain the carrier frequency $f_{c,max}$.
Set the input voltage $U_A^*/U_{dc} = 1$ and $U_A^*/U_{dc} = 0{,}8$ and explain the resulting current waveforms.

13.) * As seen in section 1.2.3 the converter behaves like an amplifier whereby the output voltage reacts with a time delay T_d after the desired value has been changed. Therefore the converter can be simplified as a block with delay time constant T_{CON} and amplification factor V_{CON}. The transfer function (1.12) is given as:

$$F_{CON}(s) = V_{CON}\ e^{-s\ T_{CON}} \approx \frac{V_{CON}}{1 + s\ T_{CON}} \tag{1.12}$$

Give the values of the parameters V_{CON} and T_{CON} as a function of the DC-bus-voltage U_{dc} and the carrier frequency f_c. For determination of the time constant T_{CON} the maximum delay at a given carrier frequency should be considered.

14.) The validity of the approximation above shall be verified by simulation.
Therefore open the file `DCM_Converter_Compare.slx`.
Insert a copy of the edited block `Converter with Load` from problem 12 and rename it as `Pulse_Converter`. Edit its content to obtain a H-bridge converter by removing all load related components. On one side the generated PWM-signal and on the other side the output voltage u_A should serve as interface.
Add two blocks of the motor model from the file `DCM_ideal_supply.slx`. For the first model use the `converter`-block to supply the armature voltage. For the second model use the output of the block `pulse_converter (Time-Delay-Approximation)`. Adjust the values of the parameters T_c, V_{CON} and T_{CON} in file `Experiment_1_DCM_Parameter.m`.
Compare the results of both models. How does the motor speed change when the switching of the converter is neglected? What advantages does this simplification have?

1.5.3 Influence of Sensing

In the following, the behaviour of the sensors are investigated. It is assumed, that the armature circuit as well as the excitation circuit are fed by a H-bridge converters. Both converters are modeled as first order delay time blocks with gain V_{CON} and delay time T_{CON}.

15.) Open the file `DCM_Sensing.slx` and add a copy the motor model from file `DCM_ideal_supply.slx`.
Use the following reference signal for the pulse converter in the excitation circuit:

$$\frac{U_E^*}{U_{EN}} = \begin{cases} 0 & \text{for} \quad t \leq 0{,}1\ [\text{s}] \\ 1 & \text{for} \quad t > 0{,}1\ [\text{s}] \end{cases} \tag{1.13}$$

The reference voltage value of the armature circuit is:

$$\frac{U_A^*}{U_{AN}} = \begin{cases} 0 & \text{for} \quad t \leq 0{,}5\,[\text{s}] \\ 1 & \text{for} \quad t > 0{,}5\,[\text{s}] \end{cases} \tag{1.14}$$

Take care of the gain factor when implementing the converter. Load the DC machine at time $t_L = 1{,}5\,[\text{s}]$ with nominal torque M_{MN}.
Assess the behavior of the motor.
Look at the measurement signals Ω_M^m, I_A^m, I_E^m and compare them with the signals from the machine model Ω_M, I_A and I_E. Give reasons for the existing differences.

16.) Smooth the current measurement signals I_A^m and I_E^m with a first-order low-pass filter with time constant $T_{f,\,I_A} = T_{f,\,I_E} = 2\,[\text{ms}]$). Also use such a filter for the angular velocity with time constant $T_{f,\,\Omega_M} = 2\,[\text{ms}]$. To complement the filter modify the block `transfer function` from the `Simulink` library `Continuous`.

After successfully smoothing the measurement signals finally evaluate the behavior of the filter by comparing the filtered signals $\hat{\Omega}_M$, $\hat{I}_A$, $\hat{I}_E$ to the measured signals Ω_M^m, I_A^m, I_E^m and the real signals Ω_M, I_A, I_E.

Experiment 2
Control of the DC Drive

2.1 Overview

In the previous experiment we derived simplified models of the DC drive components (DC machine, H-bridge converter, sensing) and validated them by simulation in an *open-loop* system. In this experiment the DC drive will be investigated in *closed-loop* operation.

The usual approach is to control the state variables *Armature Current* I_A and *Rotational Speed* Ω_M with linear PID-controllers (Proportional-Integral-Differential) in a cascade structure (see Fig. 2.1). This entails that the current controller and the speed controller are nested into each other. Two controllers have to be designed.

In industrial drive applications control parameters often get determined by the *Magnitude Optimum,* respectively *Symmetric Optimum* control guidelines. This procedure requires relatively small effort when modelling the control systems and delivers satisfying results with regard to the dynamics and stability of the closed-loop circuit.

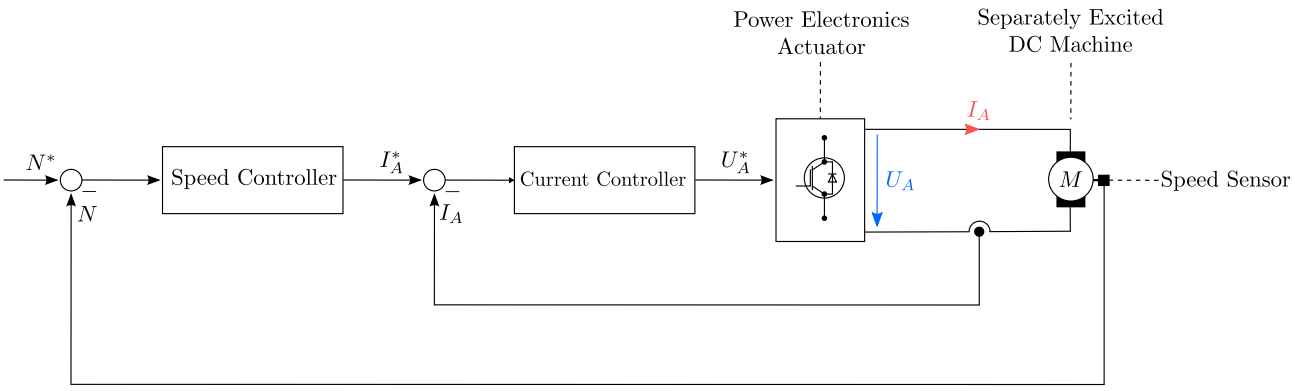

Figure 2.1: Principle Diagram of Speed and Current Control in Cascaded Structure

After a short summary of the fundamental properties of the model from experiment 1, the design of the current controller in the inner loop is considered first. In the next step the speed controller in the outer loop is designed. Finally we will check in simulation if the control objectives are achieved. The investigation is limited to the armature control range. The field weakening range is not taken into account.

2.2 Model of the DC Drive

The most important properties of the DC machine, the pulse converter and the sensory circuits in experiment 1 are summarized in this section. Relevant numerical parameters for the controller design can be found in table 2.1.

2.2.1 DC Machine

The electrical and mechanical equations of the separately excited DC machine according to (1.5) are:

$$\text{Armature Circuit:} \qquad U_A = E_A + R_A\ I_A + L_A \frac{\mathrm{d}I_A}{\mathrm{d}t} \tag{2.15a}$$

$$E_A = C_M\ \Psi_E\ \Omega_M \tag{2.15b}$$

$$M_M = C_M\ \Psi_E\ I_A \tag{2.15c}$$

$$\text{Excitation Circuit:} \qquad U_E = R_E\ I_E + \frac{\mathrm{d}\Psi_E}{\mathrm{d}t} \tag{2.15d}$$

$$\Psi_E = f(I_E)\ \text{ with }\ \Psi_E(0) = 0 \tag{2.15e}$$

$$\text{Mechanics:} \qquad M_M - M_L = \Theta_M \frac{\mathrm{d}\Omega_M}{\mathrm{d}t} \tag{2.15f}$$

The derived signal flow diagram is depicted in figure 2.2.

The excitation flux Ψ_E follows the nonlinear equation of the excitation current I_E from experiment 1:

$$\frac{\Psi_E}{\Psi_{EN}} = a_1\ \mathrm{atan}\left(\frac{I_E}{I_{EN}}\right) + a_2\ \mathrm{atan}\left(\frac{2I_E}{I_{EN}}\right) + a_3\ \mathrm{atan}\left(\frac{3I_E}{I_{EN}}\right) \tag{2.16}$$

$$\text{with } a_1 = -1.122,\ a_2 = 2.553 \text{ and } a_3 = -0.759$$

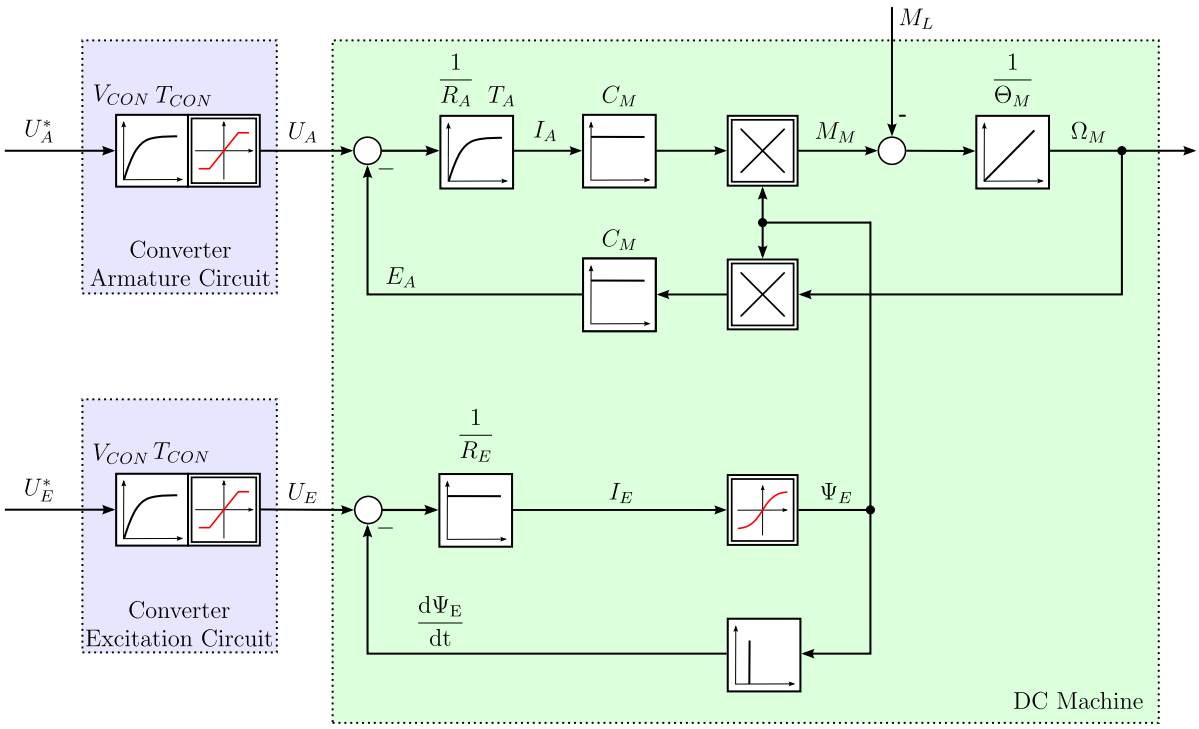

Figure 2.2: Signal Flow Diagram for a Separately Excited DC Machine with Pulse Converters for Armature and Excitation Circuit

2.2.2 Power Electronic Actuator

The armature voltage as well as the excitation voltage are supplied by pulse converters. Both converters are modeled by first-order delay elements that describe their amplifying and delay behaviour. We will see that, this approximation simplifies the controller design. Therefore, the transfer function of the power electronic actuator is:

$$F_{CON}(s) = \frac{U(s)}{U^*(s)} = V_{CON}\ e^{-sT_{CON}} \approx \frac{V_{CON}}{1 + s\ T_{CON}} \tag{2.17}$$

Here V_{CON} is the gain of the pulse converter and $T_{CON} = T_{d,max}$ is the maximum delay time for taking over the desired value (see experiment 1).

The output voltage of the converter can not exceed the DC-bus voltage U_{dc}. This is taken into account by introduction of voltage saturation in the simulation.

2.2.3 Sensing

Similar to experiment 1 the current measurement signals I_A^m and I_E^m are prone to noise. An incremental encoder determines the rotor angle. The angular velocity Ω_M is calculated by derivation with respect to time. For the controller design the sensors are assumed to show no dynamical behaviour. That means there is no time delay between the actual values I_A, I_E, Ω_M and the measured signals I_A^m, I_E^m and Ω_M^m.

The noise in the measured signal X, $X \in \{I_A^m, I_E^m, \Omega_M^m\}$ is suppressed by a first-order filter with the time constant $T_{f,X}$:

$$F_f(s) = \frac{\hat{X}(s)}{X^m(s)} = \frac{1}{1 + s\, T_{f,X}} \tag{2.18}$$

For the controllers, which will be designed in the following, **only filtered** measurement signals $\hat{I}_A$, $\hat{I}_E$ and $\hat{\Omega}_M$ are available as input signals.
In figure 2.3 all components of the controlled drive system are depicted in a compact signal flow diagram.

Physical Values	**Symbol and Value (SI)**			
Nominal Power	P_N	=	200	[W]
Nominal Rotational Speed	N_N	=	2 000	[min^{-1}]
Nominal Torque	M_{MN}	=	0,96	[Nm]
Nominal Armature Voltage	U_{AN}	=	220	[V]
Nominal Armature Current	I_{AN}	=	1	[A]
Nominal Excitation Voltage	U_{EN}	=	220	[V]
Nominal Excitation Current	I_{EN}	=	0,1	[A]
Max. Armature Current	$I_{A,\,max}$	=	3	[A]
Max. Excitation Current	$I_{E,\,max}$	=	0,3	[A]
Armature Inductance	L_A	=	0,374	[Vs A^{-1}]
Armature Resistance	R_A	=	22	[Ω]
Excitation Resistance	R_E	=	2,2	[kΩ]
Rotor Inertia Moment	Θ_M	=	1,3	[g m^2]
Product of the Machine Constant and the Nominal Excitation Flux	$C_M \Psi_{EN}$	=	0,96	[Vs]
Gain of both Pulse Converters	V_{CON}	=	220	[1]
Time Constant of both Pulse Converters	T_{CON}	=	1	[ms]
Time Constant of the First-Order Filter	$T_{f,X}$	=	2	[ms]

Table 2.1: Parameters of the Investigated Drive System

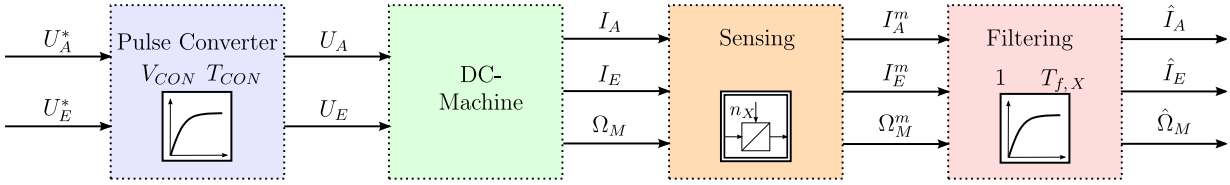

Figure 2.3: Components of the Investigated Drive System

2.3 Armature Current Control

This section focuses on the design of the current controller in the inner loop of the cascade structure (see Fig. 2.1). Therefore operation in the armature control range is a prerequisite, so $\Psi_E = \Psi_{EN}$ is valid. For the controller design the Magnitude Optimum (MO) respectively the symmetrical optimum (SO) criteria are used.

Controller Design using MO guarantees a minimum overshoot and good command response behaviour, while SO takes care of a good disturbance rejection behaviour. Following requirements have to be fulfilled to allow the controller design by MO and SO:

- The plant is exactly known.
- The system order of the plant should be $n \leq 3$.
- The plant is stable and non-oscillating, so the poles of the transfer function are real and negative.
- The transfer function of the plant exhibits a large time constants which is much higher compared to the smaller one.

Note: The exercises marked by a * should be solved as preparation.

1.) * What effect does the term "Integrator Windup" stand for in control theory? For which type of controller does it occur and what countermeasures can be taken to avoid it?

2.) * Write the transfer function of the DC machine F_{DCM} in the following form :

$$F_{DCM}(s) = \frac{\Omega_M(s)}{U_A(s)} = \frac{V_{DCM}}{1 + s\ T_M + s^2\ T_A\ T_M}$$

Insert the numerical values from table 2.1 and determine if the regarded motor fulfills the requirements for the controller design according to MO and SO? If the conditions are not satisfied, which action do you have to take to make the design by the MO or SO possible?

Hint: Solve for the poles of the transfer function.

3.) * How does the induced counter voltage (EMF) E_A affect the current control loop? To improve the dynamics of the current control it makes sense to compensate the influence of E_A. Suggest a simple method to compensate the EMF and extend the respective signal flow diagram from figure 2.2.

2.3.1 Controller Design

When designing the current controller it is assumed, that the effect of the EMF is completely compensated. Furthermore, the voltage saturation of the pulse converter is neglected.

Following requirements should hold for the current control loop:

- The current control loop is stable.
- The current controller is able to control stationary disturbances.
- The current control exhibits good command response behaviour.

4.) * Why is a good command response behaviour necessary for the current control loop?

5.) * Establish the transfer function between the **filtered** armature current $\hat{I}_A$ and the desired voltage U_A^*:

$$F_{\hat{I}_A}(s) = \frac{\hat{I}_A(s)}{U_A^*(s)} = \frac{V_{S,I_A}}{(1 + s\ T_{1,I_A})\ (1 + s\ T_{\sigma,I_A})} \tag{2.19}$$

Determine the smaller time constant T_{σ,I_A}, the larger time constant of the control system T_{1,I_A} and the amplification V_{S,I_A} as a function of the plant parameters. If necessary, merge time constants of similar magnitude.

6.) * With the help of the optimization table (see Fig. 2.6) design a current controller in accordance with the requirements of the current control loop.

2.3.2 Evaluation of the Control Performance

In the following section the properties of the **controlled** armature current loop are analyzed and evaluated by simulation.

7.) Open the model `DCM_Controller_Implementation.slx` in `Simulink`.
Add a first-order filter to smooth the measurement signals I_A^m, I_E^m and Ω_M^m, as described in section 2.2.3.
Implement your solution for the compensation of the induced voltage from problem 3.

Hint: To simplify the analysis, the dynamic behavior of the compensation block is neglected.

Open `PI_Controller.slx` and double click on the subsystem `PI-Controller`. Connect the provided blocks to create a PI-controller and save the result.
Insert an instance of the PI-controller in model `DCM_Controller_Implementation.slx` and use **symbolic variables** to express the parameters. Allocate the calculated values from problem 6 to the variables used in the file `Experiment_2_DCM_Parameter.m`.
Complete the current control loop. Complete the file `Experiment_2_DCM_Parameter.m` with the missing parameters. They get taken over by double-clicking on the `Initialize` block.

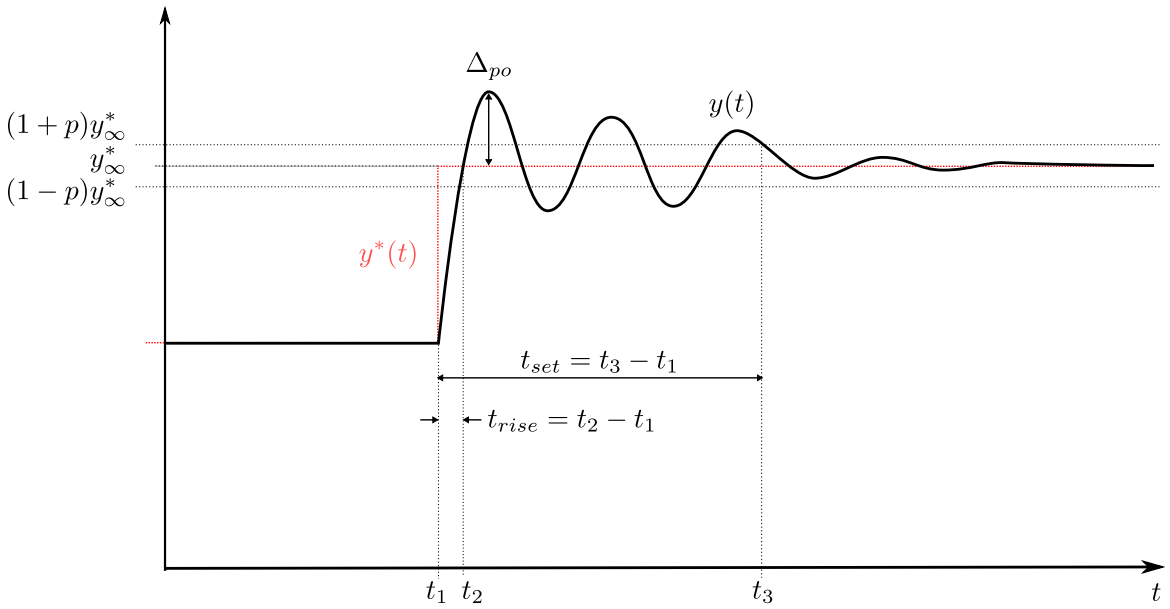

Figure 2.4: Characterization of the Control Performance of a Control Loop by its Step Response

8.) Check the current control loop for proper function by simulating and evaluating its response to the following current reference value:

$$I_A^*(t) = \frac{I_{AN}}{2}(\sigma(t - t_A) - \sigma(t - 2t_A)),\ t_A = 0.5\,[\text{s}] \tag{2.20}$$

with

$$\sigma(t) = \begin{cases} 0 & \text{for} \quad t \leq 0\,[\text{s}] \\ 1 & \text{for} \quad t > 0\,[\text{s}] \end{cases} \tag{2.21}$$

This means, that from $t_A = 0.5$ [s] onwards half of the nominal armature current $I_{AN}/2$ is applied for $0.5\,[\text{s}]$.

The quality of the control loop can be evaluated by analyzing the step response. For this purpose, at a point of time t_1, a step-wise change of the controlled variable y to a new target value y^*_∞ is considered (see Fig. 2.4). In this context, the following parameters are defined:

- Rise time t_{rise}: Time taken to reach the new target value y^*_∞ for the first time.
- Settling time t_{set}: Time elapsed from the application of a new target value to the time at which $y(t)$ has entered and remains within the specified tolerance band $2py^*_\infty$, so that

$$\forall t \geq t_1 + t_{set},\ |(y(t) - y^*_\infty)| < |py^*_\infty|$$

  In practice, $p \in [0.02; 0.05]$ is often chosen.
- Peak Overshoot Δ_{po}: Measure for the maximal occurring control error after the rise time has passed:

$$\Delta_{po} = \frac{1}{|y^*_\infty|}\left(\sup_{t \geq t_1 + t_{rise}} |y(t) - y^*_\infty|\right)$$

9.) Determine the rise time, settling time and the maximal overshoot for the tolerance band of $\pm 2\%$ for the previously simulated current response at the rising edge of the target value.
Compare your results with the specifications from the optimization table and explain the possible deviations.

10.) What effect does a failure of the EMF compensation have with respect to the armature current waveform?

2.4 Speed Control in the Armature Control Range

2.4.1 Controller Design

After optimizing the inner current control loop it is possible to design the speed controller. Here the following requirements have to be considered:

- The speed control loop is stable.
- The speed controller is able to control constant disturbances in steady-state.
- The speed control loop exhibits good disturbance rejection behaviour.

For simpler handling of the controller design, the inner current control loop is approximated as a first-order-delay-component (see Fig. 2.5). In this context, it is assumed that the influence of the EMF voltage induced in the armature winding is fully compensated. Furthermore, $\Psi_E = \Psi_{EN}$ holds true. The controller is again designed according to the Magnitude Optimum or the Symmetrical Optimum.

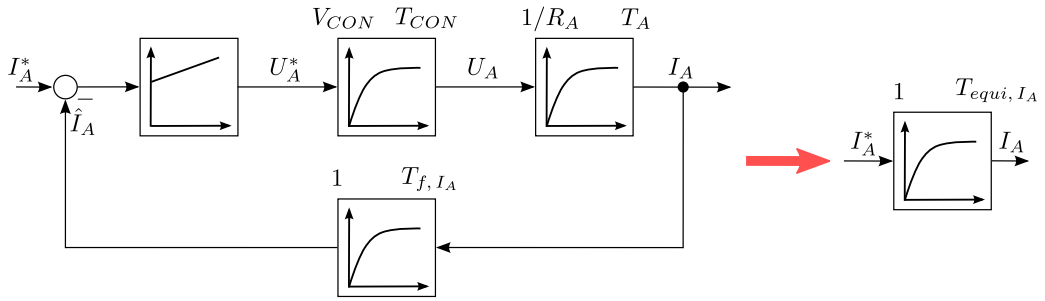

Figure 2.5: Approximation of the Current Control Loop as a First-Order-Delay-Component

11.) * Replace the current control circuit by an approximation of a PT1-block, as shown in figure 2.5. Firstly, bring the transfer function of the circuit into the following format:

$$F_{equi,I_A}(s) = \frac{1 + s\ T_{f,I_A}}{1 + s\ 2T_{\sigma,I_A} + s^2\ 2T_{\sigma,I_A}^2} \tag{2.22}$$

12.) * Then apply a polynomial division by the numerator. The transfer function can be approximated with the following $first-order-delay$ behavior and time constant T_{equi,I_A} by neglecting higher order terms:

$$F_{equi,I_A}(s) = \frac{I_A(s)}{I_A^*(s)} \approx \frac{1}{1 + s\ T_{equi,I_A}} \tag{2.23}$$

Express T_{equi,I_A} as a function of T_{σ,I_A} and T_{f,I_A}.

13.) * Taking into account the approximation made above, state the simplified transfer function between the set-point current value I_A^* and the **filtered** angular velocity Ω_M in the following form:

$$F_{\hat{\Omega}_M}(s) = \frac{\hat{\Omega}_M(s)}{I_A^*(s)} = \frac{V_{S,\Omega_M}}{s\ T_{1,\Omega_M}(1 + s\ T_{\sigma,\Omega_M})} \tag{2.24}$$

Give the expression for the small time constant T_{σ,Ω_M} as a function of T_{equi,I_A} and T_{f,Ω_M}. Determine the amplification V_{S,Ω_M}, so that:

$$T_{1,\Omega_M} = T_M = \frac{R_A\ \Theta_M}{(C_M\ \Psi_{EN})^2} \tag{2.25}$$

14.) * Design a controller, that fulfills the requirements of the speed control loop. Why is a good disturbance rejection necessary?

2.4.2 Evaluation of the Control Performance

The behavior of the speed control loop shall be validated in simulation.

15.) Extend your `Simulink`-model with the designed speed controller. Use an instance of the block `PI-Controller` from the file `PI_Controller.slx`. Add the control parameters in the file `Experiment_2_DCM_Parameter.m`.
Now test the speed control loop with the following speed waveform:

$$\Omega_M^*(t) = \frac{\Omega_{MN}}{2}\sigma(t - t_\Omega),\ t_\Omega = 0{,}5\ [\text{s}] \tag{2.26}$$

16.) Similar to the measurements of problem 9, the rise time, settling time and peak overshoot show some deviations to the optimization table. Explain where are they come from?

2.4.3 Improvement of the Control Properties

The previously designed controller exhibits a peak overshoot in the speed waveform that might be too high in many practical applications. Besides that, compliance with the maximum armature current from table 2.1 is not guaranteed.

17.) Firstly, a measure to reduce the overshoot is taken without changing the speed controller. Insert a first-order-delay-block to smooth the reference variable and adjust its time constant according to the optimization table (see Fig. 2.6).
Evaluate the speed waveform and check, if the armature current I_A stays in the permitted area for all times.

18.) For safe operation of the machine, the armature current is limited to the double of the nominal current, so $I_{A,limit} = 2I_{AN} = 2$ [A]. Hence, the speed controller is not allowed to demand current values, which are higher than the threshold value.
For that purpose, introduce a saturation block after the speed controller and re-simulate the response of the control loop.
Which differences can be detected in the speed waveform and by what effect are they generated?

19.) Remove the pre-filter from problem 17 and modify the inner structure of the speed controller. At this stage, make sure that previously detected problems are resolved and a satisfactory control performance of the speed in compliance with current saturation is achieved. If the result is not satisfying, explain what could be the reasons for that?
Then, evaluate the disturbance rejection behavior of the control loop by simulating the following load torque:

$$M_L(t) = M_{MN}\ \sigma(t - t_{M_L}),\ t_{M_L} = 1\ [\text{s}] \tag{2.27}$$

20.) Replace the block `DC_Drive` by `DC_Drive_2`, that you can find in the model with the same name and run the simulation.
Compare the results with the ones from the previous problem and explain the differences.

21.) Apply the following set-point course Ω_M^*:

$$\Omega_M^*(t) = 1{,}1\ \Omega_{MN}\ \sigma(t - t_\Omega),\ t_\Omega = 0.5\ [\text{s}] \tag{2.28}$$

Analyze the characteristics of the velocity Ω_M, the current reference value I_A^* and the resulting armature current I_A without load. If there are deviations from the desired behavior, suggest a method to eliminate them.

Optimierungstabelle

	Strecke			Regler					Verhalten bei Sprung der Führungsgröße w					Störgröße z	
Nr.	Typ	G'_S	Günstiger Bereich	Typ	G_R	Opt. Krit.	Einstellung T_R, T_n, T_v	Einstellung V_R	Einstellung $\frac{T_G}{T_\sigma}$	$\frac{t_{an}}{T_\sigma}$	$\frac{t_{ans}}{T_\sigma}(\pm 2\%)$	$\frac{x'_{max}}{w'_0}$	$\frac{x'_\infty}{w'_0}$	$\frac{T_{ers}}{T_\sigma}$	$\frac{t_{an}}{T_\sigma}$	$\frac{1}{V_S}\frac{x'_{max}}{z'_0}$	$\frac{1}{V_S}\frac{x'_\infty}{z'_0}$
1	PT_1	$\frac{V_S}{1+sT_\sigma}$	$T_\sigma = T_1 + T_2 + \ldots$	I	$\frac{V_R}{sT_n} = \frac{1}{sT_R}$	BO	$T_R = 2V_S T_\sigma$	$\frac{T_n}{2T_\sigma V_S}$	—	4.7	8.4	1.04	1	2	6.3	0.64	0
2	PT_2	$\frac{V_S}{(1+sT_1)(1+sT_\sigma)}$	$\frac{T_1}{T_\sigma} \gg 1$	P	V_R	BO	—	$\frac{T_1}{2T_\sigma V_S}$	—	(4.7)	(8.4)	$1.04\frac{x'_\infty}{w'_0}$	$\frac{V_R V_S}{1+V_R V_S}$	2	(4.7)	$\approx \frac{1}{1+V_R V_S}$	$\frac{1}{1+V_R V_S}$
3			$\frac{T_1}{T_\sigma} = 1..$	PI	$V_R\frac{1+sT_n}{sT_n}$	BO	$T_n = T_1$	$\frac{T_1}{2T_\sigma V_S}$	—	4.7	8.4	1.04	1	2	$5.5\sqrt{\frac{T_1}{T_\sigma}}$	$\frac{0.5..1.2}{T_1/T_\sigma}$	0
4			$\frac{T_1}{T_\sigma} \geq 4$	PI	$V_R\frac{1+sT_n}{sT_n}$	SO	$T_n = 4T_\sigma$	$\frac{T_1}{2T_\sigma V_S}$	—	4.7..3.1	8.4..16.5	1.04..1.43	1	—	≈ 10	$\frac{1.2..1.6}{T_1/T_\sigma}$	0
									0..4	4.7..7.6	8.4..13.3	1.04..1.08	1	2..4			
5	PT_3	$\frac{V_S}{(1+sT_1)(1+sT_2)(1+sT_\sigma)}$ $T_2 > T_\sigma$	$\frac{T_1}{T_\sigma} \gg 1$	PD	$V_R(1+sT_v)$	BO	$T_v = T_2$	$\frac{T_1}{2T_\sigma V_S}$	—	(4.7)	(8.4)	$(1.04\frac{x'_\infty}{w'_0})$	$\frac{V_R V_S}{1+V_R V_S}$	2	$4 + \frac{T_2}{T_\sigma}$	$\approx \frac{1}{1+V_R V_S}$	$\frac{1}{1+V_R V_S}$
6			$\frac{T_1}{T_\sigma} = 1..$	PID	$V_R\frac{(1+sT_n)(1+sT_v)}{sT_n}$	BO	$T_n = T_1$ $T_v = T_2$	$\frac{T_1}{2T_\sigma V_S}$	—	4.7	8.4	1.04	1	2	$4.4\sqrt{\frac{T_1 T_2}{T_\sigma^2}}$	$\frac{0.5..0.75}{\sqrt{\frac{T_1}{T_\sigma}}\sqrt{\frac{T_2}{T_\sigma}}}$	0
7			$\frac{T_1}{T_\sigma} \geq 4$	PID	$V_R\frac{(1+sT_n)(1+sT_v)}{sT_n}$	SO	$T_n = 4T_\sigma$ $T_v = T_2$	$\frac{T_1}{2T_\sigma V_S}$	—	4.7..3.1	8.4..16.5	1.04..1.43	1	—	$\approx 10^4\sqrt{\frac{T_2}{T_\sigma}}$	$\frac{1.4..1.8}{\frac{T_1}{T_\sigma}\sqrt{\frac{T_2}{T_\sigma}}}$	0
									0.4	4.7..7.6	8.4..13.3	1.04..1.08	1	2..4			
8	IT_1	$\frac{V_S}{sT_1(1+sT_\sigma)}$	$\frac{T_1}{V_S T_\sigma} \gg 1$	P	V_R	BO	—	$\frac{T_1}{2T_\sigma V_S}$	—	4.7	8.4	1.04	1	2	(4.7)	$\approx \frac{1}{V_R V_S}$	$\frac{1}{V_R V_S}$
9			$\frac{T_1}{V_S T_\sigma} > 0$	PI	$V_R\frac{1+sT_n}{sT_n}$	SO	$T_n = 4T_\sigma$	$\frac{T_1}{2T_\sigma V_S}$	—	3.1	16.5	1.43	1	—	10	$\frac{1.6}{T_1/T_\sigma}$	0
									4	7.6	13.3	1.08	1	4			
10	IT_2	$\frac{V_S}{sT_1(1+sT_2)(1+sT_\sigma)}$ $T_2 > T_\sigma$	$\frac{T_1}{V_S T_\sigma} \gg 1$	PD	$V_R(1+sT_v)$	BO	$T_v = T_2$	$\frac{T_1}{2T_\sigma V_S}$	—	4.7	8.4	1.04	1	2	$4 + \frac{T_2}{T_\sigma}$	$\approx \frac{1}{V_R V_S}$	$\frac{1}{V_R V_S}$
11			$\frac{T_1}{V_S T_\sigma} > 0$	PID	$V_R\frac{(1+sT_n)(1+sT_v)}{sT_n}$	SO	$T_n = 4T_\sigma$ $T_v = T_2$	$\frac{T_1}{2T_\sigma V_S}$	—	3.1	16.5	1.43	1	—	$\approx 10^4\sqrt{\frac{T_2}{T_\sigma}}$	$\frac{1.8}{\frac{T_1}{T_\sigma}\sqrt{\frac{T_2}{T_\sigma}}}$	0
									4	7.6	13.3	1.08	1	4			

Figure 2.6: Controller Design According to MO and SO: Optimization Table [4, Table 1.3]

Experiment 3
Model of the AC Machine

3.1 Overview

Subject of experiments 3 to 5 is the *Controlled AC drive*. Advantages compared to DC drive are low maintenance effort and a simple structure, due to elimination of the commutator. For this reason that machine type is more attractive for industrial applications.
This practical course considers the three-phase-machine to be fed by *two-level converters* (compare to Fig. 1). The two most popular machine types are the squirrel cage *asynchronous machine* and the permanent magnet *synchronous machine*. They are abbreviated to ASM and SM and their models will be derived in this chapter. Experiments 4 and 5 focus on two common control strategies for AC machines.

3.2 Fundamental Wave Model of AC Machines

3.2.1 Structure of the AC Machine

Figure 3.1 depicts the simplified structure of an AC machine. The stator consists of the coils A, B, C whereas the rotor holds the coils U, V, W. The following relations apply for the machines:

- Stator and rotor are built symmetrically.
- The coils of stator and rotor are wound symmetrically. They are displaced by 2/3 of the *pole pitch* τ_p, that means by 2/3 of the half of the spatial period of the magnetomotive force fundamental wave. The stator coils have n_s windings respectively the rotor coils have n_r windings.
- Both winding sets are connected to a star-point that is free of potential.

To determine the rotor position, the mechanical angle θ_m is defined (see Fig. 3.1). The electrical angle θ_e as well as its time derivative, the electrical speed ω_e, are related to the mechanical angle respectively the speed by the pole pair number p.

$$\begin{aligned} \theta_e &= p\ \theta_m \\ \omega_e &= p\ \omega_m \end{aligned} \tag{3.1}$$

For simplicity reasons, but without loss of generality, the number of pole pairs p is set to 1 in the experiments. Hence the coils are displayed by 120° to each other and the mechanical angle is equal to the electrical angle.

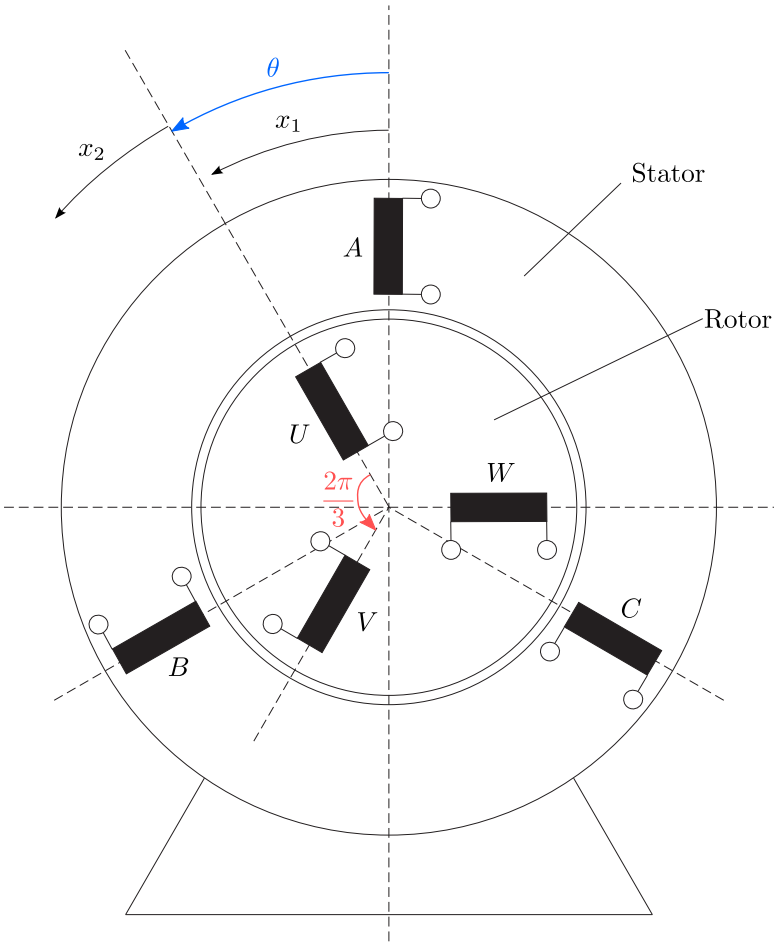

Figure 3.1: Principle Structure of an AC Machine
x_1: Coordinates with Respect to the Stator;
x_2: Coordinates with Respect to the Rotor;
θ_m: Angle between the Axes of the Coils A and U

3.2.2 Assumptions for the Fundamental Wave Model

Similar to the DC machine the electromagnetic, mechanical and thermal processes inside the AC machine are in general complex and non-linear. For this reason following assumptions are made for the fundamental wave model:

- The spatial distribution of the magneto-motive force and the magnetic field in the air gap are assumed to be sinusoidal. Hence the name fundamental wave model. In reality there are harmonic waves of higher orders. Even though some measures (choice of slot number and distribution of windings) are taken to reduce them, they are caused by the discrete position of the stator/rotor slots and windings and hence can't be suppressed completely.
- The magnetic flux has no axial component. Only the cross-sectional area (2D) is considered.
- The magnetic material exhibits linear properties. The effects of magnetic saturation and hysteresis are neglected.
- Only ohmic losses are considered. Eddy currents are neglected.
- The influence of temperature onto the resistance and the inductance are neglected.
- The coils are symmetrical, that means all of them have identical properties.

3.2.3 Electrical Differential Equations

Similar to the DC machine the electrical equivalent circuit diagram can be drawn (Fig.3.2). The general electrical differential equation for the AC machine is described by:

$$u_k = R_l \; i_k + \frac{\mathrm{d}\Psi_k}{\mathrm{d}t} \tag{3.2}$$

Where the index k stands for the coils ($k \in \{A,\, B,\, C,\, U,\, V,\, W\}$) as introduced in the previous section 3.2.1. The rotor and stator are distinguished by the index ($l \in \{1,\, 2\}$).

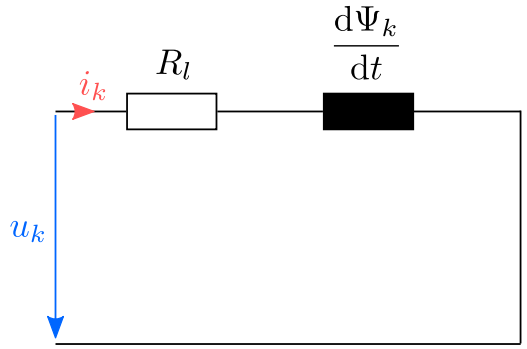

Figure 3.2: Definition of the Phase Values ($k \in \{A,\, B,\, C,\, U,\, V,\, W\}$, $l \in \{1,\, 2\}$)

If for example the indexes A and 1 are inserted the stator voltage equation is:

$$u_A = R_1 \; i_A + \frac{\mathrm{d}\Psi_A}{\mathrm{d}t} \tag{3.3}$$

Similar equations holds with the other coils and at the rotor side. This geometrical distributed physical parameters can therefore be described by a matrix notation:

$$\underline{u}_1 = \begin{bmatrix} u_A & u_B & u_C \end{bmatrix}^\top \qquad \underline{u}_2 = \begin{bmatrix} u_U & u_V & u_W \end{bmatrix}^\top$$
$$\underline{i}_1 = \begin{bmatrix} i_A & i_B & i_C \end{bmatrix}^\top \qquad \underline{i}_2 = \begin{bmatrix} i_U & i_V & i_W \end{bmatrix}^\top$$
$$\underline{\Psi}_1 = \begin{bmatrix} \Psi_A & \Psi_B & \Psi_C \end{bmatrix}^\top \qquad \underline{\Psi}_2 = \begin{bmatrix} \Psi_U & \Psi_V & \Psi_W \end{bmatrix}^\top$$

Then the basic voltage differential equations of the stator and the rotor can be simplified by the matrix notation to:

$$\underline{u}_1 = R_1 \; \underline{i}_1 + \frac{\mathrm{d}\underline{\Psi}_1}{\mathrm{d}t} \tag{3.4}$$

$$\underline{u}_2 = R_2 \; \underline{i}_2 + \frac{\mathrm{d}\underline{\Psi}_2}{\mathrm{d}t} \tag{3.5}$$

3.3 Magnetic Relations

3.3.1 Flux linkages of the individual windings

To obtain closed-form relationships, the flux linkages of the individual phases are analyzed in more detail below. In general, it is assumed that all six phases are magnetically coupled with each other.
Assuming linear magnetic conditions, the flux linkage of phase A, Ψ_A, is composed of six components:

$$\Psi_A = \underbrace{\Psi_{AA}}_{\text{I}} + \underbrace{\Psi_{AB} + \Psi_{AC}}_{\text{II}} + \underbrace{\Psi_{AU} + \Psi_{AV} + \Psi_{AW}}_{\text{III}} \tag{3.6}$$

In addition to the self-linkage expressed by term I, components II and III respectively represent the coupling with the other stator-side phases and the rotor-side coils.
As a result of the assumed magnetic linearity, each component of Ψ_A can be easily expressed in terms of the phase currents. For this purpose, inductances L_{Ak}, with $k \in \{A, B, C, U, V, W\}$, are introduced, which are independent of the magnetic state of the machine:

$$\Psi_A = L_{AA} \cdot i_A + L_{AB} \cdot i_B + L_{AC} \cdot i_C + L_{AU}(\theta) \cdot i_U + L_{AV}(\theta) \cdot i_V + L_{AW}(\theta) \cdot i_W \tag{3.7}$$

However, it must be noted that the coupling between phase A and the rotor windings depends on the rotor angle θ, so the inductances L_{AU}, L_{AV}, and L_{AW} are also functions of θ.

The flux linkages of the other phases can be determined analogously. This yields the following relationships between the vectors $\vec{\Psi}_1$ and $\vec{i}_1$, and $\vec{\Psi}_2$ and $\vec{i}_2$, respectively:

$$\vec{\Psi}_1 = \mathbf{L}_1 \cdot \vec{i}_1 + \mathbf{L}_{12}(\theta) \cdot \vec{i}_2 \tag{3.8}$$

$$\vec{\Psi}_2 = \mathbf{L}_2 \cdot \vec{i}_2 + \mathbf{L}_{21}(\theta) \cdot \vec{i}_1 \tag{3.9}$$

The resulting inductance matrices are defined as follows:

$$\mathbf{L}_1 = \begin{bmatrix} L_{AA} & L_{AB} & L_{AC} \\ L_{BA} & L_{BB} & L_{BC} \\ L_{CA} & L_{CB} & L_{CC} \end{bmatrix} \qquad \mathbf{L}_2 = \begin{bmatrix} L_{UU} & L_{UV} & L_{UW} \\ L_{VU} & L_{VV} & L_{VW} \\ L_{WU} & L_{WV} & L_{WW} \end{bmatrix}$$

$$\mathbf{L}_{12}(\theta) = \begin{bmatrix} L_{AU}(\theta) & L_{AV}(\theta) & L_{AW}(\theta) \\ L_{BU}(\theta) & L_{BV}(\theta) & L_{BW}(\theta) \\ L_{CU}(\theta) & L_{CV}(\theta) & L_{CW}(\theta) \end{bmatrix} \qquad \mathbf{L}_{21}(\theta) = \begin{bmatrix} L_{UA}(\theta) & L_{UB}(\theta) & L_{UC}(\theta) \\ L_{VA}(\theta) & L_{VB}(\theta) & L_{VC}(\theta) \\ L_{WA}(\theta) & L_{WB}(\theta) & L_{WC}(\theta) \end{bmatrix}$$

The matrices $\mathbf{L}_1$ and $\mathbf{L}_2$ describe the magnetic coupling between the phases within the stator-side and rotor-side winding sets, respectively. The matrices $\mathbf{L}_{12}(\theta)$ and $\mathbf{L}_{21}(\theta)$ represent the interactions between the two winding sets.

3.3.2 Self-inductances of the phases on the stator and rotor sides

The self-inductances of the stator-side and rotor-side winding sets are respectively represented by the diagonal elements of the matrices $\mathbf{L}_1$ and $\mathbf{L}_2$. These will be described in more detail below.

Stator-Side Winding Set

If, for example, phase A on the stator is energized by the current i_A, a magnetic field distribution is generated, which largely closes through the air gap and the rotor. This part of the field is therefore linked with the coils of all phases on both the stator and rotor sides and is referred to as the *air-gap field*. The remaining portion, known as the *leakage field*, is linked exclusively with the conductors of phase A. The resulting magnetic flux Φ_A, which penetrates the windings of phase A, can thus be divided into two components: A main flux component Φ_{hA} and a leakage flux component $\Phi_{\sigma A}$. This yields the relation: $\Phi_A = \Phi_{hA} + \Phi_{\sigma A}$. We assume that all turns of the distributed phase winding are penetrated by the same flux Φ_A. If the *reluctances* (magnetic resistances) R_{mhA} and $R_{m\sigma A}$ are assigned to the main and leakage flux paths respectively, the following relationships can be derived from Hopkinson's law:

$$\Phi_{hA} = \frac{n_1 \cdot i_A}{R_{mhA}} \tag{3.10}$$

$$\Phi_{\sigma A} = \frac{n_1 \cdot i_A}{R_{m\sigma A}} \tag{3.11}$$

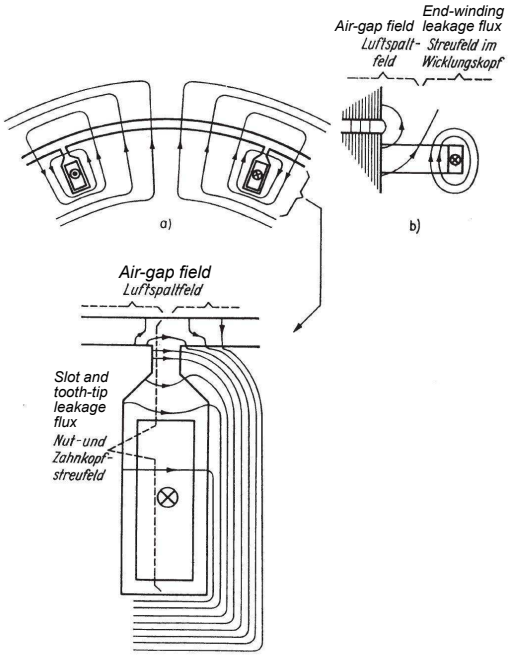

Figure 3.3: Division of a winding's magnetic field into air-gap field and leakage field [2, p. 235]
(a) Division in the cross-sectional view; (b) Division in the longitudinal section

For the flux linkage of phase A, the following applies:

$$\Psi_A = n_1 \cdot \Phi_A = \frac{n_1^2}{R_{mhA}} \cdot i_A + \frac{n_1^2}{R_{m\sigma A}} \cdot i_A \tag{3.12}$$

From equation (3.12), the main inductance L_{hA} and the leakage inductance $L_{\sigma A}$ of phase A can be defined:

$$L_{hA} = \frac{n_1^2}{R_{mhA}} \tag{3.13}$$

$$L_{\sigma A} = \frac{n_1^2}{R_{m\sigma A}} \tag{3.14}$$

The self-inductance of phase A then results, according to equation (3.12), as:

$$L_{AA} = L_{hA} + L_{\sigma A} \tag{3.15}$$

Due to the symmetrical structure of the machine and the previously assumed design features of the stator-side winding set, the same applies to phases B and C:

$$R_{mhB} = R_{mhC} = R_{mhA} = R_{mh} \tag{3.16}$$

$$R_{m\sigma B} = R_{m\sigma C} = R_{m\sigma A} = R_{m\sigma 1} \tag{3.17}$$

The inductances are then given by:

$$L_{hB} = L_{hC} = L_{hA} = L_{h1} = \frac{n_1^2}{R_{mh}} \tag{3.18}$$

$$L_{\sigma B} = L_{\sigma C} = L_{\sigma A} = L_{\sigma 1} = \frac{n_1^2}{R_{m\sigma 1}} \tag{3.19}$$

$$L_{BB} = L_{CC} = L_{AA} = L_{h1} + L_{\sigma 1} \tag{3.20}$$

Here, L_{h1} and $L_{\sigma 1}$ represent the main and leakage inductances of the stator-side winding set respectively.

Rotor-Side Winding Set

The self-inductances L_{UU}, L_{VV}, and L_{WW} of the windings mounted on the rotor can be calculated analogously. In this case, the leakage component of the magnetic flux is assigned to the reluctance $R_{m\sigma 2}$. Furthermore, it is assumed—analogous to the stator side—that the main flux component is related to the current via the magnetic reluctance R_{mh} . This leads to the following result:

$$L_{h2} = L_{hU} = L_{hV} = L_{hW} = \frac{n_2^2}{R_{mh}} \tag{3.21}$$

$$L_{\sigma 2} = L_{\sigma U} = L_{\sigma V} = L_{\sigma W} = \frac{n_2^2}{R_{m\sigma 2}} \tag{3.22}$$

$$L_{UU} = L_{VV} = L_{WW} = L_{h2} + L_{\sigma 2} \tag{3.23}$$

3.3.3 Mutual Inductances Between the Phases of a Winding Set

This section investigates the mutual terms in the matrices L_1 and L_2 , which describe the magnetic coupling between the phases within a single winding set.

Stator-Side Winding Set

It is assumed that the magnetic coupling between the phases of a winding set occurs via the air-gap field and, thus, through the magnetic reluctance R_{mh}.
If a positive current i_A flows through the windings of phase A, the assumptions stated in Section 3.2.2 lead to a sinusoidal distribution of the radial component of the air-gap field along the circumferential coordinate x_1. This component, denoted as B_r, exhibits a spatial periodicity equal to twice the pole pitch τ_p, and reaches its maximum value $\hat{B}_r$ along the axis of phase A, i.e., at $x_1 = 0$:

$$B_r = \hat{B}_r \cdot \cos\left(\frac{\pi}{\tau_p} x_1\right) \tag{3.24}$$

The winding axes of phases B and C are shifted by 2/3 and 4/3 of the pole pitch τ_p respectively, relative to the axis of phase A. At these respective positions, the radial component of the air-gap field originating from current i_A amounts to -1/2 , thereby inducing a negative flux through

the windings of phases B and C. Therefore, the following relationship holds:

$$L_{AB} = L_{AC} = -\frac{n_1^2}{2 \cdot R_{mh}} = -\frac{L_{h1}}{2} \tag{3.25}$$

The derivation of the remaining coefficients of the matrix $\mathbf{L}_1$ proceeds in a similar manner, leading to the following result:

$$\mathbf{L}_1 = \begin{bmatrix} L_{h1} + L_{\sigma 1} & -\frac{L_{h1}}{2} & -\frac{L_{h1}}{2} \\ -\frac{L_{h1}}{2} & L_{h1} + L_{\sigma 1} & -\frac{L_{h1}}{2} \\ -\frac{L_{h1}}{2} & -\frac{L_{h1}}{2} & L_{h1} + L_{\sigma 1} \end{bmatrix} \tag{3.26}$$

Rotor-Side Winding Set

Similar relationships hold for the rotor-side winding set, the matrix $\mathbf{L}_2$ takes on the following form:

$$\mathbf{L}_2 = \begin{bmatrix} L_{h2} + L_{\sigma 2} & -\frac{L_{h2}}{2} & -\frac{L_{h2}}{2} \\ -\frac{L_{h2}}{2} & L_{h2} + L_{\sigma 2} & -\frac{L_{h2}}{2} \\ -\frac{L_{h2}}{2} & -\frac{L_{h2}}{2} & L_{h2} + L_{\sigma 2} \end{bmatrix} \tag{3.27}$$

$\mathbf{L}_1$ and $\mathbf{L}_2$ are symmetric and therefore satisfy the reciprocity condition for magnetically coupled circuits.

3.3.4 Mutual Inductances Between Both Winding Sets

The approach described above can, in principle, be applied to determine the coefficients of the matrices $\mathbf{L}_{12}(\theta)$ and $\mathbf{L}_{21}(\theta)$. Howeve, in this case, it must be noted that the stator and rotor phases have different numbers of turns and that their relative position is defined by the angle θ. Moreover, the two winding sets are coupled exclusively via the air-gap field.
The resulting relationships will be derived below using the example of phases A and U. For this purpose, it is assumed that the current i_A generates a radial field distribution according to Eq. (3.24). In the special case where the axes of phases A and U are aligned, i.e., $\theta = 0$, the inductance $\mathbf{L}_{AU}$ reaches its maximum value:

$$L_{AU}(0) = \frac{n_1 \cdot n_2}{R_{mh}} = \frac{n_2}{n_1} L_{h1} \tag{3.28}$$

For an arbitrary angle θ, determining the magnetic flux through the windings of phase U caused by i_A also requires considering the radial field distribution described in Eq. (3.24). Based on

the analysis presented in Section 3.3.3, the following relation can be derived:

$$L_{AU}(\theta) = \frac{n_2}{n_1} L_{h1} \cdot \cos\theta \tag{3.29}$$

The derivation of the remaining coefficients of the matrix $\mathbf{L}_{12}(\theta)$ is carried out analogously, taking into account the shift of 2/3 of the pole pitch between the individual phases of a winding set. The resulting form of the matrix $\mathbf{L}_{12}(\theta)$ is:

$$\mathbf{L}_{12}(\theta) = \frac{n_2}{n_1} L_{h1} \begin{bmatrix} \cos\theta & \cos\left(\theta + \frac{2\pi}{3}\right) & \cos\left(\theta - \frac{2\pi}{3}\right) \\ \cos\left(\theta - \frac{2\pi}{3}\right) & \cos\theta & \cos\left(\theta + \frac{2\pi}{3}\right) \\ \cos\left(\theta + \frac{2\pi}{3}\right) & \cos\left(\theta - \frac{2\pi}{3}\right) & \cos\theta \end{bmatrix} \tag{3.30}$$

The coefficients of the matrix $\mathbf{L}_{21}(\theta)$ can be derived in a similar manner, leading to:

$$\mathbf{L}_{21}(\theta) = \frac{n_2}{n_1} L_{h1} \begin{bmatrix} \cos\theta & \cos\left(\theta - \frac{2\pi}{3}\right) & \cos\left(\theta + \frac{2\pi}{3}\right) \\ \cos\left(\theta + \frac{2\pi}{3}\right) & \cos\theta & \cos\left(\theta - \frac{2\pi}{3}\right) \\ \cos\left(\theta - \frac{2\pi}{3}\right) & \cos\left(\theta + \frac{2\pi}{3}\right) & \cos\theta \end{bmatrix} \tag{3.31}$$

It therefore follows that:

$$\mathbf{L}_{21}(\theta) = \mathbf{L}_{12}^{\top}(\theta) \tag{3.32}$$

3.4 Space Vector Representation

3.4.1 Fundamental Considerations

Equations (3.4) and (3.5), as well as (3.8) and (3.9), model the fundamental wave behavior of a rotating field machine and constitute a coupled system of six linear differential equations:

$$\vec{u}_1 = R_1 \cdot \vec{i}_1 + \mathbf{L}_1 \frac{\mathrm{d}\vec{i}_1}{\mathrm{d}t} + \mathbf{L}_{12}(\theta) \frac{\mathrm{d}\vec{i}_2}{\mathrm{d}t} + \frac{\partial \mathbf{L}_{12}(\theta)}{\partial\theta} \frac{\mathrm{d}\theta}{\mathrm{d}t} \vec{i}_2 \tag{3.33a}$$

$$\vec{u}_2 = R_2 \cdot \vec{i}_2 + \mathbf{L}_2 \frac{\mathrm{d}\vec{i}_2}{\mathrm{d}t} + \mathbf{L}_{21}(\theta) \frac{\mathrm{d}\vec{i}_1}{\mathrm{d}t} + \frac{\partial \mathbf{L}_{21}(\theta)}{\partial\theta} \frac{\mathrm{d}\theta}{\mathrm{d}t} \vec{i}_1 \tag{3.33b}$$

At this point, it is reasonable to explore potential simplifications of the differential equation system. To this end, the spatial relationships within the machine's cross-section are examined in the following, assuming that only the stator-side winding set is present (Fig.3.4).The vectors $\vec{e}_A$, $\vec{e}_B$, and $\vec{e}_C$ shown in Fig.3.4 represent unit vectors along the winding axes of phases A, B, and C. The basis $(\vec{e}_\alpha, , \vec{e}_\beta)$ defines a Cartesian coordinate system, with the assumption that $\vec{e}_A = \vec{e}_\alpha$. This coordinate system is thus referred to as the stator reference frame or (α, β)

coordinate system. The position of a point in the air gap is described by the circumferential coordinate x_1 or the angle φ.

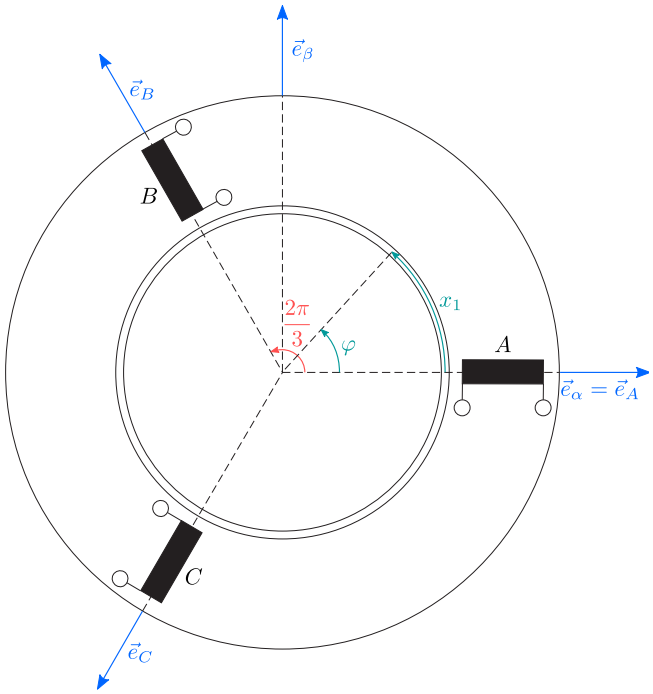

Figure 3.4: Schematic Representation of the Stator Winding Definitions in Cross Section View

As derived from (3.24), a current i_A flowing through phase A produces a sinusoidal distribution of magnetomotive force (MMF), or equivalently, a sinusoidal radial field component in the air gap, which reaches its maximum along the winding axis of phase A. It is well known that the resulting MMF ϑ_A is proportional to i_A, thus:

$$\exists\, \beta \in \mathbb{R}_+^*,\ \vartheta_A = \beta \cdot i_A \cdot \cos\varphi \tag{3.34}$$

A similar relationship holds for the MMFs generated by the currents in phases B and C:

$$\vartheta_B = \beta \cdot i_B \cdot \cos\left(\varphi - 2\pi/3\right) \tag{3.35}$$
$$\vartheta_C = \beta \cdot i_C \cdot \cos\left(\varphi + 2\pi/3\right) \tag{3.36}$$

Under the assumptions made in Section 3.2.2, particularly the assumption of linear magnetic conditions, the total MMF distribution ϑ at a given time t_0 —resulting from the individual currents $i_A(t_0)$, $i_B(t_0)$ and $i_C(t_0)$—can be expressed as the sum of the individual MMF distributions ϑ_A, ϑ_B and ϑ_C:

$$\vartheta(t_0) = \beta \left(i_A(t_0) \cdot \cos\varphi + i_B(t_0) \cdot \cos\left(\varphi - \frac{2\pi}{3}\right) + i_C(t_0) \cdot \cos\left(\varphi + \frac{2\pi}{3}\right) \right) \tag{3.37}$$

The total MMF distribution $\vartheta(t_0)$, or equivalently, the radial field component $B_r(t_0)$ also exhibits a spatial period of 2π. The amplitude of $\vartheta(t_0)$ reaches its maximum when the following

condition is satisfied:

$$\frac{\mathrm{d}\vartheta(t_0)}{\mathrm{d}\varphi} = 0 \tag{3.38}$$

From equations (3.37) and (3.38), the angle φ_0 at which the MMF $\vartheta(t_0)$ reaches its extreme can be determined as:

$$\cos\varphi_0 \cdot \frac{\sqrt{3}}{2}(i_B - i_C) - \sin\varphi_0 \cdot \left(i_A - \frac{1}{2}(i_B + i_C)\right) = 0 \tag{3.39}$$

This can be expressed as:

$$\left\| \begin{bmatrix} \cos\varphi_0 \\ \sin\varphi_0 \end{bmatrix} \times \begin{bmatrix} i_A - \frac{1}{2}(i_B + i_C) \\ \frac{\sqrt{3}}{2}(i_B - i_C) \end{bmatrix} \right\| = 0 \tag{3.40}$$

From equation (3.40), it can be deduced that the vector

$$\begin{aligned} \underline{i}_1^s &= \begin{bmatrix} i_A - \frac{1}{2}(i_B + i_C) \\ \frac{\sqrt{3}}{2}(i_B - i_C) \end{bmatrix} = i_\alpha \cdot \vec{e}_\alpha + i_\beta \cdot \vec{e}_\beta \\ &= i_A \cdot \begin{bmatrix} 1 \\ 0 \end{bmatrix} + i_B \cdot \begin{bmatrix} \cos(2\pi/3) \\ \sin(2\pi/3) \end{bmatrix} + i_C \cdot \begin{bmatrix} \cos(-2\pi/3) \\ \sin(-2\pi/3) \end{bmatrix} \\ &= i_A \cdot \vec{e}_A + i_B \cdot \vec{e}_B + i_C \cdot \vec{e}_C \end{aligned}$$

determines the points in the air gap at which the magnitude of the MMF is maximal. Consequently, knowledge of the two components i_α and i_β is sufficient to fully describe the spatial distribution of the MMF, and thus the field distribution in the air gap, at any given time t_0. The quantity $\underline{i}_1^s$ is referred to as the stator current space vector. Here, the superscript s indicates that the quantity is expressed in the stator reference frame.

3.4.2 The Clarke Transformation

The previous considerations can be generalized by introducing the following transformation:

$$\begin{aligned} \mathcal{T}_\mathcal{C}: \quad \mathbb{R}^3 &\longrightarrow \mathbb{R}^3 \\ \vec{x} = \begin{bmatrix} x_A \\ x_B \\ x_C \end{bmatrix} &\longmapsto \mathcal{T}_\mathcal{C}(\vec{x}) = \underline{x}^s = \begin{bmatrix} x_\alpha \\ x_\beta \\ x_0 \end{bmatrix} = \mathbf{T_C} \begin{bmatrix} x_A \\ x_B \\ x_C \end{bmatrix} \end{aligned} \tag{3.41}$$

The corresponding transformation matrix $\mathbf{T_C}$ is referred to as the Clarke transformation $\mathcal{T}_\mathcal{C}$:

$$\mathbf{T_C} = \frac{2}{3}\begin{bmatrix} \cos(0) & \cos\left(\frac{2\pi}{3}\right) & \cos\left(-\frac{2\pi}{3}\right) \\ \sin(0) & \sin\left(\frac{2\pi}{3}\right) & \sin\left(-\frac{2\pi}{3}\right) \\ \frac{1}{2} & \frac{1}{2} & \frac{1}{2} \end{bmatrix} = \frac{2}{3}\begin{bmatrix} 1 & -\frac{1}{2} & -\frac{1}{2} \\ 0 & \frac{\sqrt{3}}{2} & -\frac{\sqrt{3}}{2} \\ \frac{1}{2} & \frac{1}{2} & \frac{1}{2} \end{bmatrix} \tag{3.42}$$

This transformation enables the mapping of the phase quantities, which are combined into the vector $\vec{x}$, to a space vector $\underline{x}^s$ in the general case. For example, when $\mathcal{T}_\mathcal{C}$ is applied to the current vector $\vec{i}_1 = \begin{bmatrix} i_A & i_B & i_C \end{bmatrix}^\top$, the resulting stator current space vector $\underline{i}_1^s$ is obtained:

$$\underline{i}_1^s = \mathcal{T}_\mathcal{C}(\vec{i}_1) = \mathbf{T_C}\vec{i}_1 = \frac{2}{3}\begin{bmatrix} i_A - \frac{1}{2}(i_B + i_C) \\ \frac{\sqrt{3}}{2}(i_B - i_C) \\ \frac{1}{2}(i_A + i_B + i_C) \end{bmatrix} \tag{3.43}$$

The first two rows of the column vector in (3.43) correspond to the previously derived expression for $\underline{i}_1^s$. The third row represents the average of the phase quantities at the considered time and is referred to as the zero-sequence component. The factor 2/3 normalizes the space vector with respect to the amplitude of the phase quantities.
It can be easily shown that the matrix $\mathbf{T_C}$ is non-singular, thus allowing for the inverse transformation of the space vector $\underline{x}^s$ back to the corresponding phase quantities. This inverse transformation is given by:

$$\begin{aligned} \mathcal{T}_\mathcal{C}^{-1}: \quad \mathbb{R}^3 &\longrightarrow \mathbb{R}^3 \\ \underline{x}^s = \begin{bmatrix} x_\alpha \\ x_\beta \\ x_0 \end{bmatrix} &\longmapsto \mathcal{T}_\mathcal{C}^{-1}(\underline{x}^s) = \vec{x} = \begin{bmatrix} x_A \\ x_B \\ x_C \end{bmatrix} = \mathbf{T_C}^{-1}\begin{bmatrix} x_\alpha \\ x_\beta \\ x_0 \end{bmatrix} \end{aligned} \tag{3.44}$$

with

$$\mathbf{T_C}^{-1} = \begin{bmatrix} 1 & 0 & 1 \\ -\frac{1}{2} & \frac{\sqrt{3}}{2} & 1 \\ -\frac{1}{2} & -\frac{\sqrt{3}}{2} & 1 \end{bmatrix} \tag{3.45}$$

At this point, it should be noted that both the vector of combined phase quantities $\vec{x}$ and the space vector $\underline{x}^s$ are, from a mathematical perspective, three-dimensional vectors. Consequently, the Clarke transformation represents a change of basis in the vector space $\mathbb{R}^3$.
However, as shown in the previous section, the stator current space vector $\underline{i}_1^s$ describes the spatial distribution of the fundamental wave of the magnetomotive force (MMF) in the air gap, and therefore, unlike the vector $\vec{i}_1$, possesses a distinct physical significance. This distinction is reflected in the different notations used.

3.4.3 Application of the Clarke Transformation to the Modeling of AC Machines Electrical Equations

Electrical Equations

The Clarke transformation can also be applied to the stator voltage equation (3.4). In this case, the following expression is obtained:

$$\mathcal{T}_C\left(\vec{u}_1\right) = \underline{u}_1^s = \mathcal{T}_C\left(R_1 \cdot \vec{i}_1 + \frac{\mathrm{d}\vec{\Psi}_1}{\mathrm{d}t}\right) = R_1 \cdot \mathbf{T_C}\vec{i}_1 + \mathbf{T_C}\frac{\mathrm{d}\vec{\Psi}_1}{\mathrm{d}t} = R_1 \cdot \mathbf{T_C}\vec{i}_1 + \frac{\mathrm{d}(\mathbf{T_C}\vec{\Psi}_1)}{\mathrm{d}t}$$

From this, the stator voltage equation in space vector representation follows:

$$\underline{u}_1^s = R_1\underline{i}_1^s + \frac{\mathrm{d}\underline{\Psi}_1^s}{\mathrm{d}t} \tag{3.46}$$

The analysis presented in Section 3.4.1 can be extended to the rotor winding set. However, it is necessary to define a new Cartesian basis $(\vec{e}_d, \vec{e}_q)$, where the vector $\vec{e}_d$ represents a unit vector aligned with the winding axis of phase U (see Fig. 3.5). The coordinate system associated with the basis $(\vec{e}_d, \vec{e}_q)$ is referred to as the rotor reference frame, or the (d, q) coordinate system. Space vectors expressed in this coordinate system are denoted by a superscript r. Considering

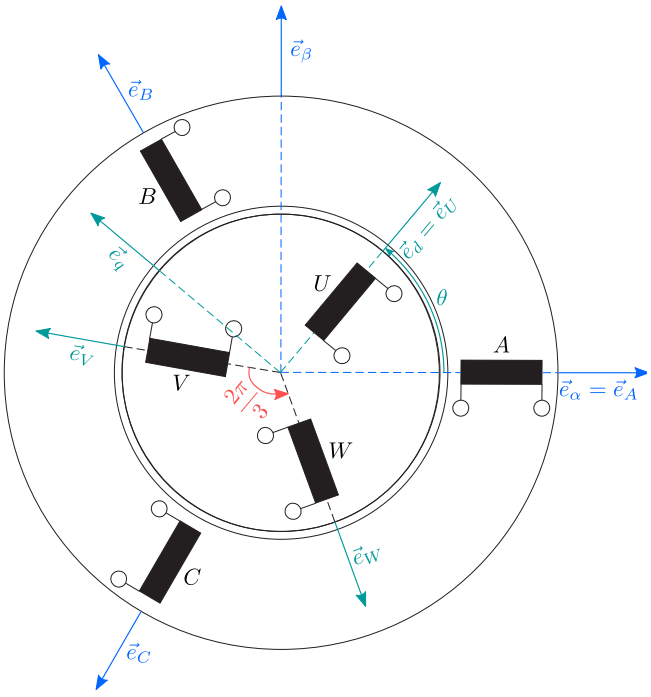

Figure 3.5: Definition of the Rotor Coordinate System for Applying the Clarke Transformation to the Rotor Winding Set

these relationships, the rotor voltage equation (3.5) in space vector representation takes the following form:

$$\underline{u}_2^r = R_2\underline{i}_2^r + \frac{\mathrm{d}\underline{\Psi}_2^r}{\mathrm{d}t} \tag{3.47}$$

Magnetic Relationships

When transforming the stator flux linkage equations (3.8) and (3.9), it must be noted that these contain both stator and rotor quantities.

The transformation of (3.8) yields:

$$\begin{aligned}\mathcal{T}_C\left(\vec{\Psi}_1\right) = \underline{\Psi}_1^s &= \mathbf{T_C}\mathbf{L}_1\vec{i}_1 + \mathbf{T_C}\mathbf{L}_{12}(\theta)\vec{i}_2 \\ &= \mathbf{T_C}\mathbf{L}_1\mathbf{T_C}^{-1}\underline{i}_1^s + \mathbf{T_C}\mathbf{L}_{12}(\theta)\mathbf{T_C}^{-1}\underline{i}_2^r\end{aligned} \tag{3.48}$$

With the definitions $\mathbf{L}_1^s = \mathbf{T_C}\mathbf{L}_1\mathbf{T_C}^{-1}$ and $\mathbf{L}_{12}^s(\theta) = \mathbf{T_C}\mathbf{L}_{12}(\theta)\mathbf{T_C}^{-1}$, the stator flux linkage space vector can be expressed as follows:

$$\underline{\Psi}_1^s = \mathbf{L}_1^s\underline{i}_1^s + \mathbf{L}_{12}^s(\theta)\underline{i}_2^r \tag{3.49}$$

the expanded form after carrying out the matrix multiplications yields:

$$\begin{bmatrix}\Psi_\alpha \\ \Psi_\beta \\ \Psi_{01}\end{bmatrix} = \begin{bmatrix}\frac{3}{2}L_{h1}+L_{\sigma1} & 0 & 0 \\ 0 & \frac{3}{2}L_{h1}+L_{\sigma1} & 0 \\ 0 & 0 & L_{\sigma1}\end{bmatrix}\begin{bmatrix}i_\alpha \\ i_\beta \\ i_{01}\end{bmatrix} + \frac{3}{2}\frac{n_2}{n_1}L_{h1}\begin{bmatrix}\cos\theta & -\sin\theta & 0 \\ \sin\theta & \cos\theta & 0 \\ 0 & 0 & 0\end{bmatrix}\begin{bmatrix}i_d \\ i_q \\ i_{02}\end{bmatrix} \tag{3.50}$$

From (3.50) it follows that, the transformed matrix $\mathbf{L}_1^s$ is diagonal, and the third component of the stator flux linkage space vector is determined solely by the zero-sequence components of the currents flowing in the stator and rotor winding sets. Based on the assumption that both winding sets have isolated neutral points, the space vectors $\underline{i}_1^s$, $\underline{i}_2^r$, and consequently $\underline{\Psi}_1^s$ are fully described by their first two components. Substituting (3.50) into the stator voltage equation (3.46) further shows that only the u_α and u_β components are nonzero.
Similarly, it can be shown that the rotor flux linkage space vector satisfies the following relationship:

$$\underline{\Psi}_2^r = \mathbf{L}_2^r\underline{i}_2^r + \mathbf{L}_{21}^r(\theta)\underline{i}_1^s \tag{3.51}$$

where $\mathbf{L}_2^r = \mathbf{T_C}\mathbf{L}_2\mathbf{T_C}^{-1}$ and $\mathbf{L}_{21}^r(\theta) = \mathbf{T_C}\mathbf{L}_{21}(\theta)\mathbf{T_C}^{-1}$. In expanded form, this yields:

$$\begin{bmatrix}\Psi_d \\ \Psi_q \\ \Psi_{02}\end{bmatrix} = \begin{bmatrix}\frac{3}{2}L_{h2}+L_{\sigma2} & 0 & 0 \\ 0 & \frac{3}{2}L_{h2}+L_{\sigma2} & 0 \\ 0 & 0 & L_{\sigma2}\end{bmatrix}\begin{bmatrix}i_d \\ i_q \\ i_{02}\end{bmatrix} + \frac{3}{2}\frac{n_2}{n_1}L_{h1}\begin{bmatrix}\cos\theta & \sin\theta & 0 \\ -\sin\theta & \cos\theta & 0 \\ 0 & 0 & 0\end{bmatrix}\begin{bmatrix}i_\alpha \\ i_\beta \\ i_{01}\end{bmatrix} \tag{3.52}$$

Here, the third component of all space vectors referring to the rotor winding set is also irrelevant, so in the following all relationships between space vectors will be examined within the subspace spanned by the basis vectors $\vec{e}_\alpha$ and $\vec{e}_\beta$ (or $\vec{e}_d$ and $\vec{e}_q$). That is, the third component will no longer be considered.
By means of the Clarke transformation, the linear combinations

$$i_A + i_B + i_C = 0$$

$$i_U + i_V + i_W = 0,$$

which hold between the three phase currents of the respective winding sets when their neutral points are isolated, can therefore be exploited to reduce the model order.
In summary, the simplified system of equations in expanded form is given by:

$$\begin{bmatrix} u_\alpha \\ u_\beta \end{bmatrix} = R_1 \begin{bmatrix} i_\alpha \\ i_\beta \end{bmatrix} + \frac{\mathrm{d}}{\mathrm{d}t} \begin{bmatrix} \Psi_\alpha \\ \Psi_\beta \end{bmatrix} \tag{3.53a}$$

$$\begin{bmatrix} \Psi_\alpha \\ \Psi_\beta \end{bmatrix} = \left(\frac{3}{2} L_{h1} + L_{\sigma 1}\right) \begin{bmatrix} 1 & 0 \\ 0 & 1 \end{bmatrix} \begin{bmatrix} i_\alpha \\ i_\beta \end{bmatrix} + \frac{3}{2} \frac{n_2}{n_1} L_{h1} \begin{bmatrix} \cos\theta & -\sin\theta \\ \sin\theta & \cos\theta \end{bmatrix} \begin{bmatrix} i_d \\ i_q \end{bmatrix} \tag{3.53b}$$

$$\begin{bmatrix} u_d \\ u_q \end{bmatrix} = R_1 \begin{bmatrix} i_d \\ i_q \end{bmatrix} + \frac{\mathrm{d}}{\mathrm{d}t} \begin{bmatrix} \Psi_d \\ \Psi_q \end{bmatrix} \tag{3.54a}$$

$$\begin{bmatrix} \Psi_d \\ \Psi_q \end{bmatrix} = \left(\frac{3}{2} L_{h2} + L_{\sigma 2}\right) \begin{bmatrix} 1 & 0 \\ 0 & 1 \end{bmatrix} \begin{bmatrix} i_d \\ i_q \end{bmatrix} + \frac{3}{2} \frac{n_2}{n_1} L_{h1} \begin{bmatrix} \cos\theta & \sin\theta \\ -\sin\theta & \cos\theta \end{bmatrix} \begin{bmatrix} i_\alpha \\ i_\beta \end{bmatrix} \tag{3.54b}$$

Using the definitions

$$\begin{aligned} L_1 &= \frac{3}{2} L_{h1} + L_{\sigma 1} \\ L_2 &= \frac{3}{2} L_{h2} + L_{\sigma 2} \\ M &= \frac{3}{2} \frac{n_2}{n_1} L_{h1} \\ \mathbf{T}(\theta) &= \begin{bmatrix} \cos\theta & -\sin\theta \\ \sin\theta & \cos\theta \end{bmatrix} \end{aligned}$$

the compact representation is:

$$\begin{aligned} \underline{u}_1^s &= R_1 \underline{i}_1^s + \frac{\mathrm{d}\underline{\Psi}_1^s}{\mathrm{d}t} \\ \underline{\Psi}_1^s &= L_1 \underline{i}_1^s + M \mathbf{T}(\theta) \underline{i}_2^r \\ \underline{u}_2^r &= R_2 \underline{i}_2^r + \frac{\mathrm{d}\underline{\Psi}_2^r}{\mathrm{d}t} \\ \underline{\Psi}_2^r &= L_2 \underline{i}_2^r + M \mathbf{T}(-\theta) \underline{i}_1^s \end{aligned} \tag{3.55}$$

The equations (3.55) in space vector form is equivalent to the original equations (3.4), (3.5), (3.8), and (3.9) in phase-variable form.

3.4.4 General Rotating Coordinate Systems

From the inspection of the above flux linkage equations, it is clear that the rotation matrix $\mathbf{T}$ expresses the angular dependence of the mutual inductance between the stator and rotor winding sets.
To further investigate these relationships and to explore the possibility of an additional simplification of the model, the following transformation is defined:

$$\begin{aligned} \mathcal{T}_{\mathcal{P}\varphi}: \quad & \mathbb{R}^2 \quad \longrightarrow \quad \mathbb{R}^2 \\ & \underline{x}^k = \begin{bmatrix} x_k \\ x_l \end{bmatrix} \longmapsto \mathcal{T}_{\mathcal{P}\varphi}(\underline{x}^k) = \underline{x}^s = \begin{bmatrix} x_\alpha \\ x_\beta \end{bmatrix} = \mathbf{T}(\varphi) \begin{bmatrix} x_k \\ x_l \end{bmatrix} = \begin{bmatrix} \cos\varphi & -\sin\varphi \\ \sin\varphi & \cos\varphi \end{bmatrix} \begin{bmatrix} x_k \\ x_l \end{bmatrix} \end{aligned} \tag{3.56}$$

$\mathcal{T}_{P\varphi}$ defines a new basis $(\vec{e_k}, \vec{e_l})$, which is rotated by an angle φ, compared with the basis

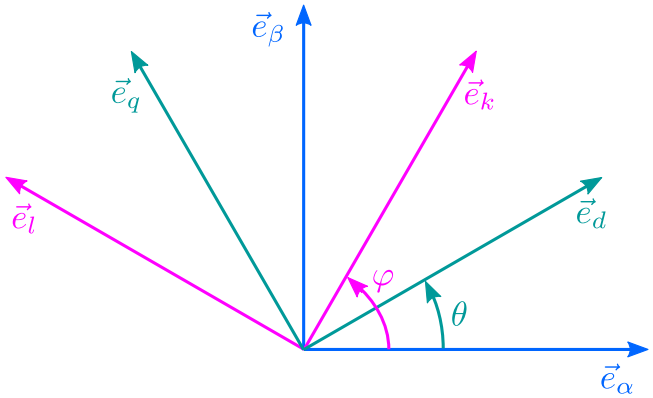

Figure 3.6: Definition of a New Coordinate System Rotated by the Angle φ with the Transformation Matrix $\mathbf{T}_{P\varphi}$

$(\vec{e_\alpha}, \vec{e_\beta})$ (Fig. 3.6). This transformation thus enables the representation of space vectors not only in the stator- or rotor-reference frame, but also in an arbitrary (k, l)-coordinate system. If a space vector $\underline{x}^k$ is expressed in this coordinate system, then $\mathcal{T}_{\mathcal{P}}(\underline{x}^k) = \mathbf{T}(\varphi)\underline{x}^k$ represents its form in the stator reference frame (α, β). $\mathcal{T}_{\mathcal{P}\varphi}$ is referred to as the *Park Transformation*.
The rotation matrix $\mathbf{T}$ is non-singular with

$$\mathbf{T}(\varphi)^{-1} = \mathbf{T}(\varphi)^\top = \mathbf{T}(-\varphi), \tag{3.57}$$

so that the inverse transformation ${\mathcal{T}_{\mathcal{P}\varphi}}^{-1}$ exists.
This inverse enables a space vector given in the (α, β) coordinate system to be transformed into (k, l)-coordinates. In the special case $\varphi = \theta$, $\mathcal{T}_{\mathcal{P}\theta}$ corresponds to a transformation from the rotor reference frame to the stator reference frame. For $\varphi = -\theta$, it corresponds to a transformation from the stator reference frame to the rotor reference frame. Due to the particular significance

of these two transformations, the notation $\mathbf{T}_{rs} = \mathbf{T}(\theta)$ and $\mathbf{T}_{sr} = \mathbf{T}(-\theta)$ will be used for the corresponding rotation matrices in the following.

It follows that the term $\mathbf{T}(\theta)\underline{i}_2^r$ in the system of equations (3.55) corresponds to the representation of the rotor current space vector in the stator reference frame, $\underline{i}_2^s$. Conversely, the term $\mathbf{T}(-\theta)\underline{i}_2^s$ represents the stator current space vector in rotor reference frame, $\underline{i}_1^r$.

Thus, the angular dependence of the mutual inductance in system (3.55) can be eliminated, allowing the equations to be further simplified:

$$\underline{u}_1^s = R_1\underline{i}_1^s + \frac{\mathrm{d}\underline{\Psi}_1^s}{\mathrm{d}t} \tag{3.58a}$$

$$\underline{\Psi}_1^s = L_1\underline{i}_1^s + M\underline{i}_2^s \tag{3.58b}$$

$$\underline{u}_2^r = R_2\underline{i}_2^r + \frac{\mathrm{d}\underline{\Psi}_2^r}{\mathrm{d}t} \tag{3.58c}$$

$$\underline{\Psi}_2^r = L_2\underline{i}_2^r + M\underline{i}_1^r \tag{3.58d}$$

If a space vector is given in a rotating coordinate system, the product rule must be applied when calculating its time derivative (cf. $\underline{\Psi}_2^r$ in (3.58c)). For the general case of a space vector $\underline{x}^k$ in an arbitrary $(k,\, l)$ coordinate system, the following applies:

$$\begin{aligned}
\frac{\mathrm{d}\underline{x}^k(t)}{\mathrm{d}t} &= \frac{\mathrm{d}[\mathbf{T}(\varphi(t))^{-1}\underline{x}^s(t)]}{\mathrm{d}t} = \frac{\mathrm{d}[\mathbf{T}(-\varphi(t))\underline{x}^s(t)]}{\mathrm{d}t} \\
&= \frac{\mathrm{d}\mathbf{T}(-\varphi(t))}{\mathrm{d}t}\underline{x}^s(t) + \mathbf{T}(-\varphi(t))\frac{\mathrm{d}\underline{x}^s(t)}{\mathrm{d}t} \\
&= \frac{\partial\mathbf{T}(-\varphi)}{\partial\varphi}\frac{\mathrm{d}\varphi}{\mathrm{d}t}\underline{x}^s(t) + \mathbf{T}(-\varphi(t))\frac{\mathrm{d}\underline{x}^s(t)}{\mathrm{d}t} \\
&= \dot{\varphi}\begin{bmatrix} -\sin\varphi & \cos\varphi \\ -\cos\varphi & -\sin\varphi \end{bmatrix}\underline{x}^s(t) + \begin{bmatrix} \cos\varphi & \sin\varphi \\ -\sin\varphi & \cos\varphi \end{bmatrix}\frac{\mathrm{d}\underline{x}^s(t)}{\mathrm{d}t} \\
&= -\dot{\varphi}\begin{bmatrix} \cos\varphi & \sin\varphi \\ -\sin\varphi & \cos\varphi \end{bmatrix}\begin{bmatrix} 0 & -1 \\ 1 & 0 \end{bmatrix}\underline{x}^s(t) + \begin{bmatrix} \cos\varphi & \sin\varphi \\ -\sin\varphi & \cos\varphi \end{bmatrix}\frac{\mathrm{d}\underline{x}^s(t)}{\mathrm{d}t} \\
&= -\dot{\varphi}\mathbf{T}(-\varphi)\mathbf{J}\underline{x}^s(t) + \mathbf{T}(-\varphi)\frac{\mathrm{d}\underline{x}^s(t)}{\mathrm{d}t}
\end{aligned} \tag{3.59}$$

with

$$\mathbf{J} = \mathbf{T}\left(\frac{\pi}{2}\right) = \begin{bmatrix} 0 & -1 \\ 1 & 0 \end{bmatrix} \tag{3.60}$$

When (3.58c) is transformed into the stator reference frame using $\mathcal{T}_{\mathcal{P}\theta}$ (and therefore by applying

the matrix $\mathbf{T}_{rs} = \mathbf{T}(\theta)$), the result is:

$$\begin{aligned}
\underline{u}_2^s &= \mathbf{T}_{rs}\underline{u}_2^r = R_2\mathbf{T}_{rs}\underline{i}_2^r + \mathbf{T}_{rs}\frac{\mathrm{d}\underline{\Psi}_2^r}{\mathrm{d}t} \\
&= R_2\underline{i}_2^s + \mathbf{T}_{rs}\frac{\mathrm{d}\mathbf{T}_{sr}\underline{\Psi}_2^s}{\mathrm{d}t} \\
&= R_2\underline{i}_2^s + \mathbf{T}_{rs}\left(-\omega\mathbf{T}_{sr}\mathbf{J}\underline{\Psi}_2^s + \mathbf{T}_{sr}\frac{\mathrm{d}\underline{\Psi}_2^s}{\mathrm{d}t}\right) \quad \text{with} \quad \omega = \dot{\theta} \\
&= R_2\underline{i}_2^s + \frac{\mathrm{d}\underline{\Psi}_2^s}{\mathrm{d}t} - \omega\mathbf{J}\underline{\Psi}_2^s
\end{aligned} \tag{3.61}$$

(3.61) represents the rotor voltage equation in the stator reference frame.

3.5 Conversion of Rotor-Referenced Quantities to the Stator Side

The system of equations (3.58) involves the rotor winding set resistance R_2, the rotor winding set inductance L_2, and the mutual inductance M. However, in practice these quantities are not always directly measurable, for instance, when the terminals of the rotor winding set are inaccessible, as is the case for squirrel-cage induction machines.
To obtain a usable model, it is therefore necessary to transform (3.58). For this purpose, the inductances L_1 and L_2 are again decomposed into main and leakage components, and equivalent quantities are subsequently introduced. For the rotor flux linkage equation (3.58d), the following holds:

$$\begin{aligned}
\underline{\Psi}_2^r &= L_2\underline{i}_2^r + M\underline{i}_1^r \\
&= \left(\frac{3}{2}L_{h2} + L_{\sigma 2}\right)\underline{i}_2^r + \frac{3}{2}\frac{n_2}{n_1}L_{h1}\underline{i}_1^r
\end{aligned}$$

Taking into account the relation $L_{h2} = \dfrac{n_2^2}{n_1^2}L_{h1}$, it follows that:

$$\begin{aligned}
\underline{\Psi}_2^r &= \left(\frac{3}{2}\frac{n_2^2}{n_1^2}L_{h1} + L_{\sigma 2}\right)\underline{i}_2^r + \frac{3}{2}\frac{n_2}{n_1}L_{h1}\underline{i}_1^r \\
\Longleftrightarrow \frac{n_1}{n_2}\underline{\Psi}_2^r &= \left(\frac{3}{2}L_{h1} + \frac{n_1^2}{n_2^2}L_{\sigma 2}\right)\frac{n_2}{n_1}\underline{i}_2^r + \frac{3}{2}L_{h1}\underline{i}_1^r
\end{aligned}$$

If the quantities are defined accordingly

$$\underline{\Psi}_r^r = \frac{n_1}{n_2}\underline{\Psi}_2^r \qquad L_{\sigma r} = \frac{n_1^2}{n_2^2}L_{\sigma 2} \qquad L_m = \frac{3}{2}L_{h1}$$

$$\underline{i}_r^r = \frac{n_2}{n_1}\underline{i}_2^r \qquad \underline{i}_s^r = \underline{i}_1^r \qquad L_r = L_m + L_{\sigma r}$$

the following equation results:

$$\underline{\Psi}_r^r = \left(L_m + L_{\sigma r}\right)\underline{i}_r^r + L_m\underline{i}_s^r = L_r\underline{i}_r^r + L_m\underline{i}_s^r = L_m\left(\underline{i}_r^r + \underline{i}_s^r\right) + L_{\sigma r}\underline{i}_r^r \tag{3.62}$$

The rotor flux linkage space vector $\underline{\Psi}_r^r$, scaled by the turns ratio, thus consists of the *main flux component* $\underline{\Psi}_h^r = L_m(\underline{i}_r^r + \underline{i}_s^r)$ and the *leakage flux component* $\underline{\Psi}_{\sigma r}^r = L_{\sigma r}\underline{i}_r^r$. If $\underline{\Psi}_r^r$ is substituted into the rotor voltage equation (3.58c), one obtains:

$$\begin{aligned} \underline{u}_2^r &= R_2\underline{i}_2^r + \frac{n_2}{n_1}\frac{\mathrm{d}\underline{\Psi}_r^r}{\mathrm{d}t} \\ \Longleftrightarrow \frac{n_1}{n_2}\underline{u}_2^r &= \frac{n_1^2}{n_2^2}R_2\underline{i}_r^r + \frac{\mathrm{d}\underline{\Psi}_r^r}{\mathrm{d}t} \end{aligned}$$

Based on these definitions,

$$\underline{u}_r^r = \frac{n_1}{n_2}\underline{u}_2^r \quad \text{und} \quad R_r = \frac{n_1^2}{n_2^2}R_2$$

(3.58c) can be rewritten as follows:

$$\underline{u}_r^r = R_r\underline{i}_r^r + \frac{\mathrm{d}\underline{\Psi}_r^r}{\mathrm{d}t} \tag{3.63}$$

Furthermore, for the stator flux linkage in the stator reference frame, the following holds:

$$\underline{\Psi}_s^s = L_s\underline{i}_s^s + L_m\underline{i}_r^s = L_m\left(\underline{i}_s^s + \underline{i}_r^s\right) + L_{\sigma s}\underline{i}_s^s \tag{3.64}$$

with

$$\underline{\Psi}_s^s = \underline{\Psi}_1^s \qquad R_s = R_1 \qquad L_s = L_m + L_{\sigma s}$$

Again, we can identify a *main flux component* $\underline{\Psi}_h^s = L_m(\underline{i}_r^s + \underline{i}_s^s)$ and a *leakage flux component* $\underline{\Psi}_{\sigma s}^s = L_{\sigma s}\underline{i}_s^s$.

Finally, using the newly introduced quantities, the electromagnetic relationships in the general fundamental-wave model of the rotating field machine are described by the following system of equations:

Stator Voltage:	$\underline{u}_s^s = R_s\underline{i}_s^s + \frac{\mathrm{d}\underline{\Psi}_s^s}{\mathrm{d}t}$	(3.65a)
Stator Flux Linkage:	$\underline{\Psi}_s^s = L_s\underline{i}_s^s + L_m\underline{i}_r^s = L_m\left(\underline{i}_s^s + \underline{i}_r^s\right) + L_{\sigma s}\underline{i}_s^s$	(3.65b)
Rotor Voltage:	$\underline{u}_r^r = R_r\underline{i}_r^r + \frac{\mathrm{d}\underline{\Psi}_r^r}{\mathrm{d}t}$	(3.65c)
Rotor Flux Linkage:	$\underline{\Psi}_r^r = L_r\underline{i}_r^r + L_m\underline{i}_s^r = L_m\left(\underline{i}_s^r + \underline{i}_r^r\right) + L_{\sigma r}\underline{i}_r^r$	(3.65d)

The system of equations (3.65) is of particular importance and is used in deriving the signal flow diagram of the generalized rotating field machine to describe the electromagnetic relationships.

However, it should be noted that the quantities L_s, L_r, R_r, and L_m — unlike R_s — do not correspond to the actual values of the respective winding parameters. For example, R_r does not represent the actual resistance of a rotor winding phase. Nevertheless, all parameter values can be determined experimentally in a straightforward manner, as will be demonstrated below.

3.6 Experimental Determination of the Model Parameters

3.6.1 Stator-Voltage-Oriented Reference Frame and Steady-State Behavior

The Park transformation $\mathcal{T}_{\mathcal{P}\varphi}$, introduced in Section 3.4, enables the definition of additional rotating reference frames, in addition to the stator reference frame and rotor reference frame already employed.
For example, starting from the basis $(\vec{e}_\alpha, \vec{e}_\beta)$ of the stator reference frame, a new basis $(\vec{e}_k, \vec{e}_l)$ rotated by an angle φ_K can be constructed, in which the space vector of the stator voltage can be described as follows:

$$\underline{u}_s = \|\underline{u}_s\|\,\vec{e}_k = \begin{bmatrix} u_{sk} \\ u_{sl} \end{bmatrix} = \begin{bmatrix} \|\underline{u}_s\| \\ 0 \end{bmatrix} \tag{3.66}$$

These relationships are illustrated in Fig. 3.7.

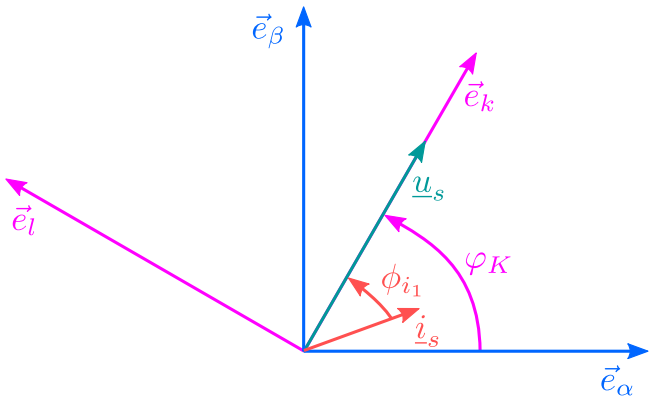

Figure 3.7: Definition of a Voltage Space Vector in the Stator Fixed (α, β)-Coordinate System and their Angles According to the Park Transformation $\mathbf{T}_P(\varphi_k)$

From the system of equations (3.65), the following relationships can be derived in the (k,l) reference frame:

$$(3.65a) \quad \Longleftrightarrow \quad \mathbf{T}(-\varphi_K)\underline{u}_s^s = \mathbf{T}(-\varphi_K)R_s\underline{i}_s^s + \mathbf{T}(-\varphi_K)\frac{\mathrm{d}[\mathbf{T}(\varphi_K)\underline{\Psi}_s^k]}{\mathrm{d}t}$$

$$\Longleftrightarrow \quad \underline{u}_s^k = R_s\underline{i}_s^k + \frac{\mathrm{d}\underline{\Psi}_s^k}{\mathrm{d}t} + \omega_K\mathbf{J}\underline{\Psi}_s^k \quad \text{mit} \quad \omega_K = \dot{\varphi}_K \tag{3.67a}$$

$$(3.65b) \quad \Longleftrightarrow \quad \underline{\Psi}_s^k = L_s\underline{i}_s^k + L_m\underline{i}_r^k = L_m\left(\underline{i}_s^k + \underline{i}_r^k\right) + L_{\sigma s}\underline{i}_s^k \tag{3.67b}$$

$$(3.65c) \quad \Longleftrightarrow \quad \mathbf{T}(\theta-\varphi_K)\underline{u}_r^r = \mathbf{T}(\theta-\varphi_K)R_r\underline{i}_r^r + \mathbf{T}(\theta-\varphi_K)\frac{\mathrm{d}[\mathbf{T}(\varphi_K-\theta)\underline{\Psi}_r^k]}{\mathrm{d}t}$$

$$\Longleftrightarrow \quad \underline{u}_r^k = R_r\underline{i}_r^k + \frac{\mathrm{d}\underline{\Psi}_r^k}{\mathrm{d}t} + (\omega_K-\omega)\mathbf{J}\underline{\Psi}_r^k \tag{3.67c}$$

$$(3.65d) \quad \Longleftrightarrow \quad \underline{\Psi}_r^k = L_r\underline{i}_r^k + L_m\underline{i}_s^k = L_m\left(\underline{i}_r^k + \underline{i}_s^k\right) + L_{\sigma r}\underline{i}_r^k \tag{3.67d}$$

For the following considerations, it is assumed that the phase voltages on the stator and rotor sides can be expressed as:

$$\begin{aligned} u_A &= \hat{u}_1\cos(\omega_e t) & u_U &= 0\\ u_B &= \hat{u}_1\cos(\omega_e t - 2\pi/3) & u_V &= 0\\ u_C &= \hat{u}_1\cos(\omega_e t - 4\pi/3) & u_W &= 0 \end{aligned}$$

where $\hat{u}_1$ and ω_e are positive constants.

By applying the Clarke transformation, one obtains:

$$\begin{bmatrix} u_\alpha \\ u_\beta \\ u_{01} \end{bmatrix} = \mathbf{T_C}\begin{bmatrix} u_A \\ u_B \\ u_C \end{bmatrix} = \hat{u}_1\begin{bmatrix} \cos(\omega_e t) \\ \sin(\omega_e t) \\ 0 \end{bmatrix}$$

$$\begin{bmatrix} u_d \\ u_q \\ u_{02} \end{bmatrix} = \mathbf{T_C}\begin{bmatrix} u_U \\ u_V \\ u_W \end{bmatrix} = \begin{bmatrix} 0 \\ 0 \\ 0 \end{bmatrix}$$

Thus, the voltage space vectors are given by:

$$\underline{u}_s^s = \hat{u}_1\begin{bmatrix} \cos(\omega_e t) \\ \sin(\omega_e t) \end{bmatrix} \qquad \underline{u}_r = \underline{0}$$

$$\underline{u}_s^k = \begin{bmatrix} \hat{u}_1 \\ 0 \end{bmatrix} \quad \text{with} \quad \omega_K = \omega_e$$

In the following, it is assumed that the rotor angular velocity ω of the general rotating-field machine is kept constant. Under these conditions, (3.67) represents a linear system of differential equations. Since the space vectors $\underline{u}_s^k$ and $\underline{u}_r^k$ are constant, the components of $\underline{i}_s^k$ and $\underline{i}_r^k$ as well as $\underline{\Psi}_s^k$ and $\underline{\Psi}_r^k$ also assume constant values in the steady state.

In this case, for example, there exists $\phi_{i_1} \in \mathbb{R}$ such that:

$$\begin{aligned}
& & \underline{i}_s^k &= \|\underline{i}_s\| \begin{bmatrix} \cos(\phi_{i_1}) \\ -\sin(\phi_{i_1}) \end{bmatrix} \\
\iff & & \underline{i}_s^s &= \mathbf{T}(\varphi_K)\underline{i}_s^k = \|\underline{i}_s\| \begin{bmatrix} \cos\varphi_K & -\sin\varphi_K \\ \sin\varphi_K & \cos\varphi_K \end{bmatrix} \begin{bmatrix} \cos(\phi_{i_1}) \\ -\sin(\phi_{i_1}) \end{bmatrix} \\
& & &= \|\underline{i}_s\| \begin{bmatrix} \cos(\omega_e t - \phi_{i_1}) \\ \sin(\omega_e t - \phi_{i_1}) \end{bmatrix} \\
\iff & & \vec{i}_1 &= \|\underline{i}_s\| \, {\mathbf{T}_\mathbf{C}}^{-1} \begin{bmatrix} \cos(\omega_e t - \phi_{i_1}) \\ \sin(\omega_e t - \phi_{i_1}) \\ 0 \end{bmatrix} \\
\iff & \begin{bmatrix} i_A \\ i_B \\ i_C \end{bmatrix} &= \|\underline{i}_s\| \begin{bmatrix} \cos(\omega_e t - \phi_{i_1}) \\ -\frac{1}{2}\cos(\omega_e t - \phi_{i_1}) + \frac{\sqrt{3}}{2}\sin(\omega_e t - \phi_{i_1}) \\ -\frac{1}{2}\cos(\omega_e t - \phi_{i_1}) - \frac{\sqrt{3}}{2}\sin(\omega_e t - \phi_{i_1}) \end{bmatrix} \\
& & &= \|\underline{i}_s\| \begin{bmatrix} \cos(\omega_e t - \phi_{i_1}) \\ \cos(\omega_e t - \phi_{i_1} - \frac{2\pi}{3}) \\ \cos(\omega_e t - \phi_{i_1} - \frac{4\pi}{3}) \end{bmatrix}
\end{aligned}$$

The phase currents of the stator winding set are also sinusoidal in steady state. They have the same angular frequency ω_e as the respective phase voltages and are time-shifted relative to them by the angle ϕ_{i_1}. Similar conclusions can be drawn for the other electrical quantities.

The steady-state analysis also allows for a simplification of (3.67a) and (3.67c), in which the time derivatives equal to zero:

$$\begin{aligned}
\underline{u}_s^k &= R_s\underline{i}_s^k + \omega_K \mathbf{J}\underline{\Psi}_s^k \\
&= R_s\underline{i}_s^k + \omega_K L_m \mathbf{J}\left(\underline{i}_s^k + \underline{i}_r^k\right) + \omega_K L_{\sigma s}\mathbf{J}\underline{i}_s^k
\end{aligned} \tag{3.68a}$$

$$\begin{aligned}
\underline{0} &= R_r\underline{i}_r^k + (\omega_K - \omega)\mathbf{J}\underline{\Psi}_r^k \\
&= R_r\underline{i}_r^k + (\omega_K - \omega) L_m \mathbf{J}\left(\underline{i}_s^k + \underline{i}_r^k\right) + (\omega_K - \omega) L_{\sigma r}\mathbf{J}\underline{i}_r^k
\end{aligned} \tag{3.68b}$$

3.6.2 Interesting Special Cases

From the system of equations (3.68), two special cases can be derived, which can be used to determine the model parameters and will therefore be examined in more detail.

The First Situation: $\omega = \omega_K$

From the assumption $\omega = \omega_K$ and (3.68b), it follows that $\underline{i}_r^k = \underline{0}$. Accordingly, (3.68a) simplifies to:

$$\begin{aligned} \underline{u}_s^k &= R_s \underline{i}_s^k + \omega_K L_m \mathbf{J} \underline{i}_s^k + \omega_K L_{\sigma s} \mathbf{J} \underline{i}_s^k \\ &= R_s \underline{i}_s^k + \omega_K L_s \mathbf{J} \underline{i}_s^k \\ &= \left(R_s \mathbf{I}_2 + \omega_K L_s \mathbf{J}\right) \underline{i}_s^k \end{aligned} \tag{3.69}$$

$$\text{with} \quad \mathbf{I}_2 = \begin{bmatrix} 1 & 0 \\ 0 & 1 \end{bmatrix}$$

From (3.69) it follows:

$$\begin{aligned} \underline{i}_s^k \cdot \underline{u}_s^k = \underline{i}_s^{k\top} \underline{u}_s^k &= \|\underline{i}_s\| \, \|\underline{u}_s\| \cos \phi_{i_1} \Big|_1 && \text{with} \quad \phi_{i_1} \in [0;\, \pi/2] \\ &= \underline{i}_s^{k\top} \left(R_s \mathbf{I}_2 + \omega_K L_s \mathbf{J}\right) \underline{i}_s^k \\ &= R_s \underline{i}_s^{k\top} \underline{i}_s^k && \text{since} \quad \underline{i}_s^{k\top} \mathbf{J} \underline{i}_s^k = 0 \\ &= R_s \, \|\underline{i}_s\|^2 \end{aligned} \tag{3.70}$$

$$\Longrightarrow \qquad R_s = \frac{\|\underline{u}_s\|}{\|\underline{i}_s\|} \cos \phi_{i_1} \Big|_1 \tag{3.71}$$

$$\begin{aligned} \left\| \underline{i}_s^k \times \underline{u}_s^k \right\| = \underline{i}_s^{k\top} \mathbf{J}^\top \underline{u}_s^k &= \|\underline{i}_s\| \, \|\underline{u}_s\| \sin \phi_{i_1} \Big|_1 && \text{with} \quad \phi_{i_1} \in [0;\, \pi/2] \\ &= \underline{i}_s^{k\top} \left(R_s \mathbf{J}^\top + \omega_K L_s \mathbf{J}^\top \mathbf{J}\right) \underline{i}_s^k \\ &= \underline{i}_s^{k\top} \left(R_s \mathbf{J}^\top + \omega_K L_s \mathbf{I}_2\right) \underline{i}_s^k \\ &= \omega_K L_s \underline{i}_s^{k\top} \underline{i}_s^k && \text{since} \quad \underline{i}_s^{k\top} \mathbf{J}^\top \underline{i}_s^k = 0 \\ &= \omega_K L_s \, \|\underline{i}_s\|^2 \end{aligned} \tag{3.72}$$

$$\Longrightarrow \qquad L_s = \frac{1}{\omega_K} \frac{\|\underline{u}_s\|}{\|\underline{i}_s\|} \sin \phi_{i_1} \Big|_1 \tag{3.73}$$

The Second Situation: $\omega = 0$

If the condition $\omega = 0$ is substituted into (3.68b), we obtain:

$$\begin{aligned} \underline{0} &= R_r \underline{i}_r^k + \omega_K L_m \mathbf{J} \left(\underline{i}_r^k + \underline{i}_s^k\right) + \omega_K L_{\sigma r} \mathbf{J} \underline{i}_r^k \\ \Longrightarrow \qquad \omega_K L_m \mathbf{J} \left(\underline{i}_r^k + \underline{i}_s^k\right) &= -R_r \underline{i}_r^k - \omega_K L_{\sigma r} \mathbf{J} \underline{i}_r^k \end{aligned}$$

In this case, (3.68a) yields:

$$\begin{aligned}\underline{u}_s^k &= R_s\underline{i}_s^k + \omega_K L_m \mathbf{J}\left(\underline{i}_s^k + \underline{i}_r^k\right) + \omega_K L_{\sigma s}\mathbf{J}\underline{i}_s^k \\ &= R_s\underline{i}_s^k - R_r\underline{i}_r^k + \omega_K L_{\sigma s}\mathbf{J}\underline{i}_s^k - \omega_K L_{\sigma r}\mathbf{J}\underline{i}_r^k \end{aligned} \tag{3.74}$$

The rotor voltage equation can also be rewritten as follows:

$$\begin{aligned} \underline{0} &= R_r\underline{i}_r^k + \omega_K L_r\mathbf{J}\underline{i}_r^k + \omega_K L_m\mathbf{J}\underline{i}_s^k \\ &= \left(R_r\mathbf{I}_2 + \omega_K L_r\mathbf{J}\right)\underline{i}_r^k + \omega_K L_m\mathbf{J}\underline{i}_s^k \\ \Longleftrightarrow \qquad \omega_K L_m\mathbf{J}\underline{i}_s^k &= -\left(R_r\mathbf{I}_2 + \omega_K L_r\mathbf{J}\right)\underline{i}_r^k \\ \Longleftrightarrow \qquad \underline{i}_s^k &= -\frac{1}{\omega_K L_m}\mathbf{J}^\top\left(R_r\mathbf{I}_2 + \omega_K L_r\mathbf{J}\right)\underline{i}_r^k \quad \text{für} \quad \omega_K \neq 0 \\ &= -\frac{R_r}{\omega_K L_m}\mathbf{J}^\top\underline{i}_r^k - \frac{L_r}{L_m}\underline{i}_r^k \\ &= -\frac{R_r}{\omega_K L_m}\mathbf{J}^\top\underline{i}_r^k - \left(1 + \frac{L_{\sigma r}}{L_m}\right)\underline{i}_r^k \end{aligned} \tag{3.75}$$

The first term on the right-hand side of (3.75) represents a component orthogonal to $\underline{i}_r^k$, while the second corresponds to a component parallel to $\underline{i}_r^k$. If the angular frequency of the stator voltage ω_K is chosen such that $\omega_K L_m \gg R_r$, the orthogonal component can then be neglected. Furthermore, in practice, the ratio $L_{\sigma r}/L_m$ is kept small by design. Under these conditions, it can be assumed as a first approximation that $\underline{i}_s^k = -\underline{i}_r^k$.
Consequently, (3.74) can be simplified to:

$$\begin{aligned}\underline{u}_s^k &= R_s\underline{i}_s^k - R_r\underline{i}_r^k + \omega_K L_{\sigma s}\mathbf{J}\underline{i}_s^k - \omega_K L_{\sigma r}\mathbf{J}\underline{i}_r^k \\ &= R_s\underline{i}_s^k + R_r\underline{i}_s^k + \omega_K L_{\sigma s}\mathbf{J}\underline{i}_s^k + \omega_K L_{\sigma r}\mathbf{J}\underline{i}_s^k \\ &= \left(R_s + R_r\right)\underline{i}_s^k + \omega_K\left(L_{\sigma s} + L_{\sigma r}\right)\mathbf{J}\underline{i}_s^k \end{aligned} \tag{3.76}$$

Analogous to the first case, the following relationships result:

$$R_s + R_r = \left.\frac{\|\underline{u}_s\|}{\|\underline{i}_s\|}\cos\phi_{i_1}\right|_2 \tag{3.77}$$

$$L_{\sigma s} + L_{\sigma r} = \left.\frac{1}{\omega_K}\frac{\|\underline{u}_s\|}{\|\underline{i}_s\|}\sin\phi_{i_1}\right|_2 \tag{3.78}$$

In good approximation, it can also be assumed that $L_{\sigma s} = L_{\sigma r}$.

3.6.3 No-load Test and Short-circuit Test

Equations (3.71), (3.73), (3.77), and (3.78) provide relationships between the model parameters R_s, L_s, $L_{\sigma s}$, R_r, $L_{\sigma r}$ and the magnitudes of the space vectors $\underline{u}_s$ and $\underline{i}_s$, as well as their relative angle, for the cases $\omega = \omega_K$ and $\omega = 0$. From the above considerations, it also follows that this angle corresponds to the phase shift between the phase currents and phase voltages.

In this way, the model parameters of an AC machine can be determined through simple experiments. For this purpose, the stator winding set is supplied by a symmetrical three-phase voltage source, and the rotor windings are short-circuited. The waveforms of a stator phase voltage and the corresponding phase current are recorded typically at rated frequency and rated voltage without mechanical load. From this *no-load test*, R_s and L_s can be determined.

To determine the remaining parameters, a test with a blocked rotor (*short-circuit test*) is carried out. In this case, the amplitude of the stator voltages is chosen so that the rated current flows, which also operating at rated frequency.

3.7 Mechanical Relationships

The previous discussion dealt exclusively with describing the electromagnetic behavior of the AC machine. However, the electromagnetic energy conversion process also results in the generation of a torque M_M, which acts on the rotor.

The expression for this torque can be derived from an energy balance. During an infinitesimally small time interval $\mathrm{d}t$, an amount of electrical energy $\mathrm{d}E_{el}$ is exchanged via the machine terminals on both the stator and rotor sides. We have:

$$\begin{aligned}
\mathrm{d}E_{el} &= \sum_{k\in\{A,B,C\}} u_k i_k \mathrm{d}t + \sum_{l\in\{U,V,W\}} u_l i_l \mathrm{d}t \\
&= \vec{u}_1^{\top}\vec{i}_1\mathrm{d}t + \vec{u}_2^{\top}\vec{i}_2\mathrm{d}t \\
&= \left(\mathbf{T_C}^{-1}\underline{u}_1^s\right)^{\top}\mathbf{T_C}^{-1}\underline{i}_1^s\mathrm{d}t + \left(\mathbf{T_C}^{-1}\underline{u}_2^r\right)^{\top}\mathbf{T_C}^{-1}\underline{i}_2^r\mathrm{d}t \\
&= \underline{u}_1^{s\top}{\mathbf{T_C}^{-1}}^{\top}\mathbf{T_C}^{-1}\underline{i}_1^s\mathrm{d}t + \underline{u}_2^{r\top}{\mathbf{T_C}^{-1}}^{\top}\mathbf{T_C}^{-1}\underline{i}_2^r\mathrm{d}t
\end{aligned} \tag{3.79}$$

With

$${\mathbf{T_C}^{-1}}^{\top}\mathbf{T_C}^{-1} = \begin{bmatrix} \frac{3}{2} & 0 & 0 \\ 0 & \frac{3}{2} & 0 \\ 0 & 0 & 3 \end{bmatrix}$$

it follows:

$$
\begin{aligned}
\mathrm{d}E_{el} &= \begin{bmatrix} u_\alpha & u_\beta & u_{01} \end{bmatrix} \begin{bmatrix} \frac{3}{2} i_\alpha \\ \frac{3}{2} i_\beta \\ 3 i_{01} \end{bmatrix} \mathrm{d}t + \begin{bmatrix} u_d & u_q & u_{02} \end{bmatrix} \begin{bmatrix} \frac{3}{2} i_d \\ \frac{3}{2} i_q \\ 3 i_{02} \end{bmatrix} \mathrm{d}t \\
&= \frac{3}{2} \left(\sum_{k \in \{\alpha, \beta\}} u_k i_k + \sum_{l \in \{d, q\}} u_l i_l \right) \mathrm{d}t + 3 \left(u_{01} i_{01} + 3 u_{02} i_{02} \right) \mathrm{d}t \\
&= \frac{3}{2} \left(\sum_{k \in \{\alpha, \beta\}} u_k i_k + \sum_{l \in \{d, q\}} u_l i_l \right) \mathrm{d}t \\
&= \frac{3}{2} \left(\underline{u}_s^{s\top} \underline{i}_s^s + \underline{u}_r^{r\top} \underline{i}_r^r \right) \mathrm{d}t = \frac{3}{2} \left(\underline{u}_s^{s\top} \underline{i}_s^s + \left(\mathbf{T}_{sr} \underline{u}_r^s \right)^\top \mathbf{T}_{sr} \underline{i}_r^s \right) \mathrm{d}t \\
&= \frac{3}{2} \left(\underline{u}_s^{s\top} \underline{i}_s^s + \underline{u}_r^{s\top} \mathbf{T}_{sr}^\top \mathbf{T}_{sr} \underline{i}_r^s \right) \mathrm{d}t = \frac{3}{2} \left(\underline{u}_s^{s\top} \underline{i}_s^s + \underline{u}_r^{s\top} \underline{i}_r^s \right) \mathrm{d}t \\
&= \frac{3}{2} \left(\underline{i}_s^{s\top} \underline{u}_s^s + \underline{i}_r^{s\top} \underline{u}_r^s \right) \mathrm{d}t
\end{aligned} \tag{3.80}
$$

The system of equations (3.65) yields:

$$
\begin{aligned}
\underline{i}_s^{s\top} \underline{u}_s^s &= \underline{i}_s^{s\top} \left(R_s \underline{i}_s^s + \frac{\mathrm{d}\underline{\Psi}_s^s}{\mathrm{d}t} \right) \\
&= \underline{i}_s^{s\top} \left(R_s \underline{i}_s^s + L_m \frac{\mathrm{d}}{\mathrm{d}t} \left(\underline{i}_s^s + \underline{i}_r^s \right) + L_{\sigma s} \frac{\mathrm{d}\underline{i}_s^s}{\mathrm{d}t} \right) \\
&= R_s \underline{i}_s^{s\top} \underline{i}_s^s + L_m \underline{i}_s^{s\top} \frac{\mathrm{d}}{\mathrm{d}t} \left(\underline{i}_s^s + \underline{i}_r^s \right) + L_{\sigma s} \underline{i}_s^{s\top} \frac{\mathrm{d}\underline{i}_s^s}{\mathrm{d}t} \\
&= R_s \left\| \underline{i}_s \right\|^2 + L_m \underline{i}_s^{s\top} \frac{\mathrm{d}}{\mathrm{d}t} \left(\underline{i}_s^s + \underline{i}_r^s \right) + \frac{\mathrm{d}}{\mathrm{d}t} \left(\frac{1}{2} L_{\sigma s} \left\| \underline{i}_s \right\|^2 \right)
\end{aligned} \tag{3.81}
$$

$$
\begin{aligned}
\underline{i}_r^{s\top} \underline{u}_r^s &= \underline{i}_r^{s\top} \mathbf{T}_{rs} \left(R_r \underline{i}_r^r + \frac{\mathrm{d}\underline{\Psi}_r^r}{\mathrm{d}t} \right) \\
&= \underline{i}_r^{s\top} \left(R_r \underline{i}_r^s + \frac{\mathrm{d}\underline{\Psi}_r^s}{\mathrm{d}t} - \omega \mathbf{J} \underline{\Psi}_r^s \right) \\
&= R_r \underline{i}_r^{s\top} \underline{i}_r^s + L_m \underline{i}_r^{s\top} \frac{\mathrm{d}}{\mathrm{d}t} \left(\underline{i}_s^s + \underline{i}_r^s \right) + L_{\sigma r} \underline{i}_r^{s\top} \frac{\mathrm{d}\underline{i}_r^s}{\mathrm{d}t} - \omega \underline{i}_r^{s\top} \mathbf{J} \underline{\Psi}_r^s \\
&= R_r \left\| \underline{i}_r \right\|^2 + L_m \underline{i}_r^{s\top} \frac{\mathrm{d}}{\mathrm{d}t} \left(\underline{i}_s^s + \underline{i}_r^s \right) + \frac{\mathrm{d}}{\mathrm{d}t} \left(\frac{1}{2} L_{\sigma r} \left\| \underline{i}_r \right\|^2 \right) - \omega \underline{i}_r^{s\top} \mathbf{J} \underline{\Psi}_r^s
\end{aligned} \tag{3.82}
$$

$$\begin{aligned}
\underline{i}_s^{s\top}\underline{u}_s^s + \underline{i}_r^{s\top}\underline{u}_r^s &= R_s\left\|\underline{i}_s\right\|^2 + L_m\underline{i}_s^{s\top}\frac{\mathrm{d}}{\mathrm{d}t}\left(\underline{i}_s^s + \underline{i}_r^s\right) + \frac{\mathrm{d}}{\mathrm{d}t}\left(\frac{1}{2}L_{\sigma s}\left\|\underline{i}_s\right\|^2\right) \\
&+ R_r\left\|\underline{i}_r\right\|^2 + L_m\underline{i}_r^{s\top}\frac{\mathrm{d}}{\mathrm{d}t}\left(\underline{i}_s^s + \underline{i}_r^s\right) + \frac{\mathrm{d}}{\mathrm{d}t}\left(\frac{1}{2}L_{\sigma r}\left\|\underline{i}_r\right\|^2\right) - \omega\underline{i}_r^{s\top}\mathbf{J}\underline{\Psi}_r^s \\
&= R_s\left\|\underline{i}_s\right\|^2 + R_r\left\|\underline{i}_r\right\|^2 + L_m\left(\underline{i}_s^s + \underline{i}_r^s\right)^\top\frac{\mathrm{d}}{\mathrm{d}t}\left(\underline{i}_s^s + \underline{i}_r^s\right) \\
&+ \frac{\mathrm{d}}{\mathrm{d}t}\left(\frac{1}{2}L_{\sigma s}\left\|\underline{i}_s\right\|^2 + \frac{1}{2}L_{\sigma r}\left\|\underline{i}_r\right\|^2\right) - \omega\underline{i}_r^{s\top}\mathbf{J}\underline{\Psi}_r^s \\
&= R_s\left\|\underline{i}_s\right\|^2 + R_r\left\|\underline{i}_r\right\|^2 + \frac{\mathrm{d}}{\mathrm{d}t}\left(\frac{1}{2}L_m\left\|\underline{i}_s + \underline{i}_r\right\|^2\right) \\
&+ \frac{\mathrm{d}}{\mathrm{d}t}\left(\frac{1}{2}L_{\sigma s}\left\|\underline{i}_s\right\|^2 + \frac{1}{2}L_{\sigma r}\left\|\underline{i}_r\right\|^2\right) - \omega\underline{i}_r^{s\top}\mathbf{J}\underline{\Psi}_r^s
\end{aligned} \tag{3.83}$$

For the expression of the exchanged electrical energy within the time interval $\mathrm{d}t$, we obtain:

$$\begin{aligned}
\mathrm{d}E_{el} &= \frac{3}{2}\left(R_s\left\|\underline{i}_s\right\|^2 + R_r\left\|\underline{i}_r\right\|^2\right)\mathrm{d}t \\
&+ \frac{3}{2}\frac{\mathrm{d}}{\mathrm{d}t}\left(\frac{1}{2}L_m\left\|\underline{i}_s + \underline{i}_r\right\|^2 + \frac{1}{2}L_{\sigma s}\left\|\underline{i}_s\right\|^2 + \frac{1}{2}L_{\sigma r}\left\|\underline{i}_r\right\|^2\right)\mathrm{d}t \\
&- \frac{3}{2}\omega\underline{i}_r^{s\top}\mathbf{J}\underline{\Psi}_r^s\mathrm{d}t
\end{aligned} \tag{3.84}$$

On the right-hand side of Eq. (3.84), three energy components can be identified:

- The thermal energy generated by ohmic losses:

$$\mathrm{d}E_{th} = \frac{3}{2}\left(R_s\left\|\underline{i}_s\right\|^2 + R_r\left\|\underline{i}_r\right\|^2\right)\mathrm{d}t \tag{3.85}$$

- The exchanged magnetic energy:

$$\mathrm{d}E_{mag} = \frac{3}{2}\frac{\mathrm{d}}{\mathrm{d}t}\left(\frac{1}{2}L_m\left\|\underline{i}_s + \underline{i}_r\right\|^2 + \frac{1}{2}L_{\sigma s}\left\|\underline{i}_s\right\|^2 + \frac{1}{2}L_{\sigma r}\left\|\underline{i}_r\right\|^2\right)\mathrm{d}t \tag{3.86}$$

- The exchanged mechanical energy:

$$\mathrm{d}E_m = -\frac{3}{2}\omega\underline{i}_r^{s\top}\mathbf{J}\underline{\Psi}_r^s\mathrm{d}t = -\frac{3}{2}p\omega_M\underline{i}_r^{s\top}\mathbf{J}\underline{\Psi}_r^s\mathrm{d}t = \omega_M\cdot M_M\mathrm{d}t \tag{3.87}$$

In Eq. (3.87), ω_M denotes the mechanical angular velocity of the rotor, p the number of pole

pairs of the machine, and M_M the torque it delivers. From this, it follows:

$$\begin{aligned} M_M &= -\frac{3}{2}p(\underline{i}_r^s)^\top \mathbf{J}\underline{\Psi}_r^s \\ &= -\frac{3}{2}p(\mathbf{T}_{rs}\underline{i}_r^r)^\top \mathbf{J}\mathbf{T}_{rs}\underline{\Psi}_r^r \\ &= -\frac{3}{2}p\underline{i}_r^{r\top}\mathbf{T}_{rs}^\top \mathbf{J}\mathbf{T}_{rs}\underline{\Psi}_r^r \\ &= -\frac{3}{2}p\underline{i}_r^{r\top}\mathbf{J}\underline{\Psi}_r^r \\ &= -\frac{3}{2}p\left(\Psi_{rd}i_{rq} - \Psi_{rq}i_{rd}\right) \end{aligned} \tag{3.88}$$

Using the stator flux linkage equation (3.65b) and the rotor flux linkage equation transformed into stator coordinates (3.65d), an expression for the motor torque as a function of the space vectors $\underline{i}_s^s$ and $\underline{\Psi}_s^s$ can be obtained:

$$\begin{aligned} (3.65b) \wedge (3.65d) \quad \Longleftrightarrow \quad & \underline{i}_r^s = \frac{1}{L_m}\left(\underline{\Psi}_s^s - L_s\underline{i}_s^s\right) \\ \wedge \quad & \underline{\Psi}_r^s = \frac{L_r}{L_m}\underline{\Psi}_s^s + \left(L_m - \frac{L_rL_s}{L_m}\right)\underline{i}_s^s \end{aligned}$$

From this, it follows:

$$\begin{aligned} M_M &= -\frac{3}{2}p(\underline{i}_r^s)^\top \mathbf{J}\underline{\Psi}_r^s \\ &= -\frac{3}{2}p\frac{1}{L_m}\left(\underline{\Psi}_s^s - L_s\underline{i}_s^s\right)^\top \mathbf{J}\left(\frac{L_r}{L_m}\underline{\Psi}_s^s + \left(L_m - \frac{L_rL_s}{L_m}\right)\underline{i}_s^s\right) \\ &= -\frac{3}{2}p\frac{1}{L_m}\left(\underline{\Psi}_s^{s\top}\mathbf{J}\left(L_m - \frac{L_rL_s}{L_m}\right)\underline{i}_s^s - \frac{L_rL_s}{L_m}\underline{i}_s^{s\top}\mathbf{J}\underline{\Psi}_s^s\right) \\ &= \frac{3}{2}p\frac{1}{L_m}\left(\left(L_m - \frac{L_rL_s}{L_m}\right)\underline{i}_s^{s\top}\mathbf{J}\underline{\Psi}_s^s + \frac{L_rL_s}{L_m}\underline{i}_s^{s\top}\mathbf{J}\underline{\Psi}_s^s\right) \\ &= \frac{3}{2}p\underline{i}_s^{s\top}\mathbf{J}\underline{\Psi}_s^s = \frac{3}{2}p\left(\Psi_{s\alpha}i_{s\beta} - \Psi_{s\beta}i_{s\alpha}\right) \end{aligned} \tag{3.89}$$

Through a torque balance, the relationship between the mechanical angular velocity of the rotor ω_M, the electromagnetic torque M_M, and the load torque M_L can be derived:

$$\Theta_M\frac{\mathrm{d}\omega_M}{\mathrm{d}t} = M_M - M_L \tag{3.90}$$

Here, Θ_M denotes the rotor's moment of inertia. For machines with a pole pair number $p > 1$, the relationship

$$\theta = p \cdot \theta_M$$

between the mechanical rotor angle θ_M and the electrical angle θ must also be taken into account.

3.8 Signal Flow Diagram of the Fundamental Wave Model

For the simulation of the electromechanical behavior of the AC machine a signal flow diagram can be drawn. The model equations are summarized in the following:

Stator Voltage:
$$\underline{u}_s^s = R_s\ \underline{i}_s^s + \frac{\mathrm{d}\underline{\Psi}_s^s}{\mathrm{d}t} \tag{3.91}$$

Stator Flux Linkage:
$$\underline{\Psi}_s^s = L_s\ \underline{i}_s^s + L_m\ \underline{i}_r^s = \underbrace{L_m\,(\underline{i}_s^s + \underline{i}_r^s)}_{\underline{\Psi}_h^s} + L_{\sigma s}\ \underline{i}_s^s \tag{3.92}$$

Rotor Voltage:
$$\underline{u}_r^r = R_r\ \underline{i}_r^r + \frac{\mathrm{d}\underline{\Psi}_r^r}{\mathrm{d}t} \tag{3.93}$$

Rotor Flux Linkage:
$$\underline{\Psi}_r^r = L_r\ \underline{i}_r^r + L_m\ \underline{i}_s^r = \underbrace{L_m\,(\underline{i}_s^r + \underline{i}_r^r)}_{\underline{\Psi}_h^r} + L_{\sigma r}\ \underline{i}_r^r \tag{3.94}$$

Electro Mechanical Torque:
$$M_M = \frac{3}{2}\ p\ \underline{i}_s^{s\top}\ \mathbf{J}\ \underline{\Psi}_s^s = \frac{3}{2}\ p\ (\Psi_{s\alpha}\ i_{s\beta} - \Psi_{s\beta}\ i_{s\alpha}) \tag{3.95}$$

Mechanic Equation:
$$\Theta_M \frac{\mathrm{d}\omega_M}{\mathrm{d}t} = M_M - M_L \tag{3.96}$$

The inputs of the signal flow diagram are the voltage space vectors $\underline{u}_s^s$, $\underline{u}_r^r$ and the load torque M_L. Their outputs generate the current space vectors $\underline{i}_s^s$, $\underline{i}_r^r$, the flux linkage $\underline{\Psi}_s^s$, $\underline{\Psi}_r^r$ and the scalar motor torque M_M with the corresponding rotor speed ω_M.
The *Blondel's leakage coefficient* σ is expressed with:

$$\sigma = \left(1 - \frac{L_m^2}{L_s\ L_r}\right) \tag{3.97}$$

3.8.1 Drawing of the Signal Flow Diagram

Note: The exercises marked by a * should be solved at the preparation.

1.) ***** Draw the signal flow diagram with the inputs $\underline{u}_s^s$, $\underline{i}_s^s$ and the output $\underline{\Psi}_s^s$.
Also draw the corresponding diagram of the rotor side with $\underline{u}_r^r$, $\underline{i}_r^r$ as input and $\underline{\Psi}_r^r$ as output.

2.) ***** Draw the signal flow diagram for the generation of the space vector $\underline{\Psi}_h^s$ with the current space vector in **stator coordinates** $\underline{i}_s^s$ and the rotor space vector in **rotor coordinates** $\underline{i}_r^r$ as inputs.
Then add another path for the calculation of $\underline{i}_s^s$ by means of the vectors $\underline{\Psi}_s^s$ and $\underline{\Psi}_h^s$.
Add a second path to derive $\underline{i}_r^r$ from the inputs $\underline{\Psi}_r^r$ and $\underline{\Psi}_h^r$. Use the following blocks 3.8 to draw the transformation of the coordinate systems.

Figure 3.8: Block symbols of the Transformation Between Rotor and Stator Coordinates

3.) * Setup the signal flow diagram for the generation of the torque M_M from the components of the stator flux space vector $\Psi_{s\alpha}$ and $\Psi_{s\beta}$, as well as the components of the stator current space vector $i_{s\alpha}$ and $i_{s\beta}$.

4.) * Draw the signal flow diagram for the mechanic subsystem with M_M and M_L as an input and ω_M, θ_M and θ_{el} as an output.

5.) * Based on the previously derived partial diagrams, draw the signal flow diagram of the fundamental wave model (Inputs: $\underline{u}_s^s$, $\underline{u}_r^r$, M_L; Outputs: ω_M, M_M, $\underline{i}_s^s$, $\underline{i}_r^r$, $\underline{\Psi}_s^s$, $\underline{\Psi}_r^r$).

The signal flow diagram is not allowed to have derivation blocks in its Simulink-Implementation. All differential equations have to be built with integrators. Otherwise the calculation of the currents and flux linkages consist an *algebraic loop*. So for every time step an equation system has to be solved by an iterative approach to determine the state variables for the next time step. This will result in a massive increase of calculation time. Hence the system has to be modified.

6.) * The elimination of the problem requires changes of the signal flow diagram. Therefore express the space vectors $\underline{i}_s^s$, $\underline{i}_r^s$ and $\underline{\Psi}_h^s$ as functions of $\underline{\Psi}_s^s$ and $\underline{\Psi}_r^s$. This approach allows the calculation of the currents by means of the flux linkages.

7.) * Draw the resulting whole signal flow diagram.

3.9 Model of the Asynchronous Machine with Squirrel Cage

In this section the derived fundamental wave model for AC machines should be applied for an asychronous machine with squirrel cage. The data sheet values of the regarded motor are stated in table 3.1:

Parameter	**Symbol and Value (SI)**			
Nominal Mechanical Power	P_N	=	2,2	[kW]
Nominal Speed	N_N	=	2 890	[min^{-1}]
Nominal Voltage (Star-Connection, Line-To-Line)	U_{NY}	=	400	[V]
Nominal Current (Star-Connection)	I_{NY}	=	4,5	[A]
Nominal Frequency	f_N	=	50	[Hz]

Table 3.1: Parameters of the Considered Asynchronous Machine

8.) * Which condition does the rotor voltage $\underline{u}_r^r$ fulfill in the case of an asynchronous machine with squirrel cage?

9.) * How many pole pairs p does the investigated machine have according to table 3.1? Calculate the nominal rotational speed ω_{MN}, the nominal torque M_{MN} and the nominal slip s_N.

From now on we assume, that the machine is fed by an ideal three phase voltage source, which delivers the following phase voltages:

$$\begin{aligned} u_A &= \hat{u_s}\cos(\omega_e t) \\ u_B &= \hat{u_s}\cos(\omega_e t - 2\pi/3) \\ u_C &= \hat{u_s}\cos(\omega_e t - 4\pi/3) \end{aligned}$$

The voltage amplitude $\hat{u_s}$ and the angular frequency ω_e are adjustable.

10.) Open the File `Investigation_ASM.slx` in the directory `Experiment_3` in `Simulink` and model the voltage source in a subsystem. Therefore use variables to set the voltage frequency and amplitude, to define these parameters in the script file `Experiment_3_ASM_Parameter.m`.

Hint: Use a `Sine` block to model the voltage source.

11.) Implement the Clarke transformation and their inverse for the calculation of the components x_α and x_β of a space vector based on the corresponding string values x_A, x_B and x_C. Generate one subsystem for each.

Hint: Use simple `Simulink` blocks as `Gains` and `Summations` to implement the Clarke transformation.

12.) Implement the Park transformation and their inverse in two different subsystems, to express space vectors in different rotating coordinate systems.

Hint: Use simple `Simulink` blocks as `Gains` and `Summations` to implement the Park transformation.

13.) Set the effective value of the line-to-line output voltage of the source to 400 [V] and their frequency to 50 [Hz]. View the time course of both components of the voltage space vector and explain them.

Hint: Consider the connection type of the phases.

14.) Import a copy of the general block `General_AC_Machine` out of the file with the same name and compare it's content with your signal flow diagram from problem 7.
Double clicking onto the block `Initialize` and simulate the start-up phase.

Evaluate the resulting courses of the stator and rotor currents. Also investigate the torque-speed-characteristic and justify your observations.

Now the machine gets coupled with a processing machine, the resulting inertia moment Θ_M changes to 0,02 [kg m^2].

15.) Explain changes in the time courses and at the torque-speed-characteristics compared to the problem before.

16.) Simulate the behavior of the machine, if the following load torque is applied:

$$M_L(t) = M_{MN}\ (\sigma(t - t_M) - \sigma(t - 2t_M)),\ t_M = 1\,[\mathrm{s}] \tag{3.98}$$

with

$$\sigma(t) = \begin{cases} 0 & \text{if} \quad t \leq 0\,[\mathrm{s}] \\ 1 & \text{if} \quad t > 0\,[\mathrm{s}] \end{cases} \tag{3.99}$$

Determine the graphical nominal speed. Does it correspond to the values given in table 3.1? Determine the space vector amount of the stator flux $\Psi_{sN} = \|\underline{\Psi}_s\|$ and the rotor flux $\Psi_{rN} = \|\underline{\Psi}_r\|$ at the nominal point.

17.) Determine the tilting torque M_T in motor operation and the corresponding tilting slip s_T. Calculate the overload ratio of the machine M_T/M_N.

3.10 Model of the Permanent Magnet Synchronous Machine

The behavior of the synchronous machine with surface mounted permanent magnets can also be described by the fundamental wave model. In this case we have to consider that there are permanent magnets mounted on the rotor, but no windings. This leads ideally to a sinusoidal distributed field in the air gap. Furthermore, the magnetic field caused by the magnets is invariant due to the rotor fixed coordinate system.
For these reasons the flux linkage space vector $\underline{\Psi}_{PM}$ is introduced. It is **constant** and expressed in the rotor frame:

$$\underline{\Psi}_r^r = \begin{pmatrix} \Psi_{PM} \\ 0 \end{pmatrix} \tag{3.100}$$

$$\underline{i}_r^r = \underline{0} \tag{3.101}$$

The stator side equations thus reduce to:

$$\text{Stator Voltage:} \qquad \underline{u}_s^s = R_s\, \underline{i}_s^s + \frac{\mathrm{d}\underline{\Psi}_s^s}{\mathrm{d}t} \tag{3.102a}$$

$$\text{Stator Flux Linkage:} \qquad \underline{\Psi}_s^s = L_s\, \underline{i}_s^s + \underline{\Psi}_{PM}^s \tag{3.102b}$$

The parameters of the considered engine in this section are given in table 3.2:

Parameter	**Symbol and Value (SI)**			
Nominal Power	P_N	=	4,4	[kW]
Nominal Rotational Speed	N_N	=	2 000	[min^{-1}]
Nominal Voltage (Star-Connection, Line-To-Line)	U_{NY}	=	400	[V]
Nominal Current (Star-Connection)	I_{NY}	=	9,9	[A]
Nominal Frequency	f_N	=	100	[Hz]
Pole Pair Number	p	=	3	[1]
Rotor Inertia Moment	Θ_M	=	$1{,}0 \times 10^{-3}$	[kg m^2]
Stator Resistance	R_s	=	1,2	[Ω]
Stator Inductance	L_s	=	12	[mH]
Permanent Magnet Flux	Ψ_{PM}	=	0,36	[Vs]

Table 3.2: Parameters of the Considered Synchronous Machine

18.) * Express the stator current space vector $\underline{i}_s^s$ as a function of $\underline{\Psi}_s^s$ and $\underline{\Psi}_{PM}^s$. Then draw the signal flow diagram for the permanent magnet synchronous machine (Inputs: $\underline{u}_s^s$, M_L; Outputs: ω_M, M_M, $\underline{i}_s^s$, $\underline{\Psi}_s^s$).

19.) * Calculate the value of the nominal torque M_{MN}.

20.) Open file `Investigation_PMSM.slx` in `Simulink`. Copy all elements previous used in the fundamental wave model into the block `PMSM`. Modify the blocks at the necessary points, to derive to the signal flow diagram of the synchronous machine. Add an instance of an ideal voltage source and connect it to the motor model.
Simulate the behavior of the permanent magnet synchronous machine from table 3.2 without load torque at the static three phase supply (400 [V], 50 [Hz]). Justify the resulting engine speed.

21.) Modify the voltage source to enable run up to the half of the nominal rotor speed. Therefore increase the frequency linear by time until the half of the nominal frequency is reached.
Can it be helpful to imprint a voltage source that is proportional to the frequency? Pay attention that the nominal current I_{NY} is not exceeded.

22.) Use the following load course, to investigate the machine:

$$M_L(t) = M_{MN}\ \sigma(t - t_M),\ t_M = 2\,[\mathrm{s}] \tag{3.103}$$

Which effect has the load torque onto the rotor speed? How does the electro-mechanical energy conversion process expire in this case? Justify your answer by figures of the relevant values.

Experiment 4
Field Oriented Control of the AC Drive

4.1 Overview

In comparison to the DC machine that is sensitive to commutator failures, the synchronous and the asynchronous machine have the advantage of a robust structure and low maintenance effort. Therefore they are popular for the realization of drive systems.
An independent control of flux and torque, as known from the DC machine is not possible without special preparations. Hence the cascade structure from experiment 2 is not directly applicable to the AC machine.
In this experiment we introduce the *field oriented control* (FOC) for AC machines and analyze it's static and dynamic functions. The stator current space vector is decomposed into a flux-forming and a torque-forming component by an appropriate coordinate transformation. Each component then is controlled individually by a linear PID (Proportional-Integral-Derivative) controller. Under these circumstances the flux and motor speed can be controlled by a super-ordinate control loop. Then the controllers can be tuned to the modulus optimum (MO) or the symmetrical optimum (SO).
Within this experiment the field oriented control of an asynchronous machine with squirrel cage, that is fed by an converter, is implemented and simulated. For this purpose the machine equations and the sensing known from the previous experiments are used.

4.2 Basic Consideration

4.2.1 Definition of the Rotor Flux Oriented Coordinate System

As demonstrated in section 3.4.4, by means of the Park transformation ($\mathbf{T}_{\mathbf{P}\varphi}$) the space vector can be transformed from stator coordinates to an arbitrary rotor coordinate system. In the previous experiment the reference system was the stator voltage space vector to show the linear properties of the AC machine. We will see that a reference system ($\vec{e}_d$, $\vec{e}_q$) linked to the rotor flux linkage simplifies the fundamental wave model clearly for control purposes. Therefore a new frame rotated by the angle φ_K is constructed, in which the rotor flux space vector can be written in following way:

$$\underline{\Psi}_r = \|\underline{\Psi}_r\|\,\vec{e}_d = \begin{bmatrix} \Psi_r^d \\ \Psi_r^q \end{bmatrix} = \begin{bmatrix} \|\underline{\Psi}_r\| \\ 0 \end{bmatrix} \tag{4.1}$$

In this case φ_K is the angle of the rotor flux space vector in stator coordinates, $\underline{\Psi}_r^s$ (see Fig. 4.1). For this the reason the defined (d, q)-coordinate system is called *rotor flux oriented* or even more common *field oriented*. Also the abbreviation *k-coordinate system* is used. Then in the space vector notation a superscripted k is used.

The rotation matrix $\mathbf{T}(\varphi_K)$, that transforms a space vector from the k-coordinate system to stator coordinates is:

$$\mathbf{T}(\varphi_K) = \begin{bmatrix} \cos\varphi_K & -\sin\varphi_K \\ \sin\varphi_K & \cos\varphi_K \end{bmatrix} \tag{4.2}$$

The notation $\mathbf{T}_{ks} = \mathbf{T}(\varphi_K)$ and $\mathbf{T}_{sk} = \mathbf{T}(-\varphi_K)$ is used.

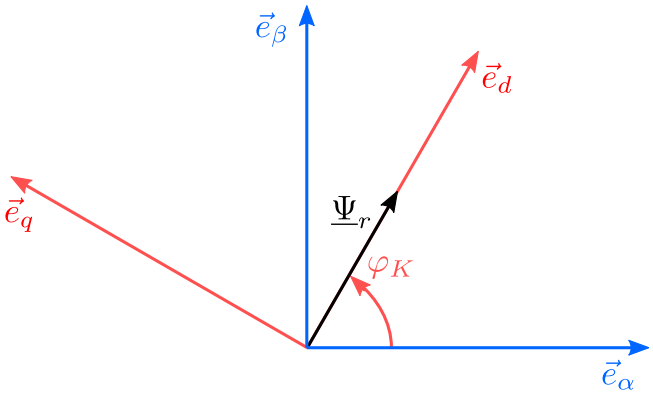

Figure 4.1: Definition of the Rotor Flux Angle φ_K Rotated into the (d, q)-Coordinate System with the Transformation $\mathbf{T}_P(\varphi_K)$

4.2.2 Model of the Asynchronous Machine in the k-Coordinate System

The mathematical relations between the electrical variables in the field-oriented coordinate system are also formulated by the equation system (3.67). Since we are looking at a squirrel cage asynchronous machine the rotor voltage space vector is zero.

$$\underline{u}_s^k = R_s\ \underline{i}_s^k + \frac{\mathrm{d}\underline{\Psi}_s^k}{\mathrm{d}t} + \omega_K\ \mathbf{J}\ \underline{\Psi}_s^k \quad \text{with} \quad \omega_K = \dot{\varphi}_K \tag{4.3a}$$

$$\underline{\Psi}_s^k = L_s\ \underline{i}_s^k + L_m\ \underline{i}_r^k = L_m\left(\underline{i}_s^k + \underline{i}_r^k\right) + L_{\sigma s}\ \underline{i}_s^k \tag{4.3b}$$

$$\underline{0} = R_r\ \underline{i}_r^k + \frac{\mathrm{d}\underline{\Psi}_r^k}{\mathrm{d}t} + (\omega_K - \omega)\ \mathbf{J}\ \underline{\Psi}_r^k \tag{4.3c}$$

$$\underline{\Psi}_r^k = L_r\ \underline{i}_r^k + L_m\ \underline{i}_s^k = L_m\left(\underline{i}_r^k + \underline{i}_s^k\right) + L_{\sigma r}\ \underline{i}_r^k \tag{4.3d}$$

To complete the model, the electromagnetic torque, M_M, has to be expressed in the k-coordinate system. This is done in equation (4.4):

$$\begin{aligned} M_M &= -\frac{3}{2}\, p\, (\underline{i}_r^s)^\top\, \mathbf{J}\, \underline{\Psi}_r^s \\ &= -\frac{3}{2}\, p\, (\mathbf{T}_{ks}\underline{i}_r^k)^\top \mathbf{J}\, \mathbf{T}_{ks}\, \underline{\Psi}_r^k = -\frac{3}{2}\, p\, \underline{i}_r^{k\top} \mathbf{T}_{ks}^\top \mathbf{J}\, \mathbf{T}_{ks}\, \underline{\Psi}_r^k \\ &= -\frac{3}{2}\, p\, \underline{i}_r^{k\top} \mathbf{J}\, \underline{\Psi}_r^k = -\frac{3}{2}\, p\, \left(\Psi_r^d\, i_r^q - \Psi_r^q\, i_r^d\right) \\ &= -\frac{3}{2}\, p\, \Psi_r^d\, i_r^q = -\frac{3}{2}\, p\, \|\underline{\Psi}_r\|\, i_r^q \end{aligned} \tag{4.4}$$

The torque is determined by the absolute value of the rotor flux space vector and the quadrature component i_r^q of the rotor current.
The direct change of the rotor currents is not possible for the asynchronous machine with squirrel cage. Therefore the model equations are rewritten to derive a relation between the M_M, the value of $\underline{\Psi}_r^d$ and the stator current space vector $\underline{i}_s^d$.
If the condition (4.1) $\Psi_r^q = 0$ respectively $\dot{\Psi}_r^q = 0$, is inserted in 4.3d:

$$\begin{aligned} \Psi_r^q = 0 &= L_r\, i_r^q + L_m\, i_s^q \\ \Longleftrightarrow i_r^q &= -\frac{L_m}{L_r}\, i_s^q \end{aligned} \tag{4.5}$$

The rotor voltage and flux linkage equation are:

$$\begin{aligned} 0 = R_r\, i_r^d + \frac{\mathrm{d}\Psi_r^d}{\mathrm{d}t} &= \frac{R_r}{L_r}(\Psi_r^d - L_m\, i_s^d) + \frac{\mathrm{d}\Psi_r^d}{\mathrm{d}t} \\ \Longleftrightarrow T_r \frac{\mathrm{d}\Psi_r^d}{\mathrm{d}t} + \Psi_r^d &= L_m i_s^d \end{aligned} \tag{4.6}$$

Here $T_r = L_r/R_r$ states the *rotor time constant*. The transformation of the equation into the Laplace domain results in:

$$\Psi_r^d(s) = \frac{L_m}{1 + s\, T_r}\, i_s^d(s) \tag{4.7}$$

Looking at equation (4.7) it can be suggested, that the absolute value of the rotor flux linkage, $\|\underline{\Psi}_r\|$, can be set by the first component of the stator current, i_s^d, with the time constant T_r. For that reason i_s^d is called the *flux forming* component.
Finally from (4.4) and (4.5) results the torque:

$$M_M = -\frac{3}{2} p\, \|\underline{\Psi}_r\|\, i_r^q = \frac{3L_m}{2L_r}\, p\, \|\underline{\Psi}_r\|\, i_s^q \tag{4.8}$$

Provided that the value of the rotor flux, $\|\underline{\Psi}_r\| = \Psi_r^d$, can be kept at a constant value, the

torque can be controlled by the quadrature component of the stator current, i_s^q without time delay. Hence i_s^q states the *torque forming* current component.
In the rotor flux oriented coordinate system a similar relation to the torque is given as the DC machine has (compare to (1.5c)). To use this property the knowledge about the amount and the angle of the rotor flux space vector is necessary. A simple method is introduced in the next section.
In summary the model equations of the asynchronous machine with squirrel cage are given in the rotor flux oriented coordinate system:

$$\text{Stator Voltage:} \qquad \underline{u}_s^k = R_s\ \underline{i}_s^k + \frac{\mathrm{d}\underline{\Psi}_s^k}{\mathrm{d}t} + \omega_K\ \mathbf{J}\ \underline{\Psi}_s^k \tag{4.9a}$$

$$\text{Stator Flux Linkage:} \qquad \underline{\Psi}_s^k = L_s\ \underline{i}_s^k + L_m\ \underline{i}_r^k \tag{4.9b}$$

$$\text{Rotor Voltage:} \qquad 0 = R_r\ \underline{i}_r^k + \frac{\mathrm{d}\underline{\Psi}_r^k}{\mathrm{d}t} + (\omega_K - \omega)\ \mathbf{J}\ \underline{\Psi}_r^k \tag{4.9c}$$

$$\text{Rotor Flux Linkage:} \qquad \underline{\Psi}_r^k = L_r\ \underline{i}_r^k + L_m\ \underline{i}_s^k \tag{4.9d}$$

$$\text{Torque:} \qquad M_M = -\frac{3}{2}\ p\ (\underline{i}_r^k)^\top\ \mathbf{J}\ \underline{\Psi}_r^k = \frac{3L_m}{2L_r}\ p\,\|\underline{\Psi}_r\|\,i_{sl} \tag{4.9e}$$

$$\text{Mechanic:} \qquad \Theta_M \frac{\mathrm{d}\omega_M}{\mathrm{d}t} = M_M - M_L \tag{4.9f}$$

4.2.3 Determination of the Rotor Flux Space Vector

In practice the flux linkage at the rotor side cannot be measured directly and the rotor flux space vector has to be replicated by available values from the model. Usually the stator currents, rotational speed and stator voltages are available, because they get measured directly or can be easily determined.
A possible approach is the use of the rotor sided voltage and flux equations in the stator coordinate system and to calculate the electrical rotor angular velocity ω and the rotor flux space vector with the stator current space vector $\underline{i}_s^s$.
Following is valid:

$$\begin{aligned}
3.94 \qquad &\Longleftrightarrow \qquad \mathbf{T}_{rs}\ \underline{u}_r^r = \underline{0} = \mathbf{T}_{rs}\ R_r\ \underline{i}_r^r + \mathbf{T}_{rs} \frac{\mathrm{d}[\mathbf{T}_{rs}\ \underline{\Psi}_r^s]}{\mathrm{d}t} \\
&\Longleftrightarrow \qquad \underline{0} = R_r\ \underline{i}_r^s + \frac{\mathrm{d}\underline{\Psi}_r^s}{\mathrm{d}t} - \omega\ \mathbf{J}\ \underline{\Psi}_r^s \\
&\Longleftrightarrow \qquad \frac{\mathrm{d}\underline{\Psi}_r^s}{\mathrm{d}t} = -R_r\ \underline{i}_r^s + \omega\ \mathbf{J}\ \underline{\Psi}_r^s
\end{aligned} \tag{4.10}$$

$$\begin{aligned}
3.95 \qquad &\Longleftrightarrow \qquad \mathbf{T}_{rs}\ \underline{\Psi}_r^r = L_r\ \mathbf{T}_{rs}\ \underline{i}_r^r + L_m\ \mathbf{T}_{rs}\ \underline{i}_s^r \\
&\Longleftrightarrow \qquad = \underline{\Psi}_r^s = L_r\ \underline{i}_r^s + L_m\ \underline{i}_s^s \\
&\Longleftrightarrow \qquad \underline{i}_r^s = \frac{1}{L_r}\,(\underline{\Psi}_r^s - L_m\ \underline{i}_s^s)
\end{aligned} \tag{4.11}$$

$$
\begin{aligned}
4.10 \wedge 4.11 \qquad &\Longleftrightarrow \qquad \frac{\mathrm{d}\underline{\Psi}_r^s}{\mathrm{d}t} = -\frac{R_r}{L_r}\left(\underline{\Psi}_r^s - L_m\ \underline{i}_s^s\right) + \omega\ \mathbf{J}\ \underline{\Psi}_r^s \\
&\Longleftrightarrow \qquad = \frac{1}{T_r}\left(L_m\ \underline{i}_s^s - \underline{\Psi}_r^s\right) + \omega\ \mathbf{J}\ \underline{\Psi}_r^s
\end{aligned} \tag{4.12}
$$

Equation (4.12) allows a practical calculation of the rotor flux space vector by integration based on the stator currents and the rotational velocity.
But here the knowledge of the *model parameters* R_r, L_r, and L_m is required. These can simply be determined experimentally by an *No-Load-Test* and *Blocked-Rotor-Test*.

4.2.4 Principle Structure of the Field Oriented Control

As derived above the rotor flux orientation enables a decomposition of the stator current space vector in the k-coordinate system in a *flux forming* value i_s^d and a *torque forming* value i_s^q. Both can be used as actuating variables for flux and torque control.
In the considered case the flux and torque (speed) control are used in a *cascade structure* with subordinated current control in the k-coordinate system (see Fig. 4.2).

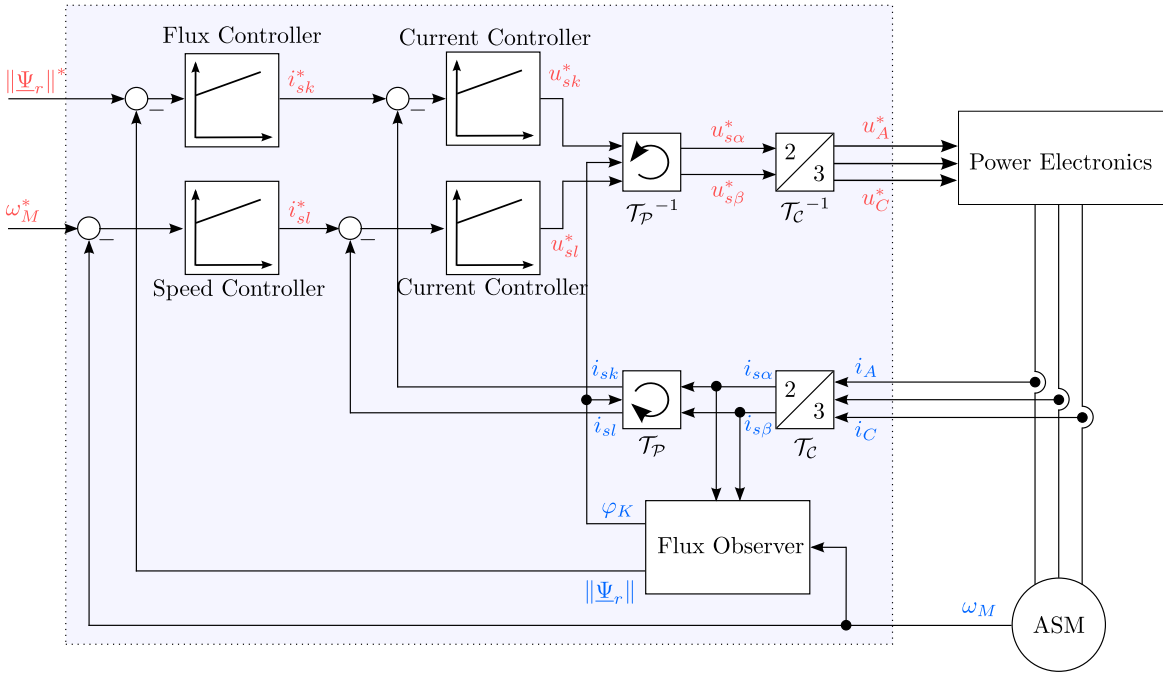

Figure 4.2: Schematic Representation of Field Oriented Speed Control with Subordinated Current Control in the Rotor Flux Coordinate System

The control of the current components in the $(d,\ q)$-coordinate system has the advantage that in steady-state operation two linear controllers can be used. The current controllers provides the reference stator voltage components u_s^{d*} and u_s^{q*}.
This concept requires the knowledge of the actual values i_s^d, i_s^q and Ψ_r^k, which are not directly mensurable. By applying the Clarke transformation the stator current space vector can be

calculated with the phase currents. The flux estimator based on equation (4.12) enables the determination of Ψ_r^k and φ_K. The Park transformation delivers the values for i_s^d and i_s^q. Furthermore, the current controllers output reference voltages in field oriented coordinates. Then the corresponding phase values u_A^*, u_B^* and u_C^* for the activation of the electronic actuators have to be calculated. This happens with the inverse transformation to the stator coordinate system and the subsequent application of the Clarke transformation.

4.3 Description of the Considered Drive System

Topic of the experiment is the design and simulation of the field oriented control of an AC machine. This consists out of an asynchronous motor with squirrel cage, H-bridge converter as electronic actuator and the sensing of the phase currents and the rotor speed. The properties of each component is described in the following section.

4.3.1 Asynchronous Motor

The data sheet parameters of the used asynchronous machine are summarized in table 4.1. The three phases of the machine are connected at a star-point and get supplied by a symmetrical power supply. Additionally the rotor inertia is given:

Physical Values	**Symbol and Value (SI)**			
Nominal Power	P_N	=	2,2	[kW]
Nominal Rotational Speed	N_N	=	2 890	[min^{-1}]
Nominal Torque	M_{MN}	=	7,3	[N m]
Nominal Voltage (Star-Connection, Line-To-Line)	U_{NY}	=	400	[V]
Nominal Current (Star-Connection)	I_{NY}	=	4,5	[A]
Nominal Frequency	f_N	=	50	[Hz]
Rotor Inertia Moment	Θ_M	=	$2{,}2 \times 10^{-3}$	[kg m^2]

Table 4.1: Data of the Considered Asynchronous Machine

In general, the field oriented has good performance, but low robustness against parameter deviations. Also the parameters for the implementation have to be determined by the no-load and blocked-rotor test. For the simulation the following parameters were measured and are summarized in table 4.2:

Value	Symbol and Value (SI)			
Stator Resistance	R_s	=	2,3	[Ω]
Rotor Resistance (Stator Coordinates)	R_r	=	2,9	[Ω]
Stator Inductance	L_s	=	340	[mH]
Rotor Inductance (Stator Coordinates)	L_r	=	340	[mH]
Coupling Inductance	L_m	=	326	[mH]
Rotor Flux	Ψ_{rN}	=	0,95	[Vs]

Table 4.2: Model Parameter of the Asynchronous Machine

4.3.2 Two-Level Converter

The asynchronous machine is fed by an *H-bridge converter* as shown in figure 4.3. In comparison to experiment 1 the DC/DC converter consists of a third leg (see Fig 1.1). The IGBT-modulus `S1` to `S6` are considered as ideal switches and get opened or closed by the binary command signals s_1 to s_6.

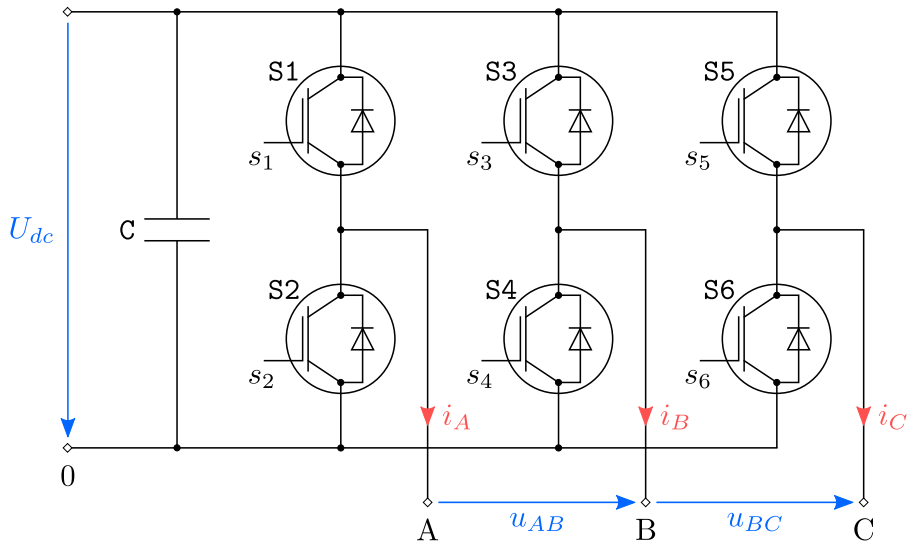

Figure 4.3: Principle Circuit Diagram of the Two-Level Converter

To prevent short circuit of the DC-bus U_{dc}, if one switch of the half bridge is closed, the counterpart has to be opened. This is performed by the logical negation of the signals s_2, s_4 and s_6 to the reference command signal s_1, s_3 and s_5.
Basically the line-to-line voltages u_{AB} and u_{BC} take the discrete value U_{dc}, 0 or $-U_{dc}$. With pulse width modulation (PWM) arbitrary average voltages in the interval $[-U_{dc}; U_{dc}]$ can be modeled (see experiment 1).
Similar to experiment 1, a PWM-modulator is used for the generation of the command signals from the desired values defined by the current controller. A triangular signal in the range of $[-1; 1]$ with the period T_c is used as reference signal (*carrier signal*). In contrast to the H-

bridge from experiment 1, each half bridge is now driven by an individual set point signal u_A^*, u_B^* and u_C^*.
The waveform of the set point signals u_A^*, u_B^* and u_C^* are sinusoidal, as is valid for AC drives in steady state. Hence, this control method is called *sine-triangle-modulation*. (see [3, Chapter 8].
Similar to the case of the H-bridge, the maximal time delay for the realization of the target values matches with the carrier period T_c. For the controller design, the converter again is approximated as an amplifying first-order delay block. Hence, the transfer functions for the phase voltages between actual and target value is defined in field oriented coordinates:

$$G_U(s) = \frac{u_{k,l}(s)}{u_{k,l}^*(s)} = \frac{U_{dc}/2}{1 + s\ T_c} \tag{4.13}$$

The parameters of the considered converter are stated in Table 1.3.

Physical Value	**Symbol and Value (SI)**
DC-Bus	$U_{dc} = 560$ [V]
Carrier Period	$T_c = 250$ [μs]

Table 4.3: Parameter of the Considered Converter

4.3.3 Sensing

The phase currents i_A and i_B are measured. The resulting measurement signals i_A^m and i_B^m are affected by noise. They are **not** filtered, so that the current measurements can be assumed to be **without delay**.
The rotor angle is determined by an incremental encoder and the rotor speed ω_M gets calculated by derivation with respect to time. Hence, the obtained speed signal ω_M^m has to be filtered. Here a first-order filter with the time constant $T_{f,\omega_M} = 2$ [ms] is implemented. For the design of the control loop, this delay has to be considered.

4.4 Implementation of the Field Oriented Control

4.4.1 Current Control Loop

Note: The exercises marked by a * shall be solved as preparation.

Similar to the case of the DC drive, both controllers of the inner current control loops have to be designed and implemented first in the field oriented coordinate system. Thus, again

linear controllers of the PID-type can be tuned according to modulus optimum (MO) or to symmetrical optimum (SO).
For the design of the current control loop the following requirements have to be met:

- The control loop has to be stable.
- The current controller has to be able to control stationary disturbances.
- The current control loop has to exhibit good command response behaviour.

1.) * From the equation set 4.9, express the two components of the stator voltage space vector u_s^d and u_s^q, in the following form:

$$u_s^d = R' \; i_s^d + L' \frac{\mathrm{d}i_s^d}{\mathrm{d}t} + a_1 \; \Psi_r^d + b_1 \; i_s^q \tag{4.14a}$$

$$u_s^q = R' \; i_s^q + L' \frac{\mathrm{d}i_s^q}{\mathrm{d}t} + a_2 \; \Psi_r^d + b_2 \; i_s^d \tag{4.14b}$$

Give expressions for the constants R' and L', the coefficients a_1, a_2, b_1 and b_2 as a function of the machine parameters and the angular speeds ω_K and ω.

Hint: Use Blondel's leakage coefficient to simplify the equation. Try to find a expression for the derivative of the rotor flux and insert the condition 4.1 just at the end of your calculation.

2.) * Transform the equation system 4.14 to the Laplace domain and draw the related signal flow diagram with i_s^d and i_s^q as outputs.
What do the values $a_1 \; \Psi_r^d + b_1 \; i_s^q$ and $a_2 \; \Psi_r^d + b_2 \; i_s^q$ represent in the current control loop? By taking Which measures can this effect be eliminated, under the assumptions of the exact knowledge of all machine parameters and $\omega_K \approx \omega_{el}$?

Hint: Remember the approach at the DC machine, that allowed to compensate the speed dependent disturbance.

In the following it is assumed, that the effects of the above values are compensated in an appropriate manner.

3.) * Determine the transfer function F_i between the current i_s^d (respectively i_s^q) and the desired voltage signal u_s^{d*} (respectively u_s^{q*}) under consideration of the converter. State the expression of the small and the big time constants $T_{\sigma,i}$ respectively $T_{1,i}$.

4.) * Design a current controller under the requirements of the current control loop. According to which optimization criteria should the controller be optimized? Justify your answer.

5.) Open the file `ASM_FOC_Implementation.slx` in the directory `Experiment_4` in `Simulink`. Next to the simplified AC drive model there exists a subsystem `Field Oriented Control` with the required transformation and flux estimation blocks. What is the block `Decoupling`

for?
Build, similar to the previous experiments, the current controller with the help of some `Gain` and `Integrator` blocks out of the `Simulink`-library.
Implement the control of the currents i_s^d and i_s^q in the subsystem `Field Oriented Control`.
Complete the file `Experiment_4_Parameter.m` by the missing parameters. Take them over by double clicking onto the `Initialize` block.

6.) State the target value of the flux forming current $i_s^d = 3\,[\mathrm{A}]$. For the torque forming current i_s^q use the following target values:

$$i_s^{q*}(t) = 2\ (\sigma(t - t_A) - \sigma(t - t_B))\ [\mathrm{A}]\,,\ t_A = 0{,}6\,[\mathrm{s}]\,,\ t_B = 0{,}8\,[\mathrm{s}] \tag{4.15}$$

where

$$\sigma(t) = \begin{cases} 0 & \text{for} \quad t \leq 0\,[\mathrm{s}] \\ 1 & \text{for} \quad t > 0\,[\mathrm{s}] \end{cases} \tag{4.16}$$

Simulate the machine behavior without load and evaluate the course of the relevant .
Determine the rise and adjust time at an tolerance band of $\pm 2\%$ as well the maximum overshoot for the simulated response of the torque forming current at the positive edge of the target value pulse. Justify possible deviations from the indication of the optimization table 2.6.

7.) Evaluate the dynamic of the rotor flux. Why does the observed behavior occur?

8.) Which effect has a failure of the decoupling onto the courses of the current components i_s^d and i_s^q? Explain the effect, that happens in this case.

4.4.2 Flux and Rotor Speed Control

After the implementation of the inner current control loops the flux and the rotor speed controller of the outer loop can be designed. For the controller design the previously optimized current control loop is approximated by a first-order-delay block (see section 2.4).

Design of the Flux Controller

9.) * Approximate the closed current control loop by the substitute transfer function with the first-order-delay-behavior and the time constant $T_{equi,\,i}$. State the expression of $T_{equi,\,i}$ as a function of the current control loop time constants. Pay attention that **no** measurement value smoothing is present.

10.) * Under consideration of the approximation from problem 9, state the transfer function, F_{Ψ_r}, between the components Ψ_{rk} of the rotor flux linkage and the target value of the flux forming current i_s^{d*}:

$$F_{\Psi_r}(s) = \frac{\Psi_r^d(s)}{i_s^{d*}(s)} \tag{4.17}$$

Determine the small and the big time constant $T_{\sigma,\,\Psi_r}$ respectively $T_{1,\,\Psi_r}$.

11.) * Design a controller, that is able to control stationary disturbances and exhibits good command response behaviour. Justify your approach.

12.) Implement the flux control loop. Use the nominal flux Ψ_{rN} as a target value and simulate the resulting machine behavior with $i_s^q = 0$ and $M_L = 0$. Evaluate the course of the flux and the flux forming current.
To prevent possible damage of the stator windings, the stator current is not allowed to exceed the 1,5 multiple of the nominal value. Verify, if this condition is satisfied. Insert, if necessary, a saturation block at the appropriate position. What effect has the saturation onto the flux course?

13.) Implement a measure to improve the control accuracy, without changing the basic type of controller.

Implementation of the Rotor Speed Control Loop

In the following the speed controller is designed. For this propose assume that the machine operates at the basic speed region, so $\Psi_r^d = \Psi_{rN}$.

14.) * State the approximated transfer function, F_{ω_M}, between the **filtered** rotational velocity $\hat{\omega}_M$ and the target value of the torque forming current i_{sl}^* in the following form:

$$F_{\omega_M}(s) = \frac{\hat{\omega}_M(s)}{i_{sl}^*(s)} = \frac{V_{S,\,\omega_M}}{T_{1,\,\omega_M} s(1 + T_{\sigma,\,\omega_M} s)} \tag{4.18}$$

Determine the amplification $V_{S,\,\omega_M}$, so that:

$$T_{1,\,\omega_M} = \frac{\Theta_M 2\pi f_N}{p M_{MN}} \tag{4.19}$$

Express $T_{\sigma,\,\omega_M}$ as a function of $T_{equi,\,i}$ and $T_{f,\,\omega_M}$.

Hint: Assume that constant flux is set to the nominal value and small time constants can be summarized for simplification as it is known from the DC machine.

15.) * Design a controller for the speed control loop. According to which criterion should be optimized? Justify your answer.

16.) Build the speed control loop with a first-order filter in the feedback path and simulate the response of the machine to the following set point speed:

$$N^*(t) = 0{,}7\ N_N\ \sigma(t - t_N)\ \left[\mathrm{U\,min^{-1}}\right],\ t_N = 0{,}2\,[\mathrm{s}] \tag{4.20}$$

Consider the current and speed courses and evaluate the control accuracy.

Ensure that the torque forming current stays below the 1,5 multiple of the nominal current and repeat the simulation. Which effect occurs now?

17.) Execute the necessary changes to reach a satisfying speed reaction without changing the type and the parameters of the controller.

4.5 Verification

In the considerations above the simplified model of the AC drive the properties of the switching converter and the sensors in general are neglected. At this place an accurate model is used to proove the suitability of the field oriented control.

18.) For this propose replace the subsystem `AC_Drive` by the block `AC_Drive_2` that is inside the same named model and simulate the response of the controlled target value of the drive in problem 16.
What difference can you notice as opposed to the previous case?

19.) Use the following load torque for the investigation of the disturbance behavior:

$$M_L(t) = M_{MN}\ \sigma(t - t_{M_L})\ [\mathrm{Nm}],\ t_{M_L} = 0{,}5\,[\mathrm{s}] \tag{4.21}$$

Evaluate the resulting course of the machine torque and the speed.

20.) Simulate the system response with the following speed target value and load torque:

$$\Omega^*(t) = 1{,}1\ \Omega_N\ \sigma(t - t_N)\ \left[\mathrm{min^{-1}}\right],\ t_N = 0{,}2\,[\mathrm{s}] \tag{4.22}$$

$$M_L(t) = 0{,}5\ M_{MN}\ \sigma(t - t_{M_L})\ [\mathrm{Nm}],\ t_{M_L} = 0{,}5\,[\mathrm{s}] \tag{4.23}$$

What problem occurs in this case? Eliminate it in an appropriate manner.

21.) What kind of difficulty can occur at the practical realization of the control strategy in this experiment?

Experiment 5
Direct Torque Control of the AC Drive

5.1 Overview

As the results from the previous experiment have shown, the AC drive can be controlled with the *field oriented* cascade structure in a way similar to the DC machine. For the execution of the coordinate transformation the exact knowledge of the rotor flux space vector and hence the machine parameters are mandatory. The machine parameters can be strongly dependent on the operating conditions, as for example the stator or rotor resistance are influenced by temperature. If the parameters of the flux estimator do not match with the actual values, an estimation error occurs. This can have negative effects on the control accuracy. For this reason the *field oriented control* is not robust against parameter variations.

In the following experiment an alternative control concept, the *direct torque control*, DTC, is investigated. Here the considerations are made in the stator fixed coordinate system. The state variables *stator flux linkage* and *torque* are imposed by nonlinear hysteresis controllers.

Topic of this experiment is the design and the simulation of the direct torque control for the AC machine used in the previous experiment. For this purpose the model of the asynchronous machine with squirrel cage and the two-level converter is used.

5.2 Theoretical Background

5.2.1 Model of the AC Drive in Stator Coordinate System

Starting point of the following thoughts is again the equation system (3.96). By applying Clarke transformation the rotor voltages and the rotor flux linkage equation can be transfered to the stator fixed (α, β)-coordinate system (see section **??**). Consequently the following relations are valid:

$$\text{Stator Voltage:} \qquad \underline{u}_s^s = R_s\ \underline{i}_s^s + \frac{\mathrm{d}\underline{\Psi}_s^s}{\mathrm{d}t} \tag{5.1a}$$

$$\text{Stator Flux Linkage:} \qquad \underline{\Psi}_s^s = L_s\ \underline{i}_s^s + L_m \underline{i}_r^s = L_m\left(\underline{i}_s^s + \underline{i}_r^s\right) + L_{\sigma s}\ \underline{i}_s^s \tag{5.1b}$$

$$\text{Rotor Voltage:} \qquad 0 = R_r\ \underline{i}_r^s + \frac{\mathrm{d}\underline{\Psi}_r^s}{\mathrm{d}t} - \omega\ \mathbf{J}\ \underline{\Psi}_r^s \tag{5.1c}$$

$$\text{Rotor Flux Linkage:} \qquad \underline{\Psi}_r^s = L_r\ \underline{i}_r^s + L_m\ \underline{i}_s^s = L_m\left(\underline{i}_s^s + \underline{i}_r^s\right) + L_{\sigma r}\ \underline{i}_r^s \tag{5.1d}$$

$$\text{Torque:} \qquad M_M = \frac{3}{2}\ p\ \left(\underline{i}_s^s\right)^\top\ \mathbf{J}\ \underline{\Psi}_s^s = \frac{3}{2}\ p\ \left(\Psi_s^\alpha\ i_s^\beta - \Psi_s^\beta\ i_s^\alpha\right) \tag{5.1e}$$

$$\text{Mechanic:} \qquad \Theta_M \frac{\mathrm{d}\omega_M}{\mathrm{d}t} = M_M - M_L \tag{5.1f}$$

The equations 5.1 are the basis for the following derivations.

5.2.2 Operation of the Two-Level Converter without Modulator

In the field oriented control the binary signals s_1, s_3 and s_5 for the switches inside of the converter (IGBT's) are determined by a modulator (see section 4.3.2).
In general the converter can be used without the modulator. Then the signals s_1, s_3 and s_5 are generated directly by an appropriate controller. The direct torque control and other control strategies for AC drives take advantage of this possibility.
The command signals of the lower switches `S2`, `S4` and `S6` are always $s_2 = \neg s_1$, $s_4 = \neg s_3$ and $s_6 = \neg s_5$, to avoid shortcircuiting of the DC-bus U_{dc}. Furthermore we assume that the switch `SX` is *closed* (that means it *conducts* current), when the corresponding command signal s_X ($X \in \{1..6\}$) takes the value 1. `SX` on the other hand is *opened* (that means it *blocks* current), if $s_X = 0$.

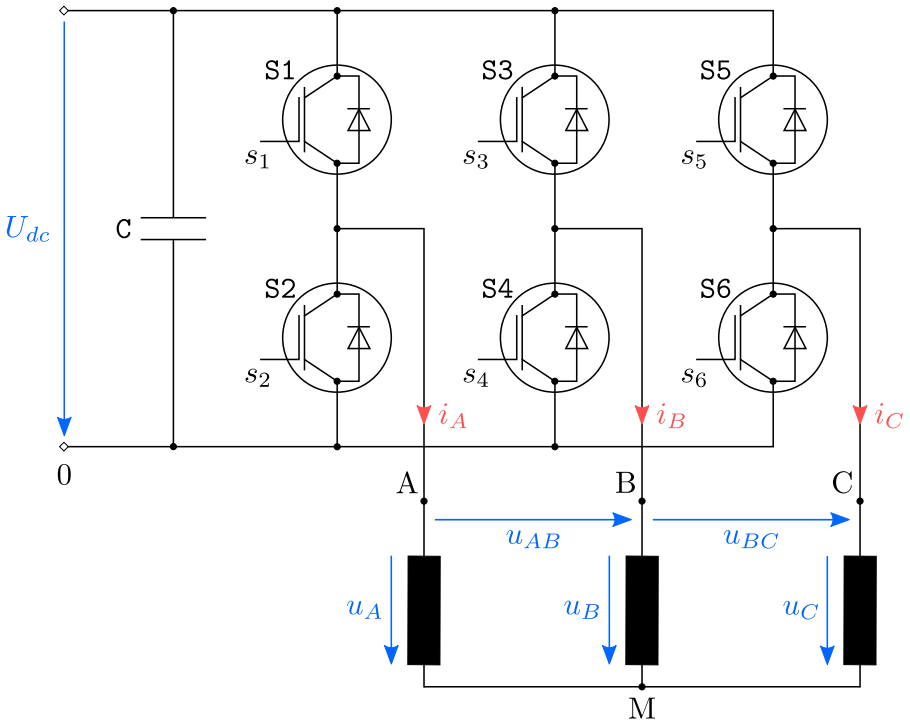

Figure 5.1: Schematic Presentation of the Converter and the Stator Strings of the AC Machine

In total the possible switching combinations are $2^3 = 8$, and the voltages u_{A0}, u_{B0} and u_{C0} can take the value U_{dc} and 0. For the line-to-line voltages u_{AB} and u_{BC} the values U_{dc}, 0 and $-U_{dc}$ can be taken. In the case of a star point connection the machine's phase voltages u_A, u_B and u_C are fixed by the following relations:

$$u_A = \frac{2s_1 - s_3 - s_5}{3} U_{dc} \tag{5.2a}$$

$$u_B = \frac{-s_1 + 2s_3 - s_5}{3} U_{dc} \tag{5.2b}$$

$$u_C = \frac{-s_1 - s_3 + 2s_5}{3} U_{dc} \tag{5.2c}$$

If the Clarke transformation $\mathbf{T}_C$ is applied to the vector of the phase voltages $\underline{u}_1 = \begin{bmatrix} u_A & u_B & u_C \end{bmatrix}^\top$, it follows that:

$$\underline{u}_s^s = U_{dc} \begin{bmatrix} \frac{2}{3}s_1 - \frac{1}{3}(s_3 + s_5) \\ \frac{\sqrt{3}}{3}(s_3 - s_5) \\ 0 \end{bmatrix} = \begin{bmatrix} u_s^\alpha \\ u_s^\beta \\ 0 \end{bmatrix} \tag{5.3}$$

Again just the first two components of the resulting voltage space vector, u_α and u_β, are important. The eight voltage space vectors generated by the converter are illustrated in figure 5.2. For better handling these have been marked by the symbol $\underline{v}_k$, ($k \in \{0..7\}$), followed by the corresponding command signals (s_1, s_3, s_5).
The space vectors $v_0(0, 0, 0)$ and $v_7(1, 1, 1)$ short circuit the load and are named *zero space vectors*. The renaming ones are the *active space vectors*.

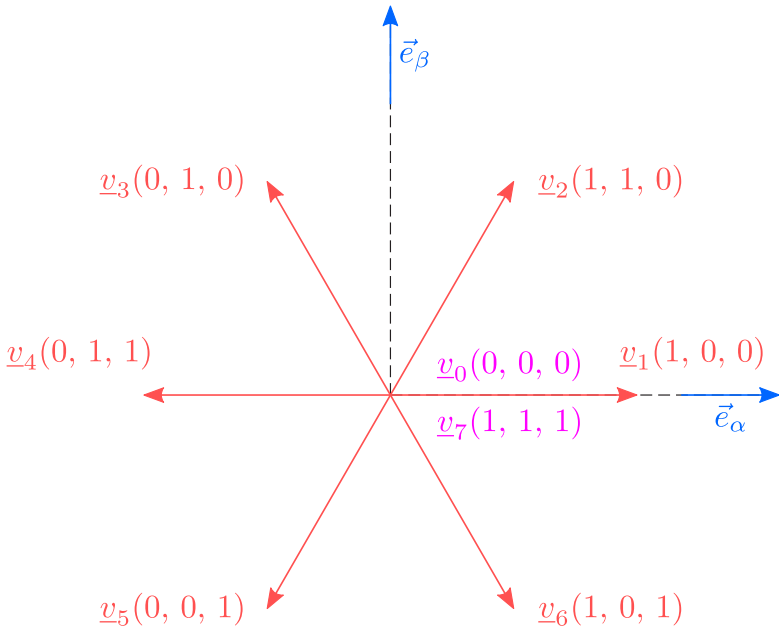

Figure 5.2: Possible Stator Voltage Space Vectors of the Two-Level Converter with Direct Activation

5.2.3 Principle of the Direct Torque Control

Approach

Foundation of the next considerations is the stator voltage equation 5.1a:

$$\underline{v}_k = \underline{u}_s^s = R_s \, \underline{i}_s^s + \frac{\mathrm{d}\underline{\Psi}_s^s}{\mathrm{d}t}, \quad k \in \{0..7\} \tag{5.4}$$

If at time t_0 the converter switches from the voltage space vector $\underline{v}_k$ to $\underline{v}_l$ ($l \in \{0..7\}, l \neq k$), within the time interval $[t_0; t_0 + T_s]$, $T_s \ll T_{\sigma s} = L_{\sigma s}/R_s$, the influence of the ohmic voltage drop in 5.4 can be neglected. The derivation of $\underline{\Psi}_s^s$ with respect to time is approximated by a difference. It holds true that:

$$\underline{v}_l = \underline{u}_s^s \approx \frac{\Delta \underline{\Psi}_s^s}{T_s}, \quad l \in \{0..7\} \tag{5.5}$$

As figure 5.3 illustrates, the application of the voltage space vector $\underline{v}_l$ during the time interval T_s leads to the following variation of the stator flux linkage:

$$\Delta \underline{\Psi}_s^s \approx T_s \, \underline{v}_l \tag{5.6}$$

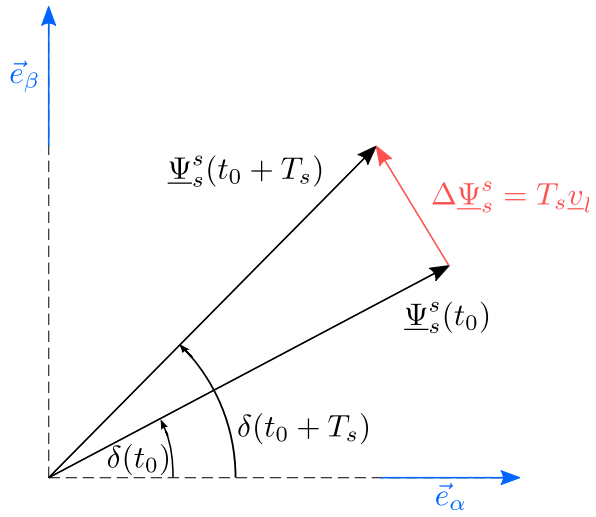

Figure 5.3: Influence of the Applied Voltage Space Vector $\underline{v}_l$ on $\underline{\Psi}_s^s$ ($l \in 0..7$)

The trajectory of the space vector $\underline{\Psi}_s^s$ in the (α, β)-plan can be determined by the application of a sequence of voltage space vectors. To take advantage of this property and derive a practical control strategy, a relation to the generated torque has to be created. This happens by expressing the stator current space vector $\underline{i}_s^s$ from the torque equation (5.1e) as a function of $\underline{\Psi}_s^s$ and $\underline{\Psi}_r^s$:

$$\underline{i}_s^s = \frac{1}{\sigma \, L_s} \left(\underline{\Psi}_s^s - \frac{L_m}{L_r} \underline{\Psi}_r^s \right) \quad \text{with} \quad \sigma = \left(1 - \frac{L_m^2}{L_s \, L_r} \right) \tag{5.7}$$

Hence for the torque it follows that:

$$
\begin{aligned}
M_M &= \frac{3p}{2\sigma L_s}\left(\underline{\Psi}_s^s - \frac{L_m}{L_r}\underline{\Psi}_r^s\right)^\top \mathbf{J}\ \underline{\Psi}_s^s \\
&= \frac{3p}{2\sigma L_s}\left((\underline{\Psi}_s^s)^\top \mathbf{J}\ \underline{\Psi}_s^s - \frac{L_m}{L_r}(\underline{\Psi}_r^s)^\top \mathbf{J}\ \underline{\Psi}_s^s\right) \\
&= -\frac{3p}{2\sigma L_s}\frac{L_m}{L_r}(\underline{\Psi}_r^s)^\top \mathbf{J}\ \underline{\Psi}_s^s \\
&= \frac{3pL_m}{2\sigma L_s L_r}\,\|\underline{\Psi}_s^s\|\,\|\underline{\Psi}_r^s\|\sin(\delta-\varphi)
\end{aligned}
\tag{5.8}
$$

where δ and φ are the angles of the stator flux space vector $\underline{\Psi}_s^s$ respectively the rotor flux space vector $\underline{\Psi}_r^s$ in the stator coordinate system (see Fig. 5.4). Thus the machine torque is determined by the absolute values of the stator and rotor flux space vector and their relative angle.

In general the rotor time constant $T_r = L_r/R_r$ is much larger then the stator time constant $T_{\sigma s} = L_{\sigma s}/R_s$ and the transfer function between $\underline{\Psi}_r^s$ and $\underline{u}_s^s$ includes second order terms. $\underline{\Psi}_r^s$ can be assumed to be constant during the time interval T_s after a switching operation. Hence, the absolute value and the angle of the stator flux space vector remain to take influence on the torque.

To control the torque M_M and the absolute value of the stator flux space vector $\|\underline{\Psi}_s\|$ independently, the torque is just controlled by changes of the angle $\delta - \varphi$. By increasing and decreasing the angle within the interval $[-\pi/2;\ \pi/2]$, the torque can be increased or decreased.

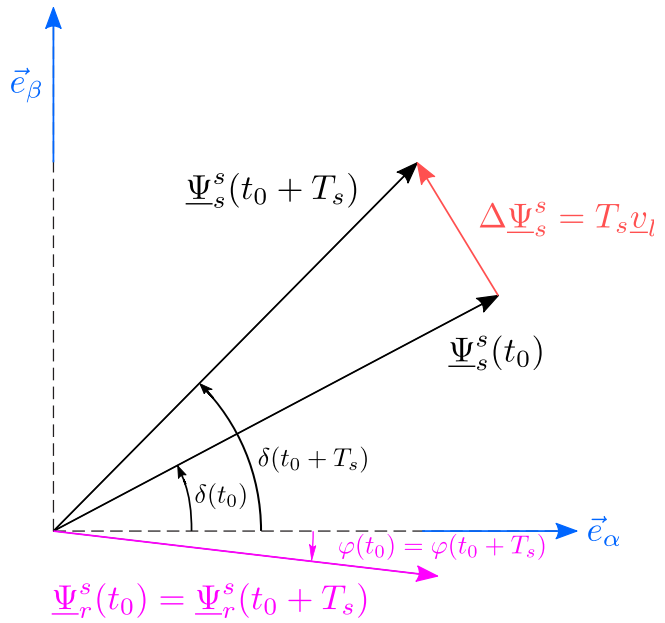

Figure 5.4: Influence of Applied Voltage Space Vector $\underline{v}_l$ on the Relative Angle Between $\underline{\Psi}_s^s$ and $\underline{\Psi}_r^s$ During the Switching Time Interval T_s

Development of a Control Concept

By means of the six active voltage space vectors of the Two-Level-Cconverter (compare Fig. 5.2) the stator flux space vector $\underline{\Psi}_s^s$ can be influenced in six different ways within the switching time interval T_s. Regardless of the machine state, three of these voltage space vectors lead to an increase of the absolute value of the flux $\|\underline{\Psi}_s\|$, while the others decrease it. According to (5.5) the application of the zero space vector has nearly no influence on the stator flux space vector and results in a conservation of its angle and absolute value.

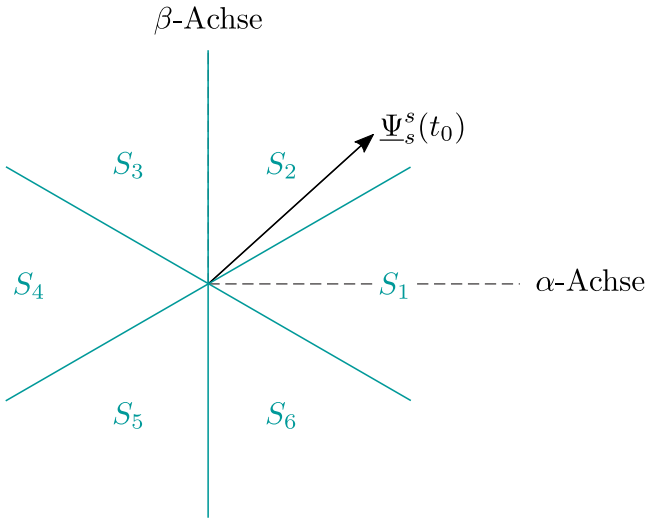

Figure 5.5: Principle Representation of the Sectors in the (α, β)-Plane

Furthermore, *three* of the six space vectors $\underline{\Psi}_s^s$ lead to a anticlockwise rotation and therefore tend to result in increase of the relative angle with the rotor flux space vector. On the other hand, the *three* other space vectors tend to decrease this angle. This has direct impact on the torque.
The concrete correlation between the space vectors and their effects is dependent on the angle δ of the stator flux space vector at the considered point of time. For this reason the (α, β)-plane is divided in *six* sectors. Each sector spans an angle of $\pi/3$. In addition, the first sector is symmetrical to the α-axis (see Fig 5.5). In each sector, *three* of the six space vectors lead to an increase of the absolute value of the flux and the other three lead to a decrease. *Two* of the six active space vectors increase the torque, *two* decrease it. The remaining *two* have a weak effect on the torque, while the sign of the effect can't be set. They are interpreted as *torque conserving* vectors.
The relation between the voltage space vectors and their effects on the flux value and torque within the respective sector is summarized in a *switching table* (see table 5.1).
The decision if the flux amount or the torque shall be increased or decreased, is made by individual hysteresis controllers. The controllers are implemented in *discrete time* and work with the switching time T_s.
The output value $h_{\underline{\Psi}_s}[(n+1)T_s]$ of the flux controller for the time interval $[nT_s; (n+1)T_s]$ ($n \in \mathbb{N}$) is determined by the control error $e_{\underline{\Psi}_s}[nT_s]$ sampled at the time instant $t_0 = nT_s$ and the controller output $h_{\underline{\Psi}_s}[nT_s]$ at this time. A similar relation holds for the torque control loop between the control error e_M and the controller output h_M. Figure 5.6 illustrates the function of both controllers.

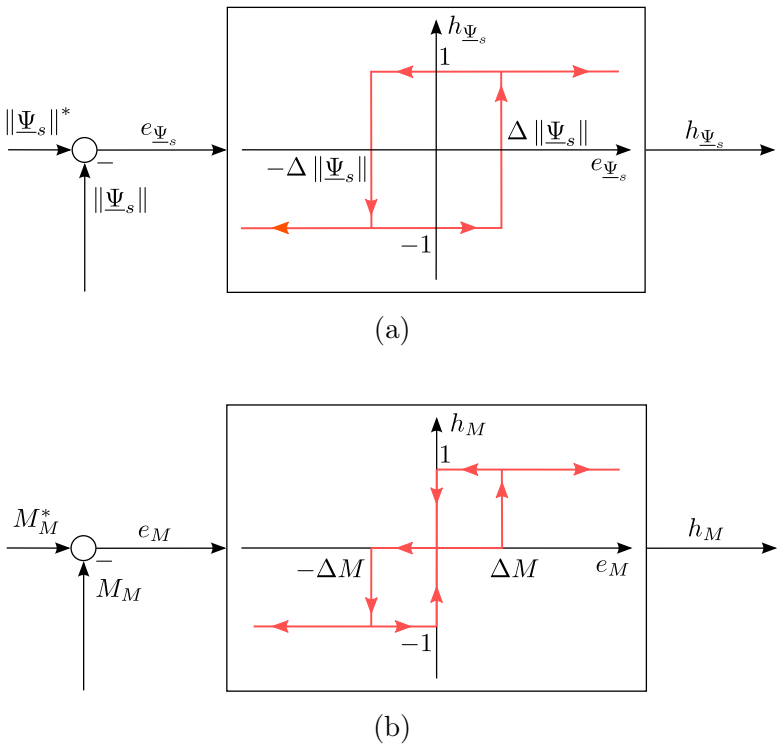

Figure 5.6: Schematic Function of the Hysteresis Controller
(a) Flux Controller; (b) Torque Controller

The output of the torque controller can take the values -1, 0 and 1. The flux controller can only take the values -1 and 1. If the controller outputs the value -1, the corresponding control variable has to be decreased. If the controller output delivers 0 or 1, the control variable should stay constant or should be increased, respectively.
From the values $h_{\underline{\Psi}_s}$ and h_M and the sector number, in which the stator flux space vector is located at the time t_0, the voltage space vector to be applied is determined by the means of the switching table 5.1. This one is going to be applied to the machine during the time interval $[nT_s;\ (n+1)T_s]$.

5.2.4 Determination of the Stator Flux Space Vector and the Torque

In practice the flux linkage on the stator side can not be measured directly and has to be recreated by a model.
From the stator voltage equation (5.1a) the following relation follows:

$$\frac{\mathrm{d}\underline{\Psi}_s^s}{\mathrm{d}t} = \underline{u}_s^s - R_s\ \underline{i}_s^s \tag{5.9}$$

After integrating equation (5.9), there exists the possibility to calculate $\underline{\Psi}_s^s$ based on the measured phase currents and phase voltages. In most applications the latter are not measured. So the target voltages are used instead. They can be calculated from the command signals of the converter with equation (5.2).

$h_{\underline{\Psi}_s}$	h_M	S_1	S_2	S_3	S_4	S_5	S_6
1	1	$\underline{v}_X$	$\underline{v}_X$	$\underline{v}_X$	$\underline{v}_X$	$\underline{v}_X$	$\underline{v}_X$
1	0	$\underline{v}_X$	$\underline{v}_X$	$\underline{v}_X$	$\underline{v}_X$	$\underline{v}_X$	$\underline{v}_X$
1	-1	$\underline{v}_X$	$\underline{v}_X$	$\underline{v}_X$	$\underline{v}_X$	$\underline{v}_X$	$\underline{v}_X$
-1	1	$\underline{v}_X$	$\underline{v}_X$	$\underline{v}_X$	$\underline{v}_X$	$\underline{v}_X$	$\underline{v}_X$
-1	0	$\underline{v}_X$	$\underline{v}_X$	$\underline{v}_X$	$\underline{v}_X$	$\underline{v}_X$	$\underline{v}_X$
-1	-1	$\underline{v}_X$	$\underline{v}_X$	$\underline{v}_X$	$\underline{v}_X$	$\underline{v}_X$	$\underline{v}_X$

Table 5.1: Switching Table for the Determination of the Voltage Space Vector to be Applied as a Function of the Controller Outputs and the Sector Number ($X \in \{0..7\}$)

Furthermore, it is possible to calculate the torque M_M with the estimated stator flux $\hat{\underline{\Psi}}_s^s$ and the stator current space vector $\underline{i}_s^s$ by taking advantage of relation (5.1e):

$$\hat{M}_M = \frac{3}{2}\, p \left(\hat{\Psi}_s^\alpha \; i_s^\beta - \hat{\Psi}_s^\beta \; i_s^\alpha \right) \tag{5.10}$$

Eventually, for the sector determination the angle of the stator flux space vector δ is required. It can be calculated with the components of $\hat{\underline{\Psi}}_s^s$ in the stator coordinate system:

$$\hat{\delta} = \operatorname{atan2}\left(\hat{\Psi}_s^\alpha,\; \hat{\Psi}_s^\beta \right) \tag{5.11}$$

In contrast to the field oriented control the direct torque control has the advantage that number of required parameters is limited to the stator resistance of the machine. Nevertheless we want to emphasize, that the method for the calculation of the stator flux space vector assumes ideal behavior of the converter and the current sensors.

5.2.5 Summary

From the considerations above, the controller structure for the direct torque control can be derived. Figure 5.7 illustrates the coaction of the two hysteresis controllers and the subsystems *flux estimator*, *torque estimator* and *switching table*. In practice, the blocks framed in blue colour are implemented in software in a real-time system.
As a consequence of the switching behavior of the hysteresis controllers the torque ideally stays within a tolerance band defined by the torque controller in steady state. The stator flux space vector creates a zigzag shaped trajectory around its set-point value in the (α, β)-plane. The resulting courses are depicted in figure 5.8.

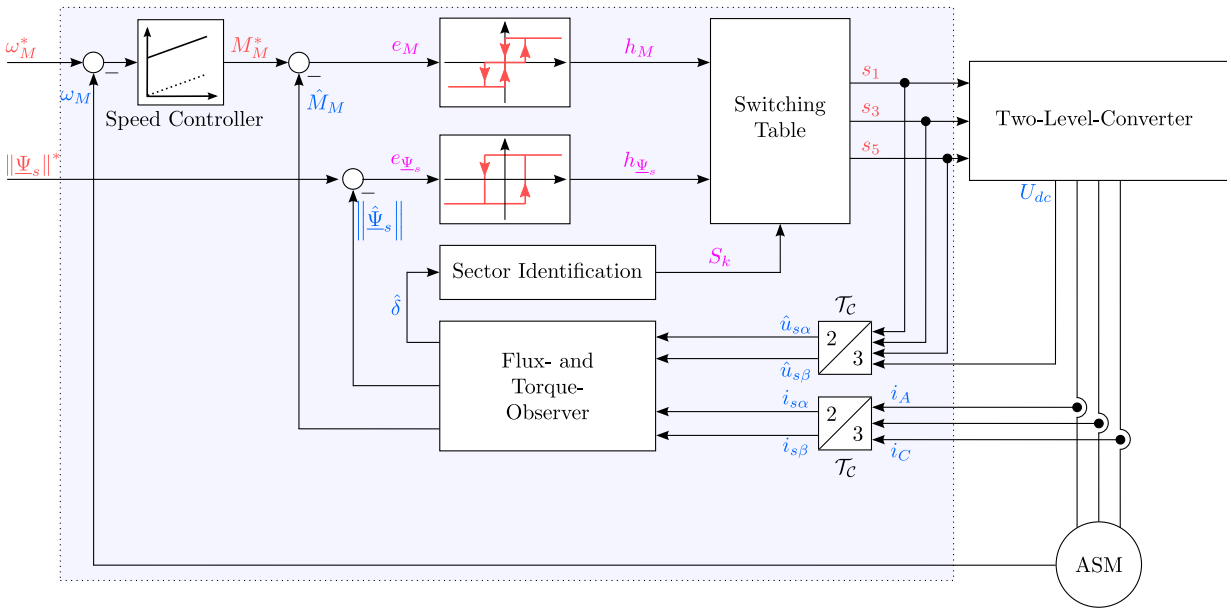

Figure 5.7: Schematic Illustration of the Direct Torque Control

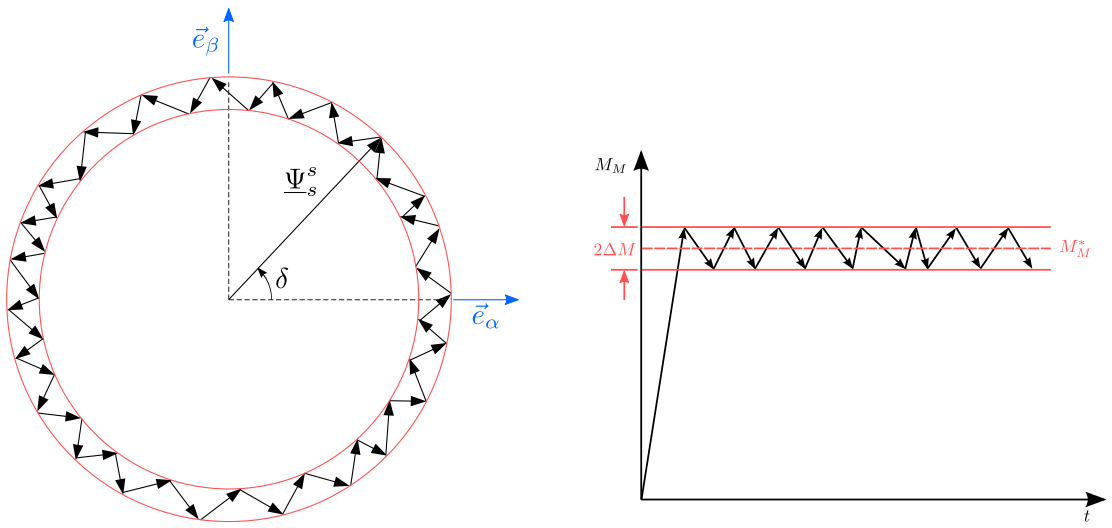

(a) (b)

Figure 5.8: Resulting Ideal Courses at Steady State Operation
(a) Space Vector of the Stator Flux Linkage; (b) Machine Torque

5.3 Implementation of the Direct Torque Control

In the following section the DTC is investigated for the drive system known from experiment 4. The necessary drive parameters are summarized in Table 5.2 and 5.3.
The influence of noise in the current measurement signal is neglected and the actual value of the rotor speed is available without any delay. First of all the flux and torque control loop is implemented. The resulting control structure of an overlaying speed control is added afterwards.

Physical Value	**Symbol and Value (SI)**			
Nominal Power	P_N	=	2,2	[kW]
Nominal Rotor Speed	N_N	=	2 890	[min^{-1}]
Nominal Torque	M_{MN}	=	7,3	[N m]
Nominal Voltage (Star-Connection, Line-To-Line)	U_{NY}	=	400	[V]
Nominal Current (Star-Connection)	I_{NY}	=	4,5	[A]
Nominal Frequency	f_N	=	50	[Hz]
Stator Resistance	R_s	=	2,3	[Ω]
Nominal Stator Flux	Ψ_{sN}	=	1,0	[Vs]
Rotor Inertia Moment	Θ_M	=	$2{,}2 \times 10^{-3}$	[kg m^2]

Table 5.2: Parameters of the Considered Asynchronous Machine

Physical Values	**Symbol and Value (SI)**			
DC-Bus Voltage	U_{dc}	=	560	[V]
Maximum Switching Frequency	$f_{s,max}$	=	4	[kHz]

Table 5.3: Parameters of the Two-Level Converter

5.3.1 Flux and Torque Control Loop

1.) * The investigated AC drive doesn't have any sensors for the measurement of phase voltages. The voltage set-point values of the controller have to be used. Draw the block diagram to recreate the stator voltage space vector $\underline{u}_s^s$ based on the command signals s_1, s_3, s_5 and the DC-bus voltage U_{dc}. If necessary indicate the Clarke transformation as is shown in figure 5.7.

2.) * Draw the signal flow diagrams of the flux and the torque estimator. Use the **estimated** stator voltage space vector $\hat{\underline{u}}_s^s$ and the stator current space vector $\underline{i}_s^s$ as inputs. The

estimated space vector of the stator flux linkage $\hat{\underline{\Psi}}_s^s$ and the estimated torque $\hat{M}_M$ are the outputs.

3.) * Draw the signal flow diagram for the determination of the absolute value and the angle of the space vector $\hat{\underline{\Psi}}_s^s$ by means of the components $\hat{\Psi}_s^\alpha$ and $\hat{\Psi}_s^\beta$.

4.) * Suggest a method to undertake the sector identification using blocks from the `Simulink`-library or few `MATLAB`-Code lines.

5.) * For each sector, think about which voltage space vector increases, decreases or conserves the flux amount respectively the torque. Fill the switching table 5.1 appropriately. Do **not** use the zero space vector.

In the following exercises the previous derived structure of the different components of the direct torque control is implemented in a `Simulink` model.

6.) Open the file `ASM_DTC_Implementation.slx` in the directory `Experiment_5` in `Simulink`. There is a block called `DTC`. Double click on it, to see its content. The measured signals of the phase currents i_A^m, i_B^m and the rotor speed ω_M^m are available as inputs. This block shall provide the binary signals s_1, s_3 and s_5 as a vector for the converter.
Firstly, construct the missing structures in the subsystem `flux and torque estimator` respecting the given inputs and outputs. Use the `Simulink`-block `discrete time integrator`, to execute the required integration in **discrete time**.

7.) Implement your suggested solution from problem 4 for the sector identification. If necessary use the block `MATLAB-Function`. Then test if your solution works properly.

8.) Build the structure of the flux and torque controller. Use the variable names `Delta_Psi` restrictively `Delta_M`, to set the hysteresis bounds. The initial values of these parameters ($\Delta \left\|\underline{\Psi}_s\right\| = 0{,}02\,[\mathrm{V\,s}],\ \Delta M = 0{,}05\,[\mathrm{N\,m}]$) are specified in the file `Experiment_5_Parameter.m`.

9.) Edit the subsystem `switching table` with the corresponding `MATLAB`-script of your solution from problem 5.

10.) Connect the subsystems and close the flux and torque control loops. Set the absolute value of the flux to the nominal value Ψ_{sN} (see table 5.2). Use the following setpoint course for the torque:

$$M_M^*(t) = \frac{M_{MN}}{4}\,(\sigma(t-t_A) - \sigma(t-t_B)),\ t_A = 0{,}3\,[\mathrm{s}]\,,\ t_B = 0{,}5\,[\mathrm{s}] \tag{5.12}$$

with

$$\sigma(t) = \begin{cases} 0 & \text{for} \quad t \leq 0\,[\mathrm{s}] \\ 1 & \text{for} \quad t > 0\,[\mathrm{s}] \end{cases} \tag{5.13}$$

Double click on the block `Initialize` to take over the simulation parameters. Check the functioning of the implemented control structure without load torque. Evaluate the

waveforms of the machine currents, the torque and the rotor speed.

By double-clicking on the block `Display Figures`, the trajectory of the stator flux space vector $\underline{\Psi}_s^s$ in the (α, β)-plane is displayed (see Fig. 5.8(a)). Analyze the results.

5.3.2 Overlaying Speed Control

The previously designed direct torque control is extended by an overlaying speed control loop. In this case the torque reference value is generated by the speed controller.

11.) For the speed controller a empirically designed PI-controller with the amplification $V_{R,\omega_m} = 10\,[\text{Nms}]$ and the Delay time $T_{n,\omega_m} = 10\,[\text{ms}]$ is used. Implement the speed controller in **discrete form** by using the `Simulink`-blocks `Gain` and `Discrete Time Integrator` and close the control loop.
Set as a command value the half of the nominal speed. Additionally load the machine with:

$$M_M^*(t) = 0{,}9\ M_{MN}\ \sigma(t - t_A),\ t_A = 0{,}5\,[\text{s}] \tag{5.14}$$

Simulate the behavior of the system and analyze the resulting speed and the stator current waveforms. Which problem occurs?

12.) Limit the set point torque value to the nominal torque M_{MN} and modify the structure of the speed controller appropriately without changing the controller type or the parameters of the controller. After rerunning the simulation, analyze the current, torque and speed waveforms.

13.) Open file `DTC_Additional_Blocks.slx` and add one instance of the block `edge counter` to the highest level of the model `ASM_DTC_Implementation.slx`. Explain its function and use it to count the number of switching operations in each inverter leg. Does the results match the maximum switching frequency from table 5.3?

The excessive switching would lead to switching losses, which could damage the converter. The number of switching operations per time unit can be reduced by specifying wider tolerance bands for the torque and flux controller or a larger sampling time T_s.
So far the sampling time of the block `DTC` was equal to the simulation time step, $T_s = 5\,[\mu\text{s}]$. With most real time computers this sampling time can not be achieved. From now $T_s = 50\,[\mu\text{s}]$ is applied, to reach meaningful results.

14.) Adjust the sampling time of the block `DTC` and simulate the system behavior. What influence does the increased sampling time have on the trajectory of the stator flux space vector and the torque? Justify your answer.

15.) What effect does an increase of the value ΔM by a factor of ten have on the torque, flux and number of switching operations? Explain this phenomena and use the value $\Delta M = 0{,}5\,[\text{Nm}]$ from now on.

16.) For the case $h_M = 0$ replace the active vectors in the switching table by zero vectors and run the simulation. How can the amount of switching be reduced by this strategy?

17.) Which other problems can occur at the practical implementation of the direct torque control?

Bibliography

[1] Andreas Binder. *Elektrische Maschinen und Antriebe - Grundlagen, Betriebsverhalten*. Berlin: Springer DE, 2012 (cit. on p. 5).

[2] Germar Mueller and Bernd Ponick. *Grundlagen elektrischer Maschinen*. New York: John Wiley & Sons, 2012 (cit. on pp. 5, 37).

[3] Dierk Schroeder. *Leistungselektronische Schaltungen - Funktion, Auslegung und Anwendung*. 3. Aufl. 2012. Heidelberg: Springer-Verlag GmbH, 2012 (cit. on p. 73).

[4] Dierk Schroeder and Joachim Boecker, eds. *Elektrische Antriebe – Regelung von Antriebssystemen*. Springer Berlin Heidelberg, 2021. DOI: 10.1007/978-3-662-62700-6 (cit. on p. 31).